TU Delft

Delft University of Technology

The Lifetime Prediction of LED Drivers and Lamps

Sun, Bo

DOI
10.4233/uuid:e83b184c-c972-402a-a0c6-418222cf11ad

Publication date
2017

Document Version
Final published version

Citation (APA)
Sun, B. (2017). *The Lifetime Prediction of LED Drivers and Lamps*. [Dissertation (TU Delft), Delft University of Technology]. https://doi.org/10.4233/uuid:e83b184c-c972-402a-a0c6-418222cf11ad

Important note
To cite this publication, please use the final published version (if applicable).
Please check the document version above.

Copyright
Other than for strictly personal use, it is not permitted to download, forward or distribute the text or part of it, without the consent of the author(s) and/or copyright holder(s), unless the work is under an open content license such as Creative Commons.

Takedown policy
Please contact us and provide details if you believe this document breaches copyrights.
We will remove access to the work immediately and investigate your claim.

This work is downloaded from Delft University of Technology.
For technical reasons the number of authors shown on this cover page is limited to a maximum of 10.

The Lifetime Prediction of LED Drivers and Lamps

THE LIFETIME PREDICTION OF LED DRIVERS AND LAMPS

Proefschrift

ter verkrijging van de graad van doctor
aan de Technische Universiteit Delft,
op gezag van de Rector Magnificus prof. ir. K.C.A.M. Luyben,
voorzitter van het College voor Promoties,
in het openbaar te verdedigen op dinsdag 26 Septembet 2017 om 15:00 uur

door

BO SUN

Betrouwbaarheid ingenieur
geboren te Taiyuan, China.

This dissertation has been approved by the

Promotor: Prof. dr. G.Q. Zhang

Composition of the doctoral committee::

Rector Magnificus,	Chairman
Prof. dr. G.Q. Zhang,	Technische Universiteit Delft
Independent members:	
Prof. dr. J.A. Ferreira,	Technische Universiteit Delft
Prof. dr. P.M. Sarro,	Technische Universiteit Delft
Prof. dr. J.L. Cao,	Fudan University, China
Prof. dr. M.G. Pecht,	University of Maryland, Maryland, USA
Prof. dr. S. Hamdioui,	Technische Universiteit Delft, reservelid
Other members:	
Prof. dr. X.J. Fan,	Lamar University, Texas, USA

Prof. X.J. Fan has contributed significantly to the creation of the dissertation.

Prof. W.D van Driel from Philips Lighting has taken part in the evaluation after the above committee granted the candidate permission to defend the dissertation in public.

Keywords: LED Driver, LED Lamp, Lifetime Prediction, Electronic-Thermal Simulation, Reliability, Solid State Lighting

Printed by: IPSKAMP Printing

Front & Back: ShangYi Design Studio

Copyright © 2017 by B. Sun

All rights reserved. No part of this publication may be reproduced, stored in a retrieval system or transmitted in any form or by any means without the prior permission of written copyright owner.

ISBN 000-00-0000-000-0

An electronic version of this dissertation is available at
http://repository.tudelft.nl/.

For we know in part, and we prophesy in part.
For now we see through a glass, darkly, but then face to face;
Now I know in part, but then shall I know even as also I am known.

Corinthians 13

Contents

1 Introduction **1**
1.1 Background 1
1.2 The Reliability of LED Drivers 4
1.2.1 Development of Drivers 4
1.2.2 Reliability of LED Drivers 6
1.3 Reliability Interactions between LED Lamps and Drivers 8
1.4 Objectives and Outlines 9
References 10

2 PoF-Simulation-Assisted Reliability Prediction for LED Drivers **21**
2.1 Introduction 22
2.2 Methodology 23
2.3 Modelling 26
2.3.1 Circuit Simulation 26
2.3.2 Thermal Simulation 27
2.3.3 Electrolytic Capacitor Degradation Model 28
2.3.4 Monte Carlo Simulation 30
2.4 Experiments 32
2.4.1 Test Set-up 32
2.4.2 Thermal Model 32
2.4.3 Electrolytic Capacitor Degradation Model 33
2.4.4 Monte Carlo Model 35
2.5 Validation 36
2.6 Results and Discussions 38
2.7 Conclusion 41
References 43

3 A Novel Lifetime Prediction for Integrated LED Lamps by Electro-Thermal Simulation **47**
3.1 Introduction 48

3.2 Degradation Models 49
3.2.1 LED Light Source 49
3.2.2 LED Driver 51
3.3 Simulation Methodology 52
3.3.1 Electronic Simulations 52
3.3.2 Thermal Simulations 54
3.3.3 Simulation Methodology 55
3.4 Parameter Extraction of LED Models 56
3.5 Result and Discussions 56
3.5.1 Lamp's Initial Temperature Distributions 56
3.5.2 Definition of Different Scenarios 57
3.5.3 Results and Discussions 59
3.6 Conclusions 63
References 64

4 A Reliability Prediction for The LED Lamp with An Electrolytic Capacitor Free Driver 69
4.1 Introduction 70
4.2 General Methodology 71
4.3 Electronic Models 71
4.3.1 Driver Circuit 71
4.3.2 LED Light Source 72
4.4 Thermal Simulation 74
4.5 Fault Tree and The Model of Failure Probability 77
4.6 Case Studies and Results 78
4.6.1 Selection of LED and Driver 78
4.6.2 Results and Discussions 79
4.7 Conclusions 85
References 86

5 A Physics and Statistics Combined Reliability Prediction Methodology for LED Drivers 91
5.1 Introduction 92
5.2 Methodology 93
5.3 Lumen Depreciation Model 94
5.4 Reliability Model of The Driver 97
5.5 Thermal Model of The LED Lamp 101

5.6 Case Studies and Results 104
5.6.1 Definition of Scenarios. 104
5.6.2 Results and Discussions 105
5.7 Conclusions. 108
References 109

6 Concluding Remarks and Recommendations 113
References 115

A Appendix A 117
A.1 An Accelerated Test Method for Outdoor LED Driver 117
A.1.1 Sampling Method 117
A.1.2 Suitability Test Method. 118
A.1.3 Accelerated Test Methods 119
A.1.4 Failure Criteria 122
References 123

B Appendix B 125
B.1 Supporting Information for Chapter 2 125

C Appendix C 131
C.1 Supporting Information for Chapter 3 131

Abbreviations, Acronyms and Notation 135

Summary 143

Samenvatting 145

List of Publications 147

Acknowledgements 151

Curriculum Vitæ 153

1

INTRODUCTION

Simplicity is prerequisite for reliability.

Edsger W. Dijkstra

1.1. BACKGROUND

SINCE the large-scale application of commercial blue Light Emitting Diode (LED), the LED lamp has now emerged as a promising product to replace conventional lighting, such as incandescent bulbs and compact fluorescent lamps (CFLs), due to its superior energy efficiency, environmental friendliness, flexible controllability and new experience of lighting [1–6]. An LED lamp is a perfect combination of illumination and semiconductors science. New technology development, new material application, and fast industrial implementation are the characteristics of LED lighting technology.

An LED lamp or luminaire is a complex system that is comprised of LED light source, electronic driver, and/or control gears, secondary optical parts, and heat dissipation components. The LED light source often has a lifetime as long as 25,000 - 100,000 hours [6, 7]. However, the customer experiences may be quite different, and some of the LED lamps can fail in a considerable time ahead of the claimed life. The discrepancies between the lifetime of LED light source and the practical life of LED lamps are mainly due to the following reasons [8]:

1. The definition of LED lamps' lifetime is vague. A complete lifetime definition should include at least four aspects: operation conditions, failure criteria, the minimum required reliability and confidence level. However, current industry standards only have uniform specifications on operation conditions and failure criteria.

2. LED's lifetime is usually obtained by constant operation conditions. However, real operation conditions may vary with time due to the degradation of LEDs and drivers. Constant condition based reliability prediction methods do not adopt the temperature change and current into consideration.

3. The lifetime mismatch between the LED lamp and the driver may occur. If driver's lifetime is much shorter than LED's, the LED lamp's life is determined by driver's lifetime. If the LED light source and the driver have comparable lifetimes, their interactions may reduce the life of the entire LED lamp.

The level of lumen depreciation, also called lumen maintenance, is typically used as failure criteria to for the claimed LED's lifetime by manufacturers. The lumen depreciation is the degradation of LED's light output during normal usage. Usually, 30% luminous drop, what is human eyes can detect, is defined as the threshold of LED's lifetime [9]. The required minimum reliability level is specified by a percentile lifetime for a population of LEDs. The confidence interval is provided based on the lumen depreciation and the required minimum reliability level [8].

Many studies have focused on LED's depreciation in different conditions [10]. For example, it is experimentally found that the lumen decay of an LED light source depends on the junction temperature, driving current and operation time [11–18]. The LED's degradation in the high temperature-humidity environment has been investigated [5, 19]. The relationships between LED structure and performance have been studied [20–22]. A control methodology for nonlinear photo-electro-thermal dynamics of LEDs has been developed [23]. LED's color shifting for various optical materials has been investigated [4, 24, 25]. Degradation tests are usually performed to obtain the lifetime of each individual LED. The industry standard LES LM-80 [26] requires a minimum of 6,000 hours of degradation testing. Based on the available lumen degradation data, the lifetime of each sample is projected by an exponential curve-fitting extrapolation as described in the standard IES TM-21 [27]. However, TM-21 uses the average degradation value for the further projection, which ignores the statistical properties and therefore the reliability information cannot be obtained from the TM-21 procedure. The degradation test methodology presented in IES LM-80 is usually performed under several specific

constant conditions. Recently an accelerated test method of luminous flux depreciation has been developed to reduce the test time from 6000 hours to 2000 hours [6, 28–30]. An increasing number of studies have also focused on the statistical properties of LED lamps. For instance, the Gamma process and copula function are implemented to model the reliability of LED lighting systems [31]. The Wiener process has been used to predict the lumen depreciation [32]. The six sigma DMAIC approach is utilized for life test for white LEDs [33]. The real operation conditions have been considered by an LED life prediction method [8].

On the other hand, significant efforts have also been made to improve driver's reliability. According to field test reports [34] shown in Figure 1.1, more than 74% of LED luminaires failures can be attributed to the LED driver, only about 7% of LED luminaires failures relate to LED light sources. The lifetime mismatch between the LED light source and the driver is usually considered as the most significant reliability problem of mainstream LED lamps or luminaires [1, 2, 35]. An LED driver has many failure modes. Among these failure modes, the electrolytic capacitor is found to be the bottleneck problems of current mainstream LED drivers. Therefore, many technologies [36–45] have been designed to eliminate electrolytic capacitors from LED drivers. It claims that these electrolytic capacitor free LED drivers have a comparable lifetime with LEDs. For such a kind of driver, the major failure modes are catastrophic failures and degradation, such as the catastrophic failure of MOSFET and the output current degradation.

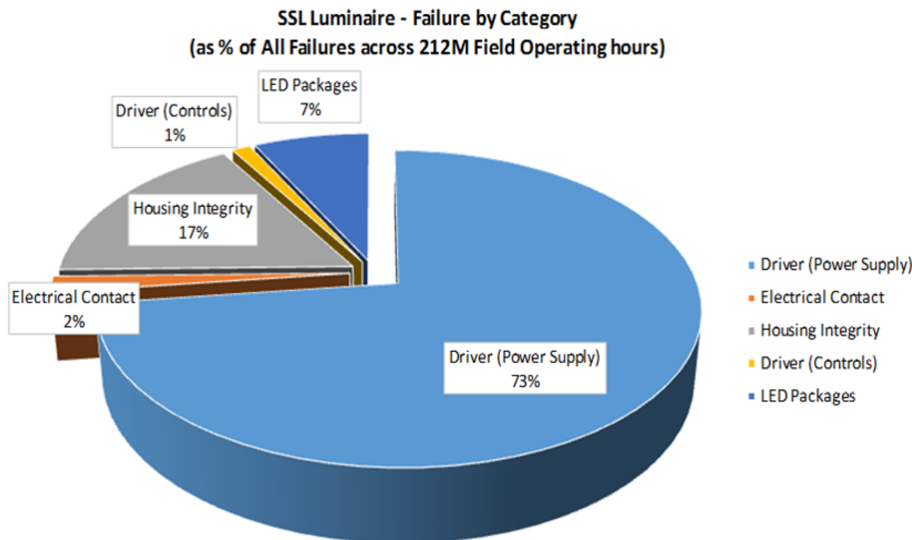

Figure 1.1: Failures of the LED Driver [2].

1

1.2. THE RELIABILITY OF LED DRIVERS

1.2.1. DEVELOPMENT OF DRIVERS

LEDs are usually driven by constant current power supplies [46], which are invented early than LEDs for lighting applications. The switched-mode power supply (SMPS) has been developed since the 1950s [47]. In 1955, self-excited oscillation push redeem transistor single transformer DC converter has been invented, initiating the pulse width modulation (PWM) control technology in power supplies [47]. In the 1960s, basic topologies of SMPS have been developed and gradually become mature technologies [46, 48–50], including buck, boost, buck-boost, fly-back, cuk, single ended primary inductor converter (SEPIC), half bridge, full bridge, active clamp forward and push-pull converter. These topologies are still used so far. Figure 1.2 displays several basic topologies of SMPS.

Despite the maturity of driver topologies, new components and new control methods of power supply have attracted more research attentions after the 1970s. Applications of new switching components, such as the giant transistors (GTR) [51], insulated gate bipolar transistor (IGBT) [52], Power MOSFET [53], V-MOSFETs and high electron mobility transistor (HEMT) [54], have significantly increased the switching frequency of SMPS higher up to 1 MHz. These components not only improve the efficiency, but also decrease the size and weight of the SMPS. With the increasing of switching frequency, the power consumption of SMPS has inevitably risen to a high level. Thus, soft switching technologies have been developed to reduce the power consumption of SMPS. These soft switching techniques, such as zero voltage switching (ZVS) [55], zero current switching (ZCS) [56], resonant [50, 57], quasi-resonant [58] and phase-shifted resonant [59] technology, can further increase the switching frequency, while keeping the high efficiency of the entire power supply.

In recent years, to improve the lifetime of LED drivers, many electrolytic capacitor free topologies have been developed, including totem-pole boost power factor correction (PFC) plus half bridge LLC resonant converter [37], valley-fill SEPIC converter [38], fly-back plus buck converter [39], power control (PC) converter [40] and PFC plus bidirectional converter [41, 42]. These topologies replace electrolytic capacitors with more reliable components [60], for instance, film capacitors, ceramic capacitors and inductors. Moreover, electrolytic capacitor elimination methods have also been developed to optimize mainstream LED drivers, such as pulsating-current driving technique [61], harmonic injection technology [62], LC filtering [63, 64] and input current shaping [65].

Meanwhile, intelligent driver and smart lighting techniques have been applied to LED drivers, such as constant light output technology [66], daylighting control [67], pre-

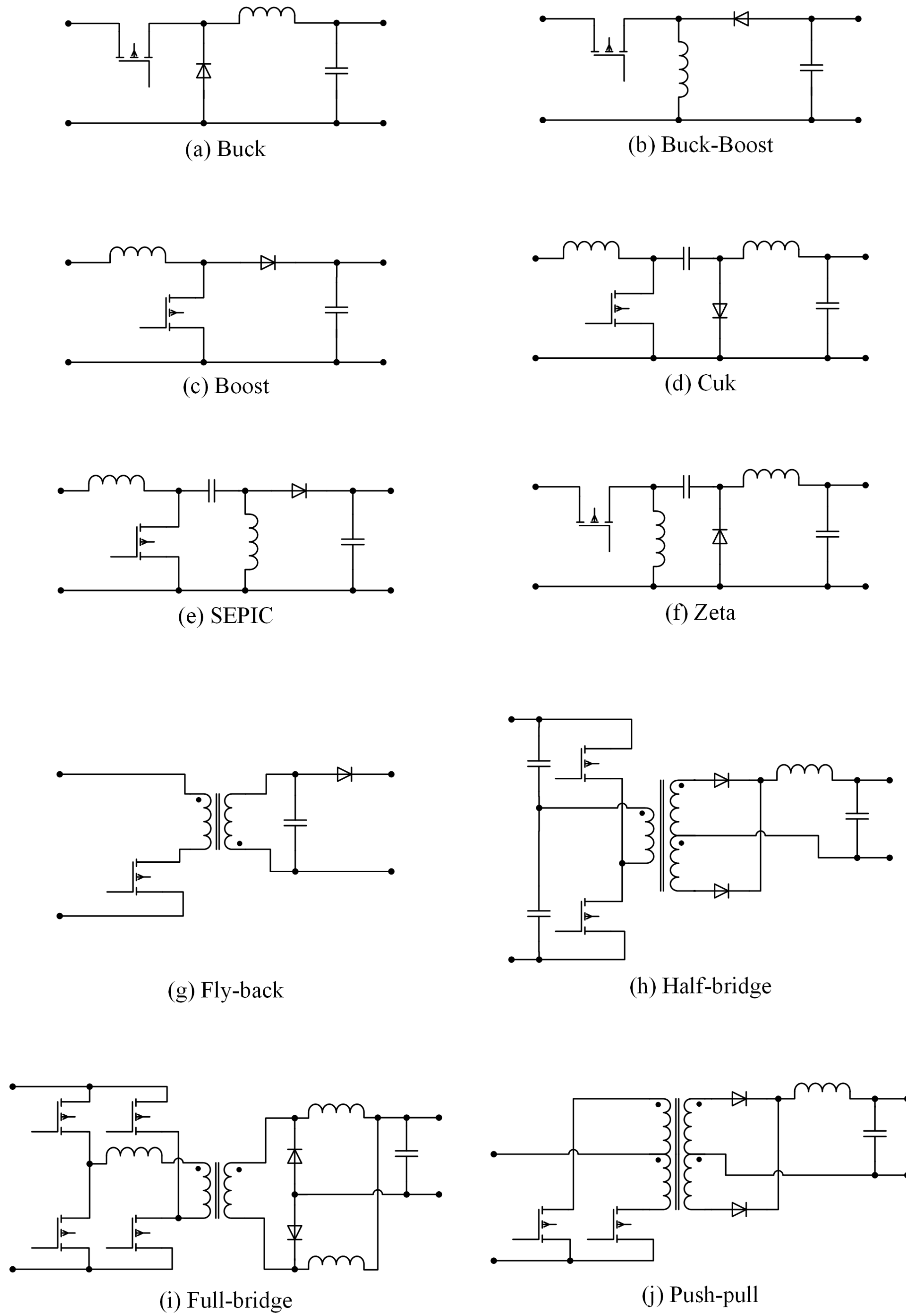

Figure 1.2: Basic Topologies of SMPS.

1

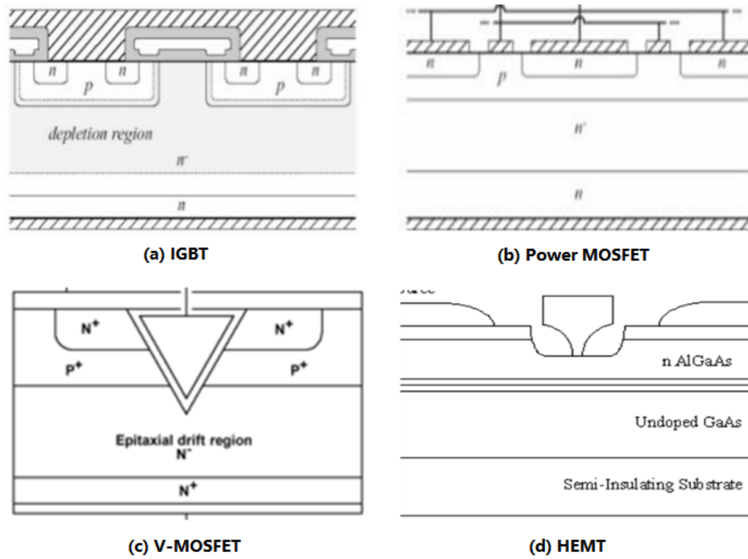

Figure 1.3: Switching Components of The SMPS.

cise dimming [68] and smart color mixing [69]. The constant light output (CLO) mode has been implemented in driver design to eliminate the lumen depreciation. In contrast with the constant current mode (CCM), LED drivers in CLO mode usually have optical feedback functions and can adjust their output current to maintain the light output. It has been claimed that such technology can eliminate the lumen depreciation during long-term operation.

1.2.2. RELIABILITY OF LED DRIVERS

Conventional lifetime prediction methods usually regard the life of the weakest component as the lifetime of the LED driver. Numerous studies [70–74] have shown that the electrolytic capacitor is the reliability bottleneck of current mainstream LED drivers [75]. Thus, various researchers have investigated the lifetime of electrolytic capacitors. For instance, a real-time failure detection method has been developed [76, 77]. Lifetime prediction models of electrolytic capacitors have been developed for switch mode power supply [78] and AC variable-frequency drivers [79]. Accelerated life test method has been designed for LED drivers [80]. Besides electrolytic capacitors, the reliability of other components and materials has been studied as well, including thin film capacitors [81], ceramic capacitors [82, 83], transformers [84], power diodes [85] MOSFET [86, 87] and molding compounds [88].

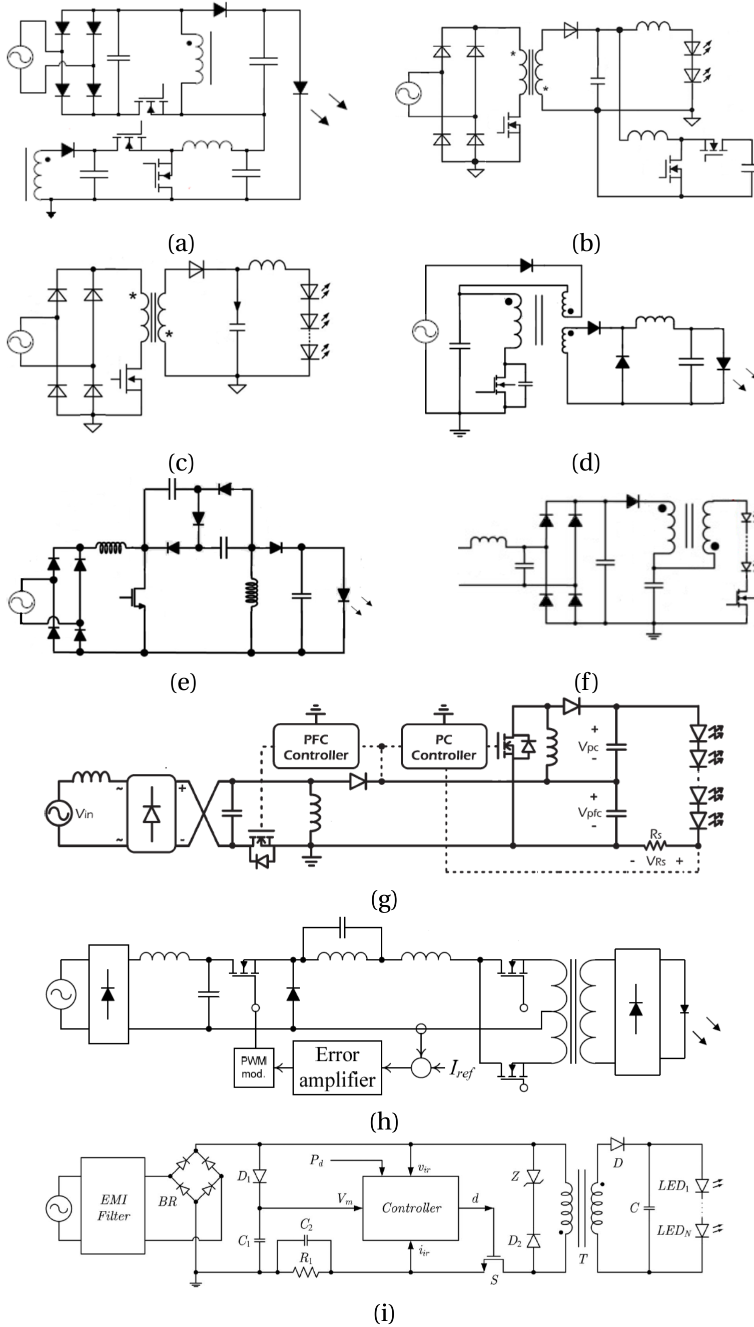

Figure 1.4: Electrolytic Capacitor-Free Technologies: (a) Buck-boost driver with ripple cancellation converter; (b) Fly-back driver with bi-directional converter; (c) Fly-back driver with LC filter; (d) Isolated AC-DC forward driver; (e) Valley-fill SEPIC driver with derived PFC (f) Pulsating current driver; (g) Optimized cascade driver; (h) Buck driver with current-fed inverter. (i) Fly-back driver with harmonic injection

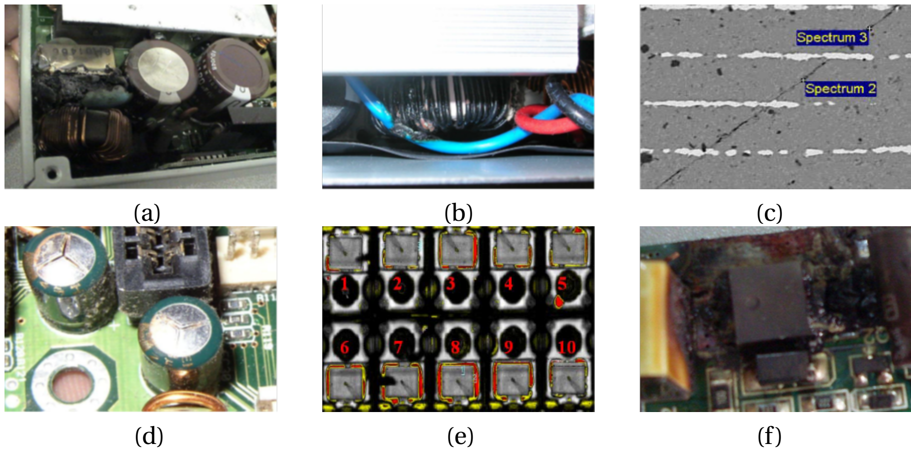

Figure 1.5: Component failures of the LED drivers: (a) Burn of Film Capacitor; (b) Burn of Inductor; (c) Crack of Ceramic Capacitor; (d) Breakdown of Electrolytic Capacitor; (e) Delamination of MOSFET; (f) Breakdown of MOSFET.

In recent years, several system-level reliability prediction methods have been developed. For example, a Markov Chain based reliability evaluation method has been developed for conventional and interleaved boost drivers [89]. The multi-physics reliability simulation has been applied to semiconductor devices in LED drivers [90, 91]. A tolerance design method has been integrated with the distribution models at each time point, degradation path models over time and SPICE simulations [92]. The particle filter technology has been used for lifetime determination of linear LED drivers [93]. An accelerated test method has been developed for outdoor LED drivers by the author which will be explained in Appendix A [94, 95].

1.3. RELIABILITY INTERACTIONS BETWEEN LED LAMPS AND DRIVERS

WHEN LED's lifetime and its driver's lifetime are far away from each other, the LED lamp's lifetime is governed by the shorter one. In other words, the "interaction" of reliability between LED and driver is insignificant. However, in the case that the LED light source and the driver have comparable lifetimes, the interaction of reliability between LED light source and LED driver must be considered [96–99]. The LED light source degrades gradually over a long period. During the degradation of LED light source, its efficacy is reduced, thus, more heat dissipation is expected. On the other hand, when the driver degrades, the output current to the LED light source will decrease over time. Such

a process will affect the heat generations of both driver and LEDs. For an integrated lamp, where the LED light source and driver are assembled together, the heat generated by LEDs and the driver will determine the junction temperature of the LED light source as well as the driver's temperature. Such temperatures continuously change over time since LED heat dissipation depends on time, temperature, and current from the driver. In the meantime, the driver's performance is also dependent on time and temperature. Ultimately the LED's lumen flux depreciation is affected by the degradations of both LED drivers and LED light source. Such a process will be even more complicated when driver's catastrophic failure modes are considered.

1.4. OBJECTIVES AND OUTLINES

AIMING at the problems discussed above, this work focuses on the four topics:

1. ***Reliability prediction for electrolytic capacitors in LED drivers***[70]. The temperature of electrolytic capacitors in LED drivers continuously increases under operation conditions. Thus, the capacitors degrade faster than that with constant temperature assumption. In this research, a physics-of-failure (PoF) based reliability prediction methodology is developed for LED drivers to consider the temperature change of electrolytic capacitor. SPICE simulation, compact thermal modeling, and Monte Carlo simulation are integrated to predict the failure rate distribution of an electrolytic capacitor of given LED driver systems.

2. ***Coupling effect of LED and driver's degradations on LED lamp's lifetime***[75]. In this research, an integrated LED lamp with an electrolytic capacitor-free driver is considered, in which the LED light source and driver have comparable lifetimes. Electronic-thermal simulation is carried out to simulate the lamp's lifetime by considering the interactions between LED and driver.

3. ***Interaction of LED driver's catastrophic failure and LED degradation***[100]. In this research, the LED driver's mean time to failure (MTTF) and the LED's lifetime in term of lumen maintenance are investigated by considering both driver's power MOSFET and diode's catastrophic failure and LED's degradation. Two distinct operation modes: constant current mode (CCM), and constant optical output (CLO) mode, are studied.

4. ***Effect of LED's stochastic lumen degradation on LED driver's reliability***[101]. In this research, the statistical property of LED's lumen depreciation is taken into consideration to study the effect on LED driver's reliability by using the Wiener

process. The reliability calculation is based on the Markov model of the LED driver. Thermal compact model is developed for an integrated lamp with a quasi-resonance driver.

Every topic will be introduced respectively by a chapter: Chapter 2 introduces the PoF based reliability prediction methodology for electrolytic capacitors of the given LED driver systems. Chapter 3 studies the impact of the interaction between the degradations of LED light source and driver on lumen depreciation. Chapter 4 investigates the LED driver's MTTF and the LED's lifetime in term of lumen maintenance. Chapter 5 discusses the influence of statistical property of lumen depreciation on the driver's reliability. Finally, Chapter 6 concludes the entire work and gives recommendations to future works.

REFERENCES

[1] W. D. van Driel and X. J. Fan, *Solid state lighting reliability: components to systems* (Springer Science & Business Media, 2012).

[2] *LED luminaire lifetime: recommendations for testing and reporting, Third Edition* (Department of Energy (DoE), United States, 2014).

[3] J. Huang, D. S. Golubović, S. W. Koh, D. Yang, X. Li, X. J. Fan, and G. Q. Zhang, *Degradation modeling of mid-power white-light LEDs by using wiener process,* Optics Express **23**, A966 (2015).

[4] G. Lu, W. D. van Driel, X. J. Fan, M. Y. Mehr, J. Fan, K. Jansen, and G. Q. Zhang, *Degradation of microcellular PET reflective materials used in LED-based products,* Optical Materials **49**, 79 (2015).

[5] J. Huang, D. S. Golubovic, S. Koh, D. Yang, X. Li, X. J. Fan, and G. Q. Zhang, *Degradation mechanisms of mid-power white-light LEDs under high-temperature-humidity conditions,* IEEE Transactions on Device and Materials Reliability **15**, 220 (2015).

[6] C. Qian, X. J. Fan, J. Fan, C. Yuan, and G. Q. Zhang, *An accelerated test method of luminous flux depreciation for LED luminaires and lamps,* Reliability Engineering & System Safety **147**, 84 (2016).

[7] J. Fan, K. C. Yunga, and M. Pecht, *Prognostics of lumen maintenance for high power white light emitting diodes using a nonlinear filter-based approach,* Reliability Engineering and System Safety (2013).

[8] X. Qu, H. Wang, X. Zhan, F. Blaabjerg, and H. S. H. Chung, *A lifetime prediction method for LEDs considering real mission profiles,* IEEE Transactions on Power Electronics **PP**, 1 (2016).

[9] Y. John Bullough, N. Narendran, and J. Taylor, *LED Life for General Lighting, Vol.1* (Alliance for Solid-State Illumination Systems and Technologies (ASSIST), 2005).

[10] M. H. Chang, D. Das, P. Varde, and M. Pecht, *Light emitting diodes reliability review,* Microelectronics Reliability **52**, 762 (2012).

[11] M. Dal Lago, M. Meneghini, N. Trivellin, G. Mura, M. Vanzi, G. Meneghesso, and E. Zanoni, *Phosphors for LED-based light sources: Thermal properties and reliability issues,* Microelectronics Reliability **52**, 2164–2167 (2012).

[12] B. Hamon, B. Bataillou, A. Gasse, and G. Feuillet, *N-contacts degradation analysis of white flip chip LEDs during reliability tests,* in *2014 IEEE International Reliability Physics Symposium* (IEEE).

[13] E. F. Schubert, T. Gessmann, and J. K. Kim, *Light emitting diodes* (Wiley Online Library, 2005).

[14] D. S. Meyaard, Q. Shan, J. Cho, E. F. Schubert, S. H. Han, M. H. Kim, C. Sone, S. J. Oh, and J. K. Kim, *Temperature dependent efficiency droop in gainn light-emitting diodes with different current densities,* Applied Physics Letters (2012).

[15] J. Piprek, *Efficiency droop in nitride-based light-emitting diodes,* physica status solidi (a) (2010).

[16] J. Huang, D. S. Golubović, S. Koh, D. Yang, X. Li, X. J. Fan, and G. Q. Zhang, *Lumen degradation modeling of white-light LEDs in step stress accelerated degradation test,* Reliability Engineering & System Safety **154**, 152 (2016).

[17] M. Cai, D. Yang, K. Tian, W. Chen, X. Chen, P. Zhang, X. J. Fan, and G. Q. Zhang, *A hybrid prediction method on luminous flux maintenance of high-power LED lamps,* Applied Thermal Engineering **95**, 482 (2016).

[18] J. Huang, D. S. Golubović, S. Koh, D. Yang, X. Li, X. J. Fan, and G. Q. Zhang, *Optical degradation mechanisms of mid-power white-light LEDs in LM-80-08 tests,* Microelectronics Reliability **55**, 2654 (2015).

[19] J. Huang, D. S. Golubović, S. Koh, D. Yang, X. Li, X. J. Fan, and G. Q. Zhang, *Rapid degradation of mid-power white-light LEDs in saturated moisture conditions,* IEEE Transactions on Device and Materials Reliability (2015).

[20] H. T. Chen, Y. F. Cheung, H. W. Choi, S. C. Tan, and S. Y. Hui, *Reduction of thermal resistance and optical power loss using thin-film light-emitting diode (LED) structure,* IEEE Transactions on Industrial Electronics **62**, 6925 (2015).

[21] J. Fan, C. Yu, C. Qian, X. J. Fan, and G. Q. Zhang, *Thermal/luminescence characterization and degradation mechanism analysis on phosphor-converted white LED chip scale packages,* Microelectronics Reliability .

[22] C. Qian, Y. Li, J. Fan, X. J. Fan, J. Fu, L. Zhao, and G. Q. Zhang, *Studies of the light output properties for a gan based blue LED using an electro-optical simulation method,* Microelectronics Reliability (2017).

[23] J. Dong and G. Zhang, *Identification and robust control of the nonlinear photoelectrothermal dynamics of LED systems,* IEEE Transactions on Industrial Electronics **64**, 2215 (2017).

[24] G. Lu, W. van Driel, X. J. Fan, M. Yazdan Mehrb, J. Fan, K. Jansenf, and G. Q. Zhang, *Color shift investigations for LED secondary optical designs: Comparison between bpa-pc and pmma,* Optical Materials (2015).

[25] G. Lu, W. D. V. Driel, X. J. Fan, M. Y. Mehr, J. Fan, C. Qian, K. M. B. Jansen, and G. Q. Zhang, *Colour shift and mechanism investigation on the pmma diffuser used in LED-based luminaires,* Optical Materials **54**, 282 (2016).

[26] *LM-80-2008 Approved Method for Measuring Lumen Maintenance of LED Light Sources* (Illuminating Engineering Society, 2008).

[27] *TM-21-2011 Projecting Long Term Lumen Maintenance of LED Light Sources* (Illuminating Engineering Society, 2011).

[28] S. Koh, C. Yuan, B. Sun, B. Li, X. J. Fan, and G. Q. Zhang, *Product level accelerated lifetime test for indoor LED luminaires,* in *2013 14th International Conference on Thermal, Mechanical and Multi-Physics Simulation and Experiments in Microelectronics and Microsystems (EuroSimE)* (IEEE, 2013).

[29] *CSA-020-2013 Accelerating depreciation test method for LED lighting products* (China Solid State Lighting Alliance, 2013).

[30] *GB-T-33720-2017 Accelerating depreciation test method for LED lighting products* (Standardization Administration of China, 2017).

[31] H. Hao, C. Su, and C. Li, *LED lighting system reliability modeling and inference via random effects gamma process and copula function,* International Journal of Photoenergy (2015).

[32] *MIL-HDBK-217F: Reliability Prediction of Electronic Equipment* (Department of Defense (DoD), United States, 1995).

[33] J. Fan, C. Qian, K. C. Yung, X. J. Fan, G. Q. Zhang, and M. Pecht, *Optimal design of life testing for high-brightness white LEDs using the six sigma DMAIC approach,* IEEE Transactions on Device and Materials Reliability (2015).

[34] *Hammer Testing Findings for Solid-State Lighting Luminaires* (Department of Energy (DoE), United States, 2013).

[35] P. Lall, P. Sakalaukus, and L. Davis, *Reliability and failure modes of solid-state lighting electrical drivers subjected to accelerated aging,* IEEE Access **3**, 531 (2015).

[36] S. Y. Hui, S. N. Li, X. H. Tao, W. Chen, and W. M. Ng, *A novel passive offline LED driver with long lifetime,* IEEE Transactions on Power Electronics, **25**, 2665 (2010).

[37] H. Ma, J.-S. J. Lai, C. Zheng, and P. Sun, *A high-efficiency quasi-single-stage bridge-less electrolytic capacitor-free high-power AC-DC driver for supplying multiple LED strings in parallel,* IEEE Transactions on Power Electronics **31**, 5825 (2016).

[38] H. Ma, J. S. Lai, Q. Feng, W. Yu, C. Zheng, and Z. Zhao, *A novel valley-fill SEPIC-derived power supply without electrolytic capacitor for LED lighting application,* Power Electronics, IEEE Transactions on **27**, 3057 (2012).

[39] H. Valipour, G. Rezazadeh, and M. R. Zolghadri, *Flicker-free electrolytic capacitor-less universal input offline LED driver with PFC,* IEEE Transactions on Power Electronics **31**, 6553 (2016).

[40] D. Camponogara, D. Ribeiro Vargas, M. Dalla Costa, J. M. Alonso, J. Garcia, and T. Marchesan, *Capacitance reduction with an optimized converter connection applied to LED drivers,* IEEE Transactions on Industrial Electronics (2015).

[41] Y. Yang, X. Ruan, L. Zhang, J. He, and Z. Ye, *Feed-forward scheme for an electrolytic capacitor-less AC/DC LED driver to reduce output current ripple,* IEEE Transactions on Power Electronics **29**, 5508 (2014).

[42] S. Wang, X. Ruan, K. Yao, S. C. Tan, Y. Yang, and Z. Ye, *A flicker-free electrolytic capacitor-less AC-DC LED driver,* Power Electronics, IEEE Transactions on **27**, 4540 (2012).

[43] W. Chen and S. Y. R. Hui, *Elimination of an electrolytic capacitor in AC/DC light-emitting diode (LED) driver with high input power factor and constant output current,* Power Electronics, IEEE Transactions on **27**, 1598 (2012).

[44] S. Dietrich, S. Strache, R. Wunderlich, and S. Heinen, *Get the LED out: Experimental validation of a capacitor-free single-inductor, multiple-output LED driver topology,* Industrial Electronics Magazine, IEEE **9**, 24 (2015).

[45] P. Fang and Y. F. Liu, *An electrolytic capacitor-free single stage buck-boost LED driver and its integrated solution,* in *2014 IEEE Applied Power Electronics Conference and Exposition - APEC 2014* (IEEE, 2014) pp. 1394–1401.

[46] Y. Wang, J. M. Alonso, and X. Ruan, *A review of LED drivers and related technologies,* IEEE Transactions on Industrial Electronics **PP**, 1 (2017).

[47] B. Williams, *Switched-mode power supplies,* in *Power Electronics* (Springer, 1987) pp. 309–329.

[48] R. W. Erickson and D. Maksimovic, *Fundamentals of power electronics* (Springer Science & Business Media, 2007).

[49] N. Mohan and T. M. Undeland, *Power electronics: converters, applications, and design* (John Wiley & Sons, 2007).

[50] K. H. Billings, *Switchmode power supply handbook* (McGraw-Hill Professional, 1999).

[51] B. K. Bose, *The past, present, and future of power electronics [guest introduction],* IEEE Industrial Electronics Magazine **3**, 7 (2009).

[52] K. Sheng, B. W. Williams, and S. J. Finney, *A review of IGBT models,* IEEE transactions on Power Electronics **15**, 1250 (2000).

[53] S. Oktyabrsky and D. Y. Peide, *Fundamentals of III-V semiconductor MOSFETs* (Springer, 2010).

[54] I. Angelov, H. Zirath, and N. Rosman, *A new empirical nonlinear model for HEMT and MESFET devices,* IEEE Transactions on Microwave Theory and Techniques **40**, 2258 (1992).

[55] K. Liu and F. C. Lee, *Zero-voltage switching technique in DC/DC converters,* IEEE transactions on power electronics **5**, 293 (1990).

[56] J. G. Cho, J. A. Sabate, G. Hua, and F. C. Lee, *Zero-voltage and zero-current-switching full bridge PWM converter for high-power applications,* IEEE transactions on power electronics **11**, 622 (1996).

[57] X. Qu, S. C. Wong, and C. K. Tse, *Resonance-assisted buck converter for offline driving of power LED replacement lamps,* Power Electronics, IEEE Transactions on **26**, 532 (2011).

[58] F. C. Lee, *High-frequency quasi-resonant converter technologies,* Proceedings of the IEEE **76**, 377 (1988).

[59] V. Vlatkovic, J. A. Sabate, R. B. Ridley, F. C. Lee, and B. H. Cho, *Small-signal analysis of the phase-shifted PWM converter,* IEEE Transactions on power Electronics **7**, 128 (1992).

[60] A. Lazaro, A. Barrado, M. Sanz, V. Salas, and E. Olias, *New power factor correction AC-DC converter with reduced storage capacitor voltage,* Industrial Electronics, IEEE Transactions on **54**, 384 (2007).

[61] J. C. Lam and P. K. Jain, *A high power factor, electrolytic capacitor-less AC-input LED driver topology with high frequency pulsating output current,* IEEE Transactions on Power Electronics (2015).

[62] L. Gu, X. Ruan, M. Xu, and K. Yao, *Means of eliminating electrolytic capacitor in AC/DC power supplies for LED lightings,* IEEE Transactions on Power Electronics (2009).

[63] B. Wang, X. Ruan, K. Yao, and M. Xu, *A method of reducing the peak-to-average ratio of LED current for electrolytic capacitor-less AC-DC drivers,* Power Electronics, IEEE Transactions on **25**, 592 (2010).

[64] X. Ruan, B. Wang, K. Yao, and S. Wang, *Optimum injected current harmonics to minimize peak-to-average ratio of LED current for electrolytic capacitor-less AC–DC drivers,* IEEE Transactions on Power Electronics (2011).

[65] G. G. Pereira, M. A. D. Costa, J. M. Alonso, M. F. de Melo, and C. H. Barriquello, *LED driver based on input current shaper without electrolytic capacitor,* IEEE Transactions on Industrial Electronics **PP**, 1 (2017).

[66] Philips, *Constant Light Output (CLO)* (2014).

[67] A. Pandharipande and D. Caicedo, *Daylight integrated illumination control of LED systems based on enhanced presence sensing,* Energy and Buildings **43**, 944 (2011).

[68] A. T. Lee, H. Chen, S. C. Tan, and S. R. Hui, *Precise dimming and color control of LED systems based on color mixing,* IEEE Transactions on Power Electronics **31**, 65 (2016).

[69] C. C. Sun, I. Moreno, Y. C. Lo, B. C. Chiu, and W. T. Chien, *Collimating lamp with well color mixing of red/green/blue LEDs,* Optics express **20**, A75 (2012).

[70] B. Sun, X. J. Fan, C. Qian, and G. Q. Zhang, *PoF-simulation-assisted reliability prediction for electrolytic capacitor in LED drivers,* IEEE Transactions on Industrial Electronics **63**, 6726 (2016).

[71] B. Sun, X. J. Fan, C. Yuan, C. Qian, and G. Q. Zhang, *A degradation model of aluminum electrolytic capacitors for LED drivers,* in *Thermal, Mechanical and Multi-Physics Simulation and Experiments in Microelectronics and Microsystems (EuroSimE), 2015 16th International Conference on* (IEEE, 2015) pp. 1–4.

[72] P. S. Almeida, D. Camponogara, M. D. Costa, H. Braga, and J. M. Alonso, *Matching LED and driver life spans: A review of different techniques,* Industrial Electronics Magazine, IEEE **9**, 36 (2015).

[73] C. Branas, F. J. Azcondo, and J. M. Alonso, *Solid-state lighting: a system review,* Industrial Electronics Magazine, IEEE **7**, 6 (2013).

[74] Y. M. Chen, H. C. Wu, M. W. Chou, and K. Y. Lee, *Online failure prediction of the electrolytic capacitor for LC filter of switching-mode power converters,* Industrial Electronics, IEEE Transactions on **55**, 400 (2008).

[75] B. Sun, X. Fan, W. van Driel, H. Ye, J. Fan, C. Qian, and G. Zhang, *A novel lifetime prediction for integrated LED lamps by electronic-thermal simulation,* Reliability Engineering & System Safety, Accepted **163**, 14 (2017).

[76] K. Abdennadher, P. Venet, G. Rojat, J. M. Retif, and C. Rosset, *A real-time predictive-maintenance system of aluminum electrolytic capacitors used in uninterrupted power supplies,* Industry Applications, IEEE Transactions on **46**, 1644 (2010).

[77] Y. Zhou, X. Ye, and G. Zhai, *Degradation model and maintenance strategy of the electrolytic capacitors for electronics applications,* in *2011 Prognostics and System Health Managment Confernece* (IEEE, 2011) pp. 1–6.

[78] A. Lahyani, P. Venet, G. Grellet, and P. J. Viverge, *Failure prediction of electrolytic capacitors during operation of a switchmode power supply,* Power Electronics, IEEE Transactions on **13**, 1199 (1998).

[79] M. L. Gasperi, *Life prediction modeling of bus capacitors in AC variable-frequency drives,* Industry Applications, IEEE Transactions on **41**, 1430 (2005).

[80] L. Han and N. Narendran, *An accelerated test method for predicting the useful life of an LED driver,* Power Electronics, IEEE Transactions on **26**, 2249 (2011).

[81] S. Gandhi, M. R. Pulugurtha, H. Sharma, P. Chakraborti, and R. R. Tummala, *High-k thin-film capacitors with conducting oxide electrodes on glass substrates for power-supply applications,* IEEE Transactions on Components, Packaging and Manufacturing Technology **6**, 1561 (2016).

[82] X. Xu, A. S. Gurav, P. M. Lessner, and C. A. Randall, *Robust BME class-i MLCCs for harsh-environment applications,* IEEE Transactions on Industrial Electronics **58**, 2636 (2011).

[83] W. Minford, *Accelerated life testing and reliability of high k multilayer ceramic capacitors,* IEEE Transactions on Components, Hybrids, and Manufacturing Technology **5**, 297 (1982).

[84] T. W. Dakin, E. N. Henry, and G. A. Mullen, *Life testing of electronic power transformers-part II,* IEEE Transactions on Electrical Insulation , 13 (1968).

[85] R. Wu, F. Blaabjerg, H. Wang, and M. Liserre, *Overview of catastrophic failures of freewheeling diodes in power electronic circuits,* Microelectronics Reliability **53**, 1788 (2013).

[86] H. Chen and S. Lu, *Fault diagnosis digital method for power transistors in power converters of switched reluctance motors,* IEEE Transactions on Industrial Electronics **60**, 749 (2013).

[87] S. Lan, C. M. Tan, and K. Wu, *Methodology of reliability enhancement for high power LED driver,* Microelectronics Reliability **54**, 1150 (2014).

[88] A. Garcia, N. Warner, N. A. D'Souza, E. Tuncer, L. Nguyen, M. Denison, and J. T. Fong, *Reliability of high-voltage molding compounds: Particle size, curing time, sample thickness, and voltage impact on polarization,* IEEE Transactions on Industrial Electronics **63**, 7104 (2016).

[89] A. Khosroshahi, M. Abapour, and M. Sabahi, *Reliability evaluation of conventional and interleaved DC-DC boost converters,* IEEE Transactions on Power Electronics **30**, 5821 (2015).

[90] S. Tarashioon, W. van Driel, and G. Zhang, *Multi-physics reliability simulation for solid state lighting drivers,* Microelectronics Reliability **54**, 1212 (2014).

[91] S. Tarashioon, A. Baiano, H. van Zeijl, C. Guo, S. Koh, W. van Driel, and G. Zhang, *An approach to "design for reliability" in solid state lighting systems at high temperatures,* Microelectronics Reliability **52**, 783 (2012).

[92] G. Zhai, Y. Zhou, and X. Ye, *A tolerance design method for electronic circuits based on performance degradation,* Quality and Reliability Engineering International **31**, 635 (2015).

[93] S. Lan and C. M. Tan, *Application of particle filter technique for lifetime determination of a LED driver,* IEEE Transactions on Device and Materials Reliability **15**, 163 (2015).

[94] B. Sun, C. A. Yuan, X. J. Fan, S. W. Koh, and G. Q. Zhang, *An accelerated lifetime test method for DC or AC supplied electronic control gear for led modules of outdoor led lighting products,* in *2013 10th China International Forum on Solid State Lighting (ChinaSSL)* (2013) pp. 65–68.

[95] *CSA-029-2015 Accelerated Test Method for DC or AC Supplied Electronic Control Gear for LED Modules of Outdoor Lighting Products* (China Solid State Lighting Alliance, 2015).

[96] S. Lan, C. M. Tan, and K. Wu, *Reliability study of LED driver–a case study of black box testing,* Microelectronics Reliability (2012).

[97] D. Ang and C. Ling, *On the time-dependent degradation of LDD n-MOSFETs under hot-carrier stress,* Microelectronics Reliability **39**, 1311 (1999).

[98] X. Shao, *Research on Reliability Assessment Method of The LED Driver Power Supply,* Thesis (2012).

[99] Z. Yuege, Z. Yi, L. Xiang, and Z. Guofu, *Performance reliability assessment of LED drivers for lighting.* Electric Machines & Control/Dianji Yu Kongzhi Xuebao **18** (2014).

[100] *A reliability prediction for integrated LED lamp with electrolytic capacitor-free driver,* IEEE Transactions on Components, Packaging and Manufacturing Technology **7**, 1081 (2017).

[101] B. Sun, X. J. Fan, C. Q. Chui, and G. Q. Zhang, *A stochastic process based reliability prediction method for LED driver,* Reliability Engineering & System Safety **submitted**.

2

PoF-Simulation-Assisted Reliability Prediction for LED Drivers

The temperature of electrolytic capacitor in LED drivers continuously increases under operation conditions, thus the capacitors degrade faster than that with constant temperature assumption. In this chapter, a physics-of-failure based reliability prediction methodology is developed for LED drivers to consider the temperature change of electrolytic capacitor. SPICE simulation, compact thermal modeling, and Monte Carlo simulation are integrated to predict the failure rate distribution of an electrolytic capacitor of given LED driver systems. The simulation results agree well with the accelerated test results for an RC linear AC-DC converter. Furthermore, a buck-boost DC-DC converter is simulated to understand the degradation behavior of electrolytic capacitor. It has been found that the temperature of an output stage capacitor increases significantly during operation time. The capacitor's performance without taking temperature change into account results in an overestimated driver lifetime by more than 38% for the selected case study.

Parts of this chapter have been published in IEEE Transactions on Industrial Electronics **63(11)**, pp.6726-6735, (2016) [1].

2.1. Introduction

Light emitting diode (LED) has now emerged as a promising technology to replace conventional lighting, such as incandescent bulbs and compact fluorescent lamps, due to its superior energy efficiency, environmental friendliness, and particularly long lifetime (in the range of 25,000 to 100,000 hours) [2–7]. An LED lamp or luminaire is mainly comprised of LED light source, electronic driver and/or control gears, secondary optical parts, and heat dissipation components. Among these components, the LED driver, which provides a DC current to LEDs, is considered as the weakest link in LED lamps or luminaires [2, 3]. It implies the LED driver usually does not have a long enough lifetime to match the lifetime of LEDs. The lifetime prediction of LED drivers thus plays an important role in the reliability design of LED luminaires [3, 8]. Moreover, the reliable lifetime prediction has high potential to reduce the development and material cost and testing time, thus saving the cost of LED lighting products eventually.

Electrolytic capacitors are often used [9–15] in commercial LED drivers. In most of the single- and two-stage mainstream commercial LED drivers, electrolytic capacitors are used as energy storages and buffers [9, 10]. Electrolytic capacitors are also commonly used at the output end of fly-back drivers [11]. Although a number of new technologies, such as resonance-assisted filter [12] and variable on-time control method [13], have been reported that the lifetime of electrolytic capacitors in buck converters can be made comparable to LEDs, the electrolytic capacitor is still considered as the weakest component in LED drivers [16, 17]. In recent years, several electrolytic capacitor-less LED drivers have also been presented to maximize the lifetime of the overall LED system [18–23]. Nevertheless, the applications of electrolytic capacitors in LED drivers remain widespread and dominant in commercial LED luminaires [8, 10–17].

The performance of electrolytic capacitor is complicated and highly affected by its operation conditions such as voltage, current, frequency, and temperature. In addition, the electrolytic capacitor is also affected by its degradation process [16, 24–26]. During degradation, the electrolytic liquid inside capacitor will be evaporated gradually, which will cause the rise of equivalent series resistance (ESR) and the fall of capacitance. Many researchers have investigated the degradation of electrolytic capacitors. For instance, a real-time failure detection method has been developed for the changes of voltage [26], ESR and capacitance [27] of electrolytic capacitors. Lifetime prediction models of electrolytic capacitors have been developed for switch mode power supply [24] and AC variable-frequency drivers [25]. Accelerated life-test method has been developed for LED drivers that use electrolytic capacitors at the output stage [16]. The ingress of moisture into the aluminum electrolytic capacitor in LED drivers has been studied to assess

the reliability in harsh environment applications [17]. However, in above mentioned models and accelerated tests, electrolytic capacitors are usually assumed at a constant temperature under operation condition. There is little systematic research on reliability prediction of electrolytic capacitors at a continually changing temperature condition during operation.

The capacitance and ESR of an electrolytic capacitor change continually during operation due to degradation. This will alter the power consumption in driver system. As a consequence, the capacitor temperature will continually increase, thus, will degrade faster than that at a constant temperature condition assumption [27, 28]. To consider the temperature change during degradation, this chapter develops a Physics of Failure (PoF) approach that integrates SPICE simulation, thermal modeling and Monte Carlo simulation. For a given driver circuit, the prediction begins with a circuit simulation to obtain power consumption of an electrolytic capacitor. A thermal simulation is performed to obtain capacitor temperature [29, 30]. As capacitor further degrades, capacitance falls and ESR rises. This leads to circuit performance change. Therefore, electronic simulation needs to be updated, which will change the capacitor's temperature. The interactions among capacitor degradation, temperature rise, and the circuit behavior can be adequately simulated by an iteration process. The end of the lifetime can be obtained from the iterated simulation. The Monte Carlo simulation is then performed to obtain the probability of failure.

An RC linear AC-DC converter is used for an accelerated test to verify the simulation results. A buck-boost LED driver is applied as an example for the detailed results and discussions. The chapter is organized as follows. Section 2.2 explains an overview of the proposed methodology; Section 2.3 describes the theory of each model, including SPICE model, thermal model, degradation model and Monte Carlo method. In Section 2.4, the parameters of electrolytic capacitor degradation model used in the chapter are determined experimentally. The experimental results of the accelerated test on an RC linear converter and the validation of the proposed prediction methodology are presented in Section 2.5. Section 2.6 discusses the results of a case study for a buck-boost converter. Section 2.7 concludes this work finally.

2.2. METHODOLOGY

THIS work proposes a hybrid, building-block approach that relies on combining PoF simulations with a statistical approach for lifetime prediction. Figure 2.1 illustrates the building blocks of the proposed methodology for lifetime prediction of an electronic

component in a system. As such a methodology is not limited to study the reliability of an electrolytic capacitor, the term "component" is used to represent any component in interest (electrolytic capacitor, for instance). The proposed method is also not limited to LED driver only.

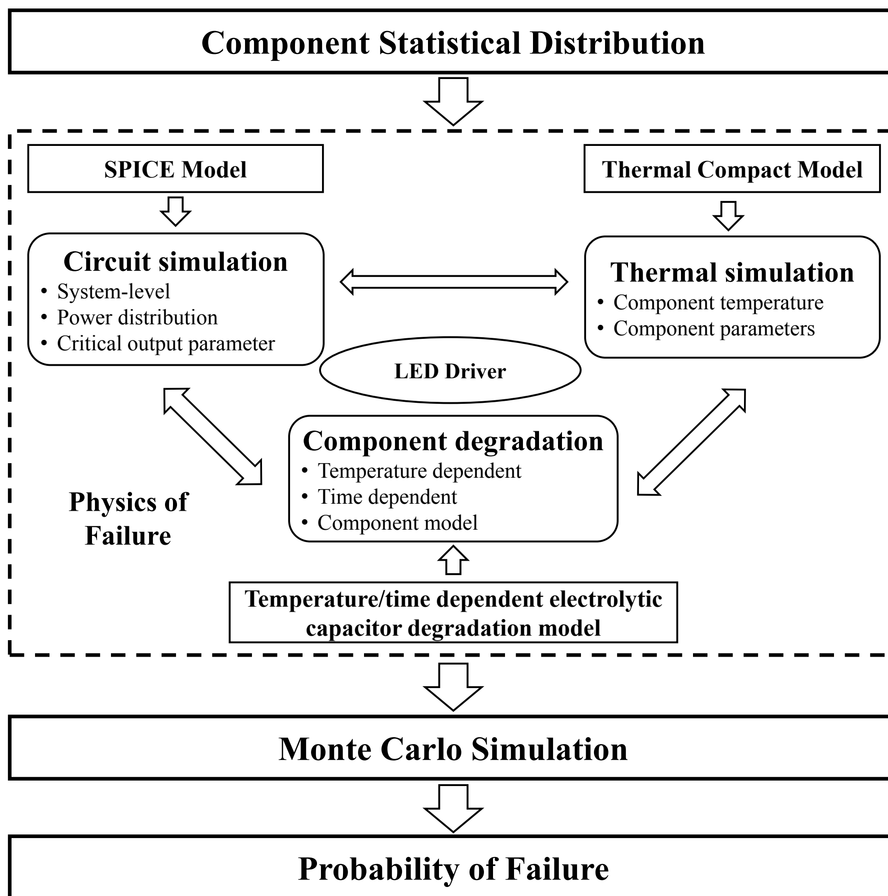

Figure 2.1: Building Blocks for Combining PoF-based Modeling and Empirical-Statistical Approaches for Reliability Prediction for LED Driver System.

For a given electronic system, circuit simulation is carried out to obtain power distributions and output parameters such as output current and voltage. Thermal simulations are preformed based on power distribution to obtain the temperature distributions of the component. Since circuit simulation requires component's parameters, such as ESR and capacitance, which are dependent on temperature and time due to degradation, thermal and electronic simulations are coupled through capacitor's degradation

models, and therefore, iteration process among electronic and thermal simulation is required, as shown in Figure 2.1. Then Monte Carlo simulation can be applied to obtain the probability of failure.

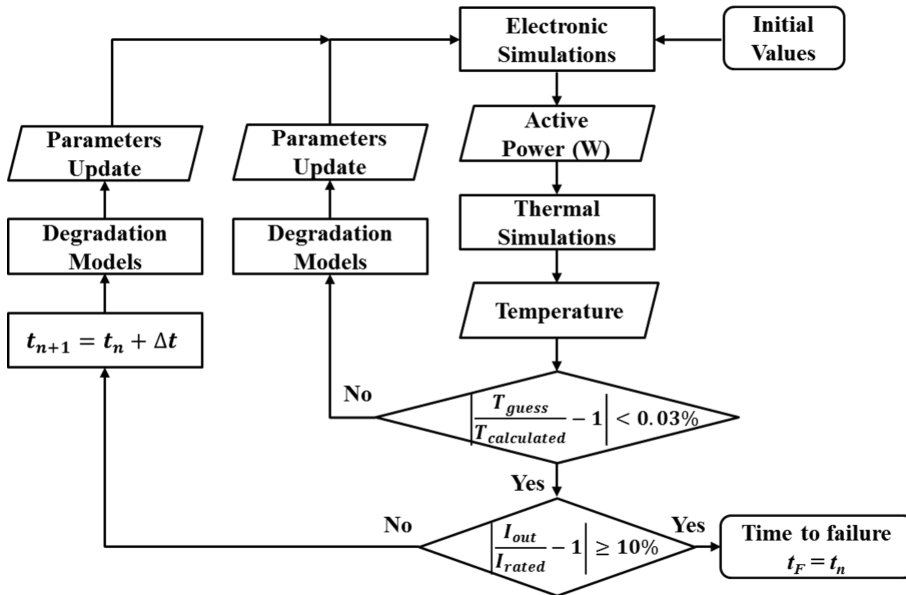

Figure 2.2: Flowchart of the Iteration Process in Circuit-Thermal Simulation.

Figure 2.2 displays the flowchart of iteration processes in the electronic-thermal simulation. At time zero, since capacitor's initial temperature (during operation) is not known, an initial guess is needed for initial ESR and initial capacitance for electronic simulations. An iteration process is not complete until the guess temperature is within the allowed error range compared to the calculated temperature from thermal simulations. The temperature difference between the guessed temperature and calculated temperature less than 0.03% of the calculated temperature is used as convergence criterion in the present study. Once the iteration process is complete between electronic and thermal simulation at time t, the final output parameter, such as output current, can be obtained at the time t. Based on the selected failure criterion (110% rated output current, for instance), if the output current is within the specified value, then simulations advance to next time step. The present study uses 5% of the total investigated time as time increment to advance to next time step. For example, if the lifetime is expected to be 10000 hours, the time increment 500 hours (t in Figure 2.2) is used. At the time $t + \Delta t$, the ESR and capacitance are functions of time and temperature, and must be updated. Since temperature is not known, the new iteration process is needed. When time

$t = t_F$, and the output current exceeds the specified value, the simulation stops, and t_F is considered as the lifetime of the component.

Given the statistical distribution nature of component parameters, shown on the top block in Figure 2.1, the iteration process is needed each time for a given set of parameters, and based on Monte Carlo method, the cumulative failure rate and the predicted mean time to failure (MTTF) of the component can be obtained finally.

2.3. Modelling

2.3.1. Circuit Simulation

A single inductor buck-boost DC-DC converter shown in Figure 2.3 is selected in the present study. This type of driver is one of the most commonly used drivers that can achieve high efficiency, wide output voltage range, and low distortion of line current with a simple topology in LED applications[31]. The electrolytic capacitor C4 at output stage is considered critical[16], and its degradation behavior is investigated in the present study. Other failure modes, such as MOSFET failure and power diode breakdown, are not considered. The operating conditions of LED driver are as follows: switching frequency is 300 kHz, input voltage range is 9-20 Vdc, rated output current is 380 mA, the duty cycle is 25%, and the maximum power is 5.0W. The circuit simulation is performed by the LTSPICE software. Device models in LTSPICE are provided from virtual testing of commercial driver designs by manufacturers. These device models have been widely used in LED-based products and well validated. The error of circuit simulation is less than 2% in terms of output current against experimental results[32].

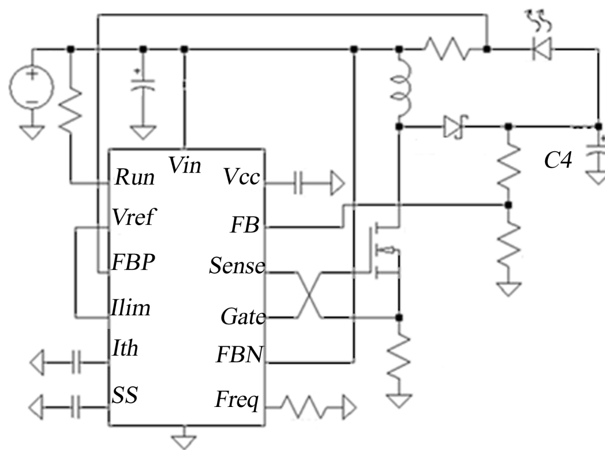

Figure 2.3: Single Inductor Buck-Boost DC-DC Converter [33].

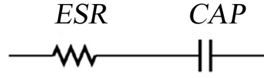

Figure 2.4: Equivalent Circuit of an Electrolytic Capacitor.

As shown in Figure 2.4, the electrolytic capacitor is considered equivalent to an ideal capacitor (CAP) connected in series with a resistor (ESR). An additional equivalent series inductance (ESL) may also be included. However, for the LED driver used in our study, the ESL is very small and can be negligible[26]. As a dominant wear-out mechanism of an electrolytic capacitor is the evaporation and deterioration of electrolyte, the capacitor temperature determines the lifetime of the capacitor.

Different operation load results in variations on current, thermal power and thus the capacitor temperature. The thermal power at time t, $P_{th,C}$, dissipated by electrolytic capacitor can be obtained by the following equation:

$$P_{th,C}(t) = I_{RMS}^2(t) \cdot ESR(T,t) \tag{2.1}$$

where $I_{RMS}(t)$ is the root mean square value of capacitor current at time t and $ESR(T,t)$ is equivalent series resistance of electrolytic capacitors at temperature T and time t.

2.3.2. THERMAL SIMULATION

Temperature distributions on an LED driver system, in principle, can be obtained through system-level computational fluid dynamics (CFD) or finite element analysis (FEA), provided that the power dissipation of each component, the thermal properties of materials, and the geometrical information are known. Since the present study focus on an output stage electrolytic capacitor, a compact thermal model for an electrolytic capacitor is applied. According to previous studies[34], the interactions of the junction temperature of chips within one package are not significant. Thus, board-level thermal dissipation interactions between capacitors and other components may be neglected. As illustrated in Figure 2.5, a simplified compact thermal model, which consists of two thermal resistances, R_{th1} and R_{th2}, respectively, is used for a capacitor. R_{th1} is thermal conduction resistance from core to surface, and R_{th2} is the convective thermal resistance. R_{th1} can be determined from thermal properties of the capacitor and its structure given by manufactures. R_{th2} depends on ambient convective heat transfer condition, and will be calibrated through experiment. The capacitor temperature rise at time t can be calculated

by:

$$\Delta T_{cap}(t) = P_{th,C}(t) \cdot (R_{th1} + R_{th2}) \tag{2.2}$$

where $P_{th,C}(t)$ is the thermal power at time t determined by Equation 2.1.

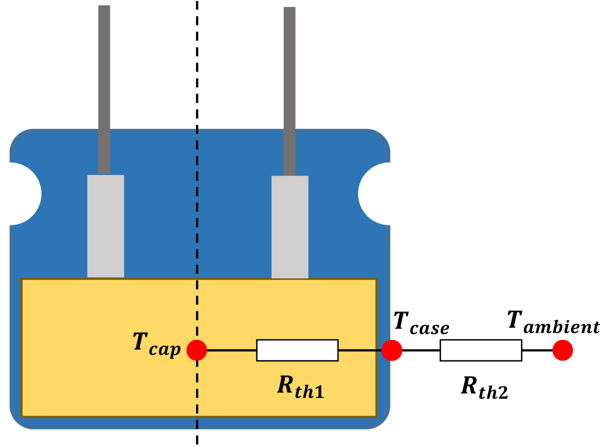

Figure 2.5: Compact Thermal Model of an Electrolytic Capacitor.

2.3.3. Electrolytic Capacitor Degradation Model

The degradation of an electrolytic capacitor is a time, temperature, and also frequency dependent process. Since the operation frequency usually remains unchanged during the aging process, the degradation models are obtained at the specified frequencies. When a constant capacitor temperature is considered, the CAP degrades linearly with time t, whereas the ESR has an exponential relationship with time t [27, 28], as follows:

$$CAP(t) = CAP_T \cdot (1 + A \cdot t) \tag{2.3}$$

$$ESR(t) = ESR_T \cdot e^{C \cdot t} \tag{2.4}$$

where CAP_T and ESR_T are the initial capacitance and ESR, A and C describe temperature-dependent degradation rates. In this work, A and C are assumed to follow the Arrhenius Equation:

$$A(t) = A_0 \cdot e^{-E_{a1}/(\kappa \cdot T)} \tag{2.5}$$

$$C(t) = C_0 \cdot e^{-E_{a2}/(\kappa \cdot T)} \tag{2.6}$$

where A_0 and C_0 are base degradation rates, E_{a1} and E_{a2} are the activation energies, κ is the Boltzmann constant. CAP_T and ESR_T in Equations 2.3 and 2.4 are related to capacitor's geometry and basic material properties [35, 36] as following:

$$CAP_T = \varepsilon_0 \cdot \varepsilon \cdot \frac{A_{cap}}{d} \tag{2.7}$$

$$ESR_T = \frac{d}{A_{cap} \cdot \sigma} \tag{2.8}$$

where A_{cap} is the surface area of the electrolytic capacitor, ε_0 is the absolute permittivity, ε is relative permittivity, d is the average distance, σ is the conductivity. According to the characteristics of permittivity and conductivity [36–38], ε and σ are functions of temperature T:

$$\varepsilon = \varepsilon^{(0)} \cdot e^{B/T} \tag{2.9}$$

$$\sigma = \sigma_A \cdot [1 + D \cdot (T - T_A)] \tag{2.10}$$

where $\sigma^{(0)}$ is basic conductivity, σ_A is conductivity at reference temperature T_A.

If temperature $T(t)$ changes as a function of time, the increment of capacitance and ESR in a period of Δt can be described by:

$$\Delta \frac{CAP[T(t), t]}{CAP_T} = A[T(t)] \cdot \Delta t \tag{2.11}$$

$$ln\Delta \frac{ESR[T(t), t]}{ESR_T} = C[T(t)] \cdot \Delta t \tag{2.12}$$

Thus, from time 0 to time x, the accumulated capacitance and ESR can be described by:

$$\frac{CAP[T(t), x]}{CAP_T} = \sum_0^x \Delta \frac{CAP[T(t), t]}{CAP_T} \tag{2.13}$$

$$\frac{ESR[T(t), x]}{ESR_T} = \sum_0^x \Delta \frac{ESR[T(t), t]}{ESR_T} = ln \prod_0^x \Delta \frac{ESR[T(t), t]}{ESR_T} \tag{2.14}$$

In the integral form, the accumulated capacitance and ESR can be described by:

$$\frac{CAP[T(t), x]}{CAP_T} = \int_0^x A[T(t)] \cdot dt + E \tag{2.15}$$

$$\frac{ESR[T(t), x]}{ESR_T} = e^{\int_0^x C[T(t)] \cdot dt + D} \tag{2.16}$$

The boundary conditions are:

$$CAP[T(0),0] = CAT_T \tag{2.17}$$

$$ESR[T(0),0] = ESR_T \tag{2.18}$$

Thus, $E = 1$ and $D = 0$, as a result:

$$\frac{CAP[T(t),x]}{CAP_T} = \int_0^x A[T(t)] \cdot dt + 1 \tag{2.19}$$

$$\frac{ESR[T(t),x]}{ESR_T} = e^{\int_0^x C[T(t)] \cdot dt} \tag{2.20}$$

Figure 2.6 displays the measured and fitted results of the capacitance and ESR at a temperature of 399K. Similar results are also obtained at other temperatures. It confirms that the CAP follows a linear degradation pattern with time, while ESR can be described by an exponential function of time t. Considering temperature $T(t)$ changes as a function of time t during aging process, the accumulated $CAP[T(t),t_f]$ and $ESR[T(t),t_f]$ from 0 to time t_f can be finally obtained from Equation 2.3 and 2.4 as:

$$CAP[T(t),t_f] = CAP_T \cdot \int_0^{t_f} A[T(t)] \cdot dt + 1 \tag{2.21}$$

$$ESR[T(t),t_f] = ESR_T \cdot e^{\int_0^{t_f} C[T(t)] \cdot dt} \tag{2.22}$$

Combining Equation 2.7, 2.8, 2.9, 2.10, 2.21 and 2.22, when both temperature and time changes during degradation, the accumulated capacitance and ESR can be described as[28]:

$$CAP[T(t),t_f] = CAP_0 \cdot e^{B/T(t_f)} \int_0^{t_f} \{1 + A[T(t)] \cdot dt]\} \tag{2.23}$$

$$ESR[T(t),t_f] = \frac{ESR_0}{1 + D[T(t_f) - T_A]} \cdot e^{\int_0^{t_f} C[T(t)] \cdot dt} \tag{2.24}$$

where the parameters CAP_0, A_0, B, E_{a1} for capacitance and ESR_0, C_0, D, E_{a2} for ESR need to be determined experimentally.

2.3.4. Monte Carlo Simulation

For a given set of parameters, the electronic-thermal simulation provides the definite value of the lifetime. However, the initial values of capacitance and equivalent series resistance usually have certain randomness, leading to a statistical distribution. There-

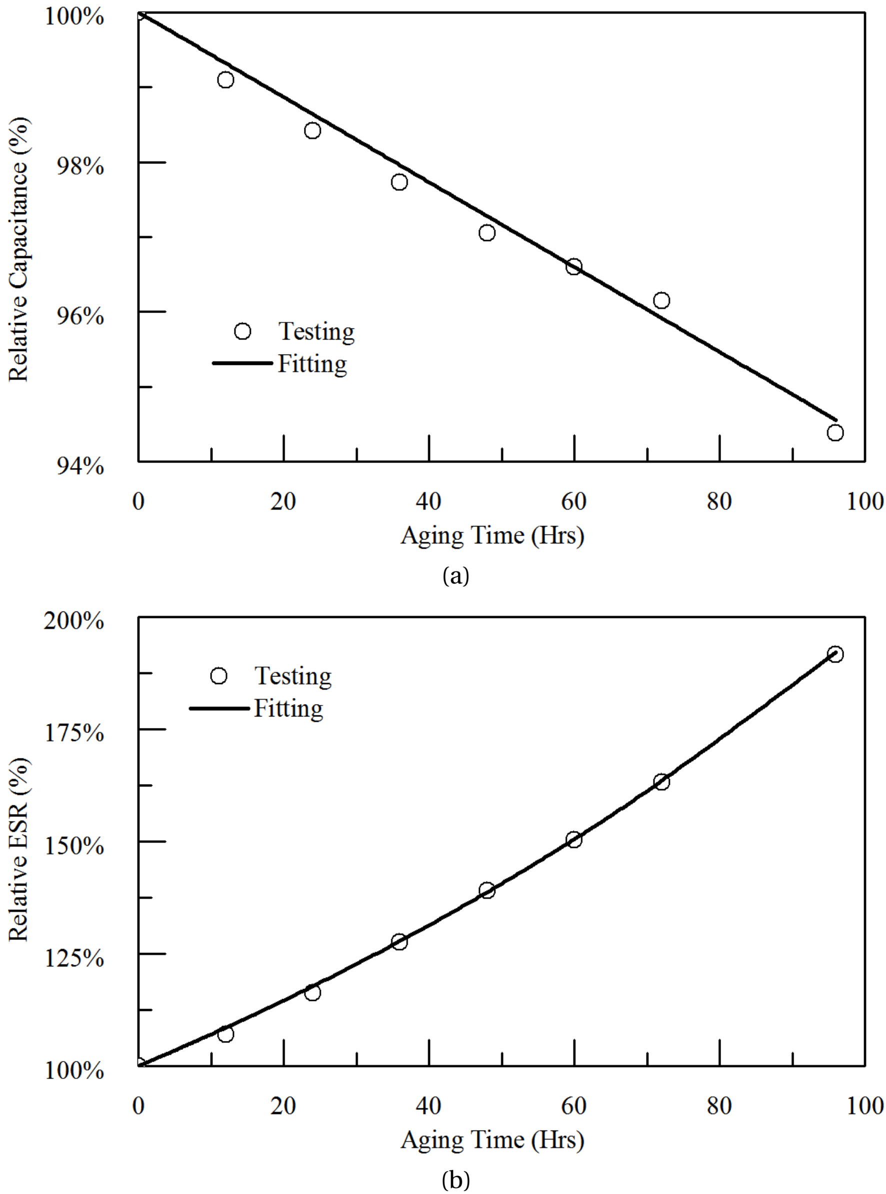

Figure 2.6: (a) Relative Capacitance and (b) ESR of LED.

fore, Monte Carlo simulation is introduced to calculate a complete distribution of failure rate and the predicted mean-time-to-failure (MTTF). In this process, a certain number of parameter combinations are simulated through iterated electronic-thermal simulation.

The probability density functions of CAP and ESR can be expressed as[39]:

$$f_{CAP}(CAP) = \frac{CAP_{mean}}{\sigma_1 \cdot \sqrt{2\pi}} \cdot e^{-(\frac{CAP - CAP_{mean}}{\sqrt{2}\sigma_1})^2} \tag{2.25}$$

$$f_{ESR}(ESR) = \frac{ESR_{mean}}{\sigma_2 \cdot \sqrt{2\pi}} \cdot e^{-(\frac{ESR - ESR_{mean}}{\sqrt{2}\sigma_2})^2} \tag{2.26}$$

where, $f_{CAP}(CAP)$ and $f_{ESR}(ESR)$ are probability density functions; CAP and ESR are random values of capacitance and ESR; CAP_{mean} and ESR_{mean} are mean values of CAP and ESR; σ_1 and σ_2 are standard deviations. The mean values CAP_{mean} and ESR_{mean} and standard deviations σ_1 and σ_2 will be determined experimentally for a given population of samples in Section 2.4. Assuming N times of circuit-thermal simulations with a random combination of CAP and ESR, each case is carried out from beginning to time t, the cumulative failure rate $g(t)$ can be calculated as the frequency of failure occurrence[40]:

$$g(t) = \frac{\text{Number of failures in time } t}{N} \tag{2.27}$$

The cumulative failure rate $g(t)$ is then used for calculation of the Mean Time To Failure (MTTF) t_{MTTF} of the component under study[39]:

$$t_{MTTF} = t_{MAX} - \int_0^{t_{MAX}} g(t) \cdot dt \tag{2.28}$$

where t_{MAX} is total operation time of the whole group of samples.

2.4. Experiments

2.4.1. Test Set-up

Figure 2.7 shows the test set-up to determine the degradation characteristics of a selected type of electrolytic capacitor. A total of 60 samples were used. Four different groups of experiments were carried out for capacitor temperature ranging from 308K to 400K. The case temperature of each capacitor is measured by the thermal couple. From the thermal model, both case temperature and capacitor temperature can be calculated. The measured case temperature will be used to verify the thermal model.

2.4.2. Thermal Model

For thermal model, R_{th1} is obtained from the tested component specification[41] as $0.1R_{th2}$ in convection free condition. To calibrate R_{th2}, a group of samples was tested

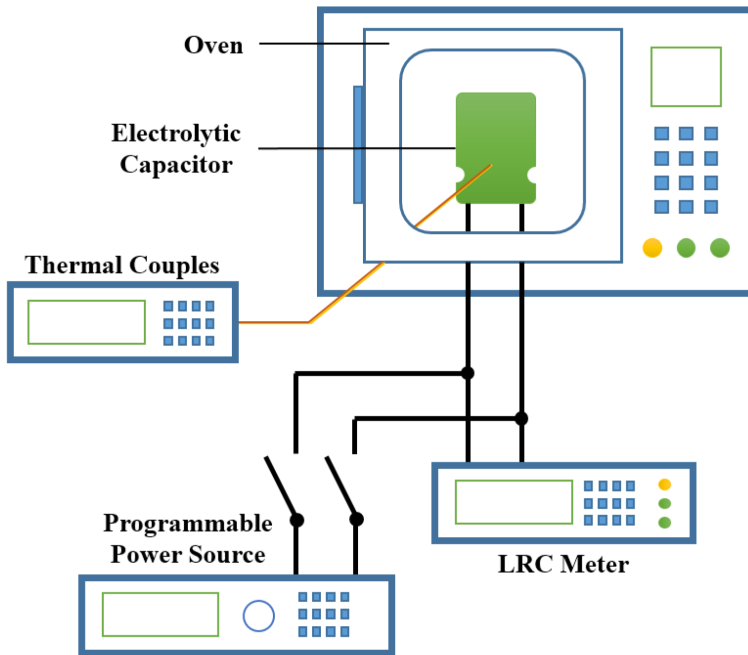

Figure 2.7: Test Set-up for Electrolytic Capacitors.

in an ambient condition of 298K by the test platform shown in Figure 2.7. In this test, samples were placed in a controlled environmental chamber with natural convection only per specification, and various input voltage levels were then applied to generate different thermal powers. The power consumption of each sample can be measured directly by the programmable power source. By adjusting the magnitude of AC input, the thermal power of each sample can be controlled. Then the thermal resistance R_{th2} is calibrated as 161.0 K/W. With the experimentally obtained R_{th1} and R_{th2} values, the calculated case temperature of the capacitor agrees well the experimental data, as shown in Figure 2.8. The maximum error between calculated case temperature by thermal simulation and tested case temperature is less than 5% of the tested value.

2.4.3. ELECTROLYTIC CAPACITOR DEGRADATION MODEL

To obtain the parameters in Equations 2.23 and 2.24, the least square method is applied to fit the experimental data at various temperatures. Table 2.1 and 2.2 summarize the mean values of the eight parameters: CAP_0, ESR_0 E_{a1},E_{a2}, A_0,C_0, B and D. Please note that the initial values of capacitance and ESR depend on frequency, and are given in Table 2.2 separately. The details of experimental data analysis, test procedures, and the

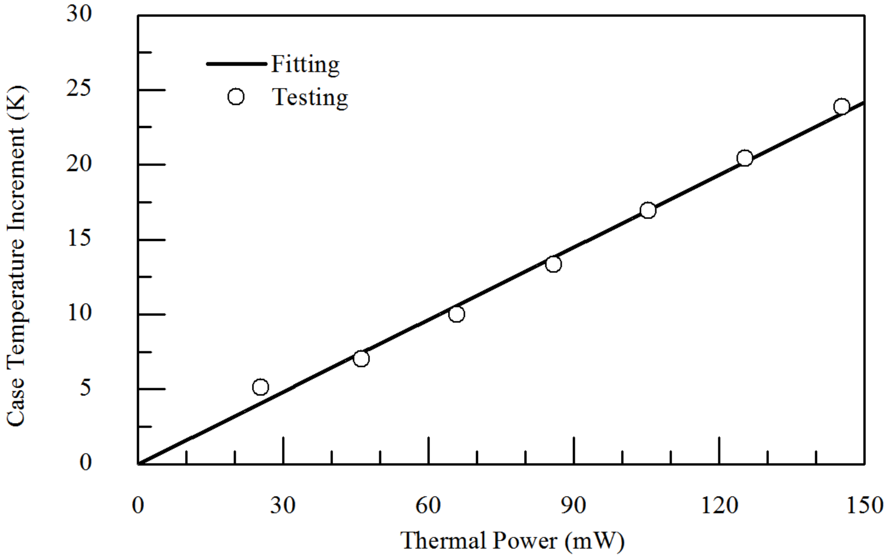

Figure 2.8: Case Temperature Increase vs Thermal Power.

fitting analysis are referred to[28]. The final normalized fitting results agree well with the experimental results, as shown in Figure 2.9. 100Hz frequency will be used for RC linear AC-DC converter, and 300KHz frequency will be used for buck-boost DC-DC converter, to be described in subsequent sections.

Table 2.1: Determined Parameters of the Degradation Models

Symbol	Value	Symbol	Value
E_{a1}	$0.774\ eV$	A_0	-3.46×10^6
B	-1.12×10^2	E_{a2}	$0.700\ eV$
C_0	-4.54×10^6	D	-4.07×10^6

Table 2.2: Intial capacitance and ESR

Frequency (Hz)	CAP_0 Mean (μF)	ESR_0 Mean (Ω)
100	6.31	40.1
300K	5.89	17.2

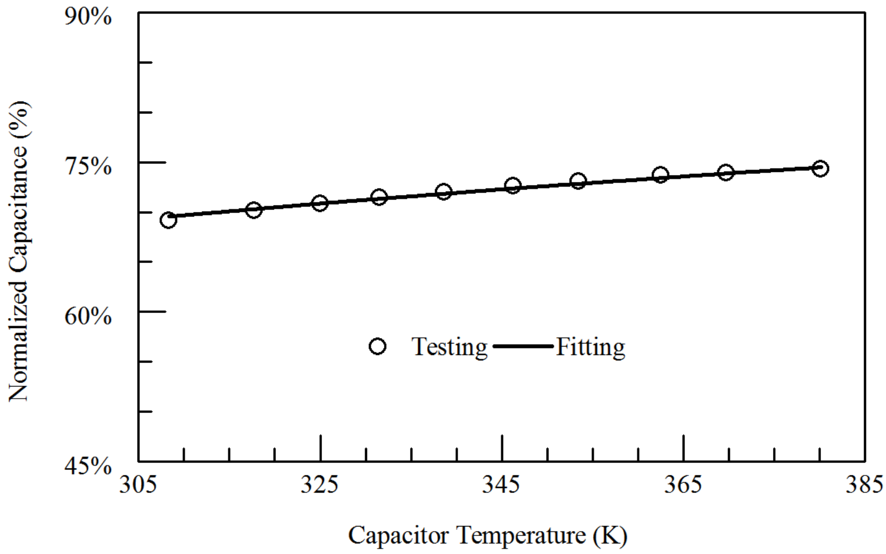

(a)

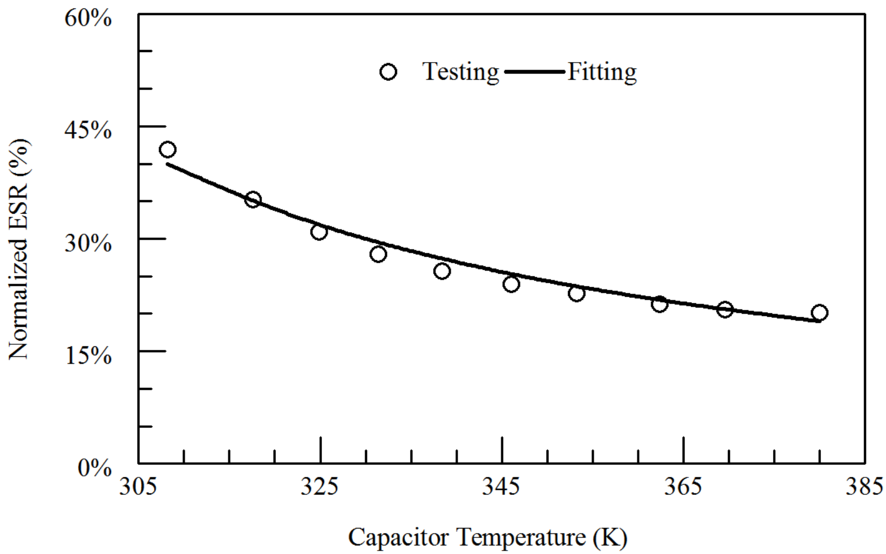

(b)

Figure 2.9: Normalized (a)Capacitance and (b)ESR vs Capacitor Temperature.

2.4.4. MONTE CARLO MODEL

60 additional samples were also used to determine the statistical distributions of the initial values of capacitance and equivalent series resistance. Table 2.3 shows the summary

Table 2.3: Normal Distribution Parameters in Equation 2.25 and 2.26

	Capacitance (μF)	ESR (Ω)
Standard Deviation	2.74×10^{-2}	40.1
P Value	0.275	0.652

of the standard deviation and P values for normality test. The P-value is an indicator of statistics to represent the probability whether the observed sample results follow assumed distribution. $P = 0.05$ is the threshold value for the normality test in statistics. The larger P value, the better the distribution follows the assumed distribution. In Table 2.3, P values of capacitance and ESR are much higher than 0.05, thus normal distribution in Equation 2.25 and 2.26 is confirmed. These values in Table 2.3 will be used in performing Monte Carlo simulations.

2.5. Validation

To validate the proposed prediction method, an accelerated test, which was similar to the test setup in the literature [16], was performed on electrolytic capacitors in an RC linear AC-DC converter as shown in Figure 2.10. This driver is a simplest LED driver in which the failure of the electrolytic capacitor can be conveniently detected during tests. Thus, the degradation of the electrolytic capacitor in an RC linear AC-DC converter directly leads to the degradation of output power which can be conveniently measured. For other drivers such as buck-boost DC-DC converter, they are complicated and contains more components. Accelerated tests may trigger not only the electrolytic capacitor's failure, but also the failures of other components. These failures may complicate the test results.

In the validation test, a total of nine electrolytic capacitors were aged individually at an ambient temperature of 398K. The relative output power of the RC linear driver to a stable LED load was measured as a function of time. Through the simulation, the relative output power can also be obtained as a function of time.

Figure 2.11 and Table 2.4 show the predicted time vs. different power consumption against experiments. These prediction results are in good agreements with the test results. The maximum error between the test and simulation is no larger than 5%. Due to the time limit and lab constraints, the test beyond 300 hours was not carried out. Nevertheless, the ESR of each sample already increased up to more than 300% of its initial

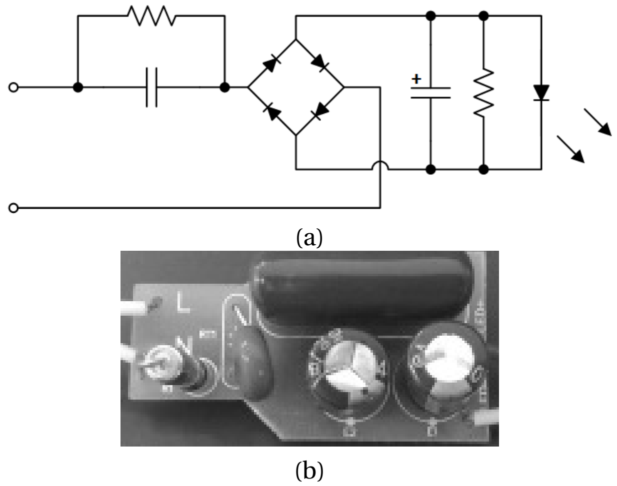

Figure 2.10: (a) Circuit and (b) Layout of the RC Linear AC-DC Converter.

value at 300 hours, and the capacitor is considered near the end of functioning.

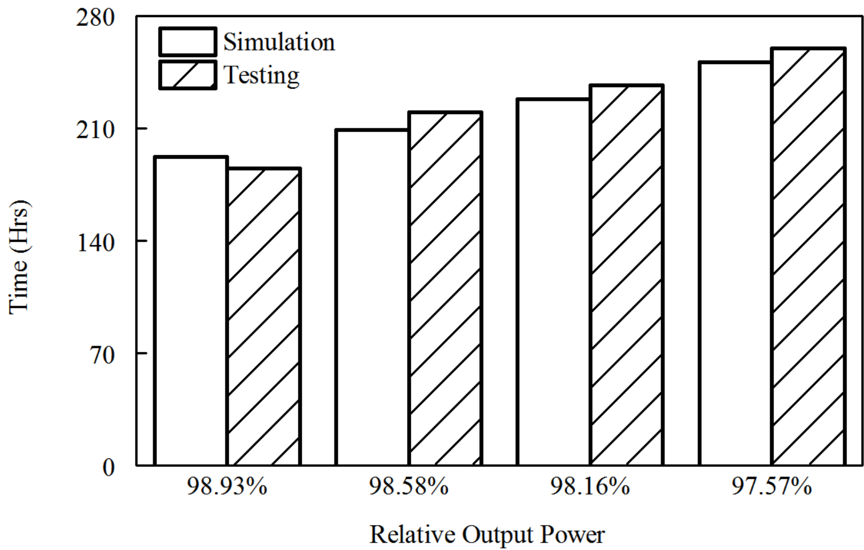

Figure 2.11: The Predicted Time vs. Different Power Consumption.

Table 2.4: The Predicted Time vs. Different Power Consumption

Power Consumption	Predicted Time	Aging Time	Error
98.93%	192 Hrs	185 Hrs	3.78%
98.58%	209 Hrs	220 Hrs	5.00%
98.16%	228 Hrs	237 Hrs	3.80%
97.57%	251 Hrs	260 Hrs	3.46%

2.6. Results and Discussions

In this section, a single inductor buck-boost converter, as shown in Figure 2.3, is simulated to investigate the capacitor C4's degradation behavior. The degradation models described in Table 2.1 and 2.2 are used for study, as well as the distribution models described in Table 2.3. The ambient temperature in the study is supposed as 328K.

Figure 2.12 displays the capacitor temperature rise as a function of time. The upper bound, mean value and the lower bound of temperature are presented based on the distributions from Equation 2.25 and 2.16, as well as Table 2.3. The simulation results clearly show that the capacitor temperature is not constant, but increasing with time during operation condition, due to the aging process. It also appears that the upper bound and lower bound of capacitor temperature distribute symmetrically with respect to the mean value at 0 hour, but such a distribution is no longer symmetric after aging. In Figure 2.12, the simulation ends at 10,000 hours as the output current at 10,000 hours exceeds the rated value by 10% already (see Figure 2.14 next). The failure criterion is defined as within 10% of the rated current increase. The upper bound of capacitor temperature achieves a plateau (not decreasing) in Figure 2.12 is an indication that capacitor's ESR has been increasing exponentially, and the current through capacitor may be decreasing.

Figure 2.13 shows the results of the predicted relative CAP and ESR versus time. The relative CAP and ESR are defined as the ratio of the current value and initial value (time zero). The upper bound, mean value and the lower bound of CAP and ESR are shown in these figures. As a comparison, by assuming a constant capacitor temperature, dashed lines represent the degradation curves without taking capacitor temperature changes into consideration. It shows that the capacitance does not degrade significantly, but ESR increases exponentially. When ESR's value is doubled compared to its initial value, the capacitor is near the end of functioning, and the current in capacitors may be decreasing. From Figure 2.13, it can be seen that the ESR without taking considerations of capacitor temperature change underestimates the rate of degradation.

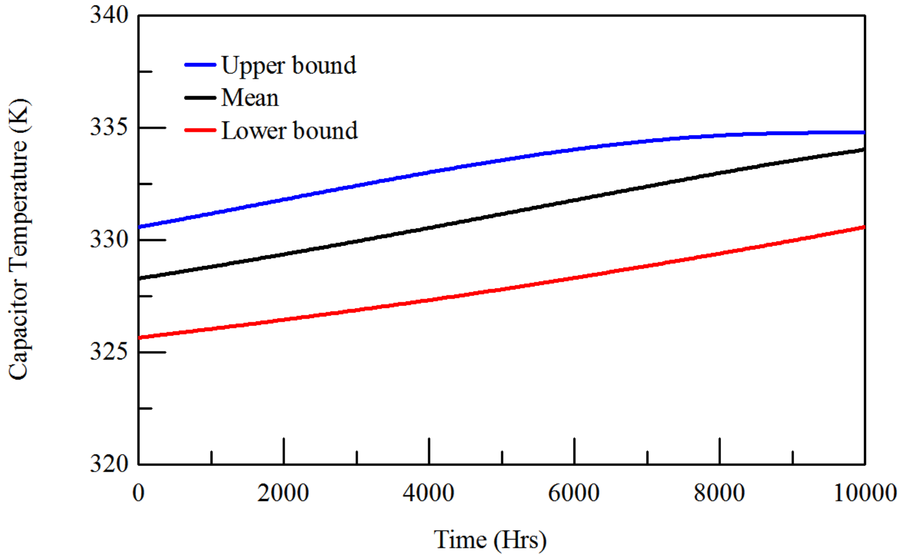

Figure 2.12: Capacitor Temperature in the Buck-Boost Converter.

Figure 2.14 shows the output current and ripple current degradations. In the present study, the output current is defined as the root-mean-square value of LED currents (not capacitor), whereas the ripple current is defined as the peak-to-peak value of LED currents. The mean of output current increases about 20% of its initial value, and the ripple current increases about 82% within 10,000 hours. Meanwhile, the upper and lower bounds of output currents increase about 28% and 11%, and the upper and lower bounds of ripple current increase about 115% and 45% respectively. Such results are consistent with the *ESR* results to imply that the capacitor is degrading significantly. In addition, compared with the output current, the ripple current is more sensitive to degradation. Output current has a significant influence on the optical output of LEDs, such as lumen flux and color temperature.

Finally, the predicted failure rate can be obtained by the Monte Carlo simulation, as shown in Figure 2.15. For comparison, the failure rate curves obtained by constant capacitor temperature analysis (the dash line) and using ambient temperature (328K) as capacitor temperature (the dot line) are also plotted in Figure 2.15. The predicted mean time to failure (MTTF) can then be obtained by Equation 2.28. The MTTFs predicted by the present method, "the constant capacitor temperature" analysis, and "ambient temperature as capacitor temperature" are 5125 hours, 7107 hours and 12565 hours, respectively. In other words, the conventional methods overestimate the MTTF by 38.7%

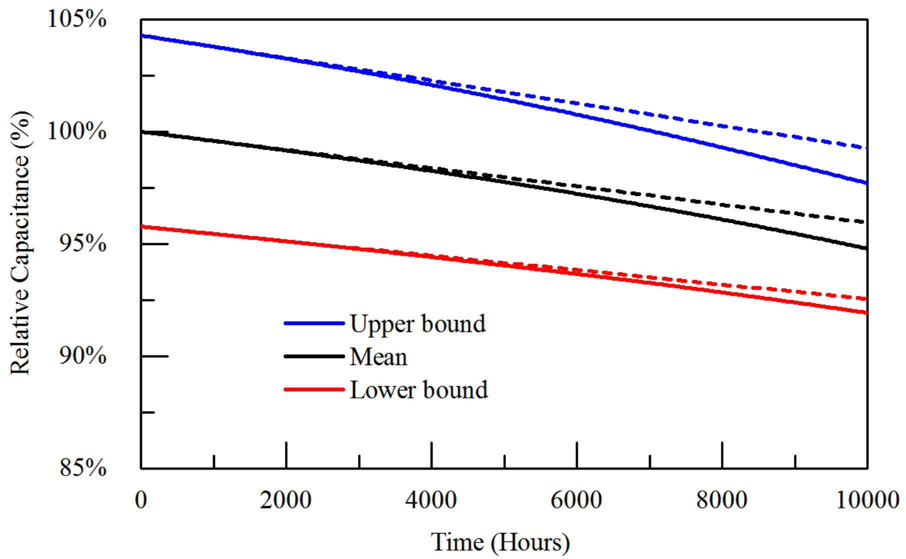

(a)

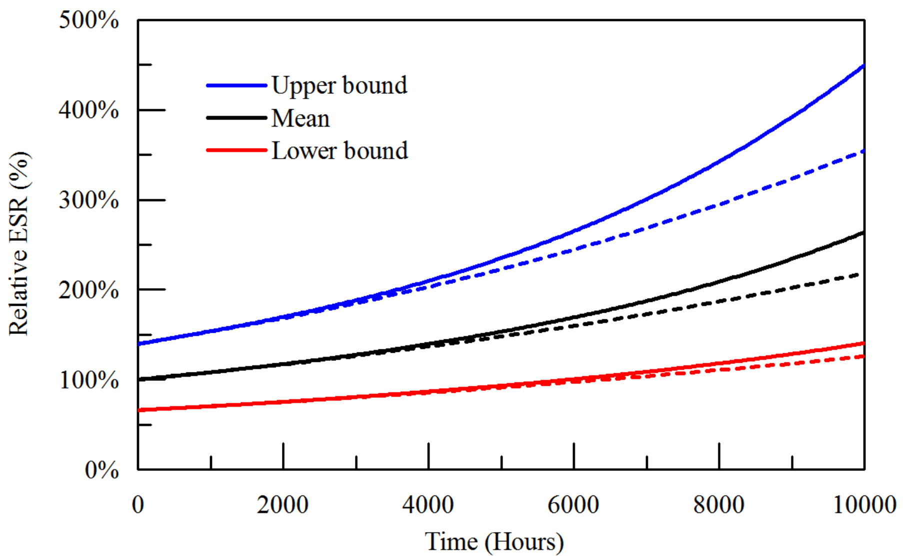

(b)

Figure 2.13: Comparisons of Degradation between the Present Analysis (solid lines) and Constant Capacitor Temperature Analysis (dash lines) (a) Capacitance and (b) ESR.

and 145.2% respectively, compared to the present method.

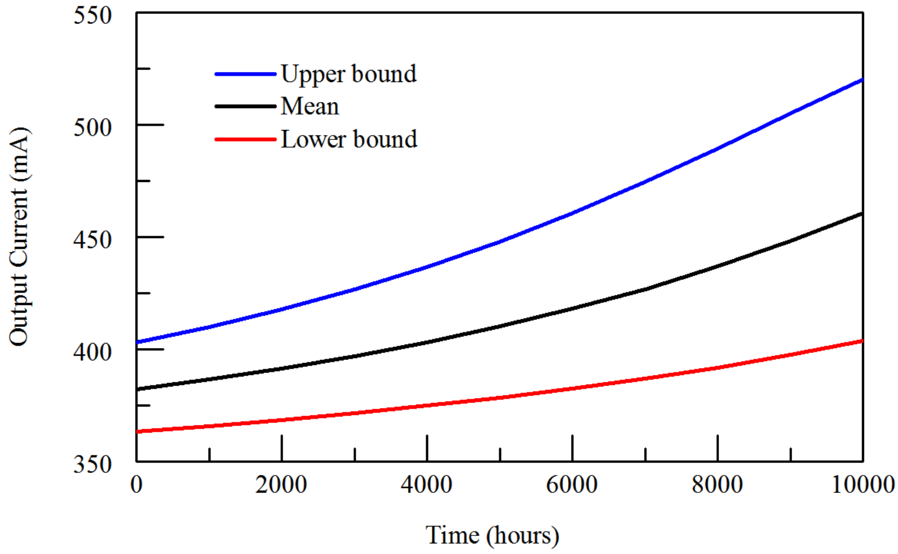

(a)

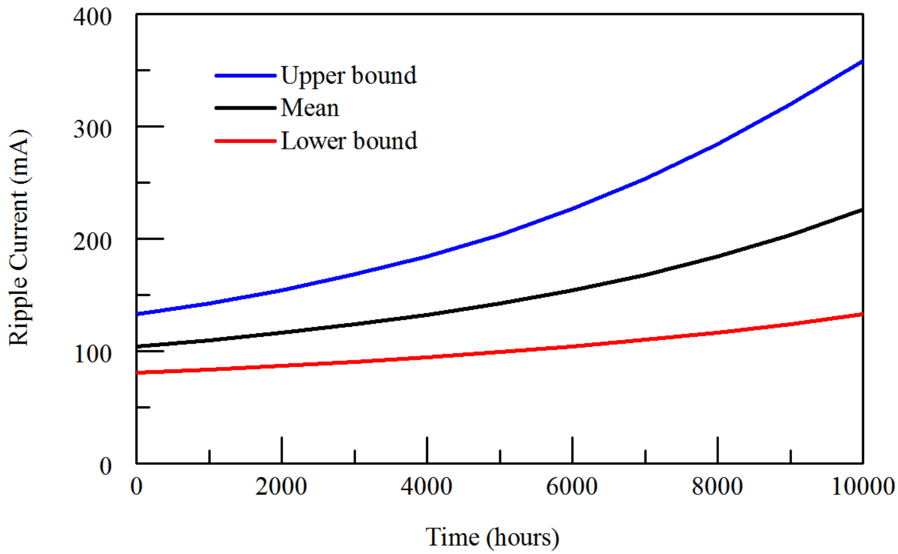

(b)

Figure 2.14: (a) Output Current and (b) Ripple Current of LED.

2.7. CONCLUSION

IN this chapter, a hybrid hierarchical building-block approach that relies on combining a PoF simulation with the statistical-empirical approach for LED driver lifetime

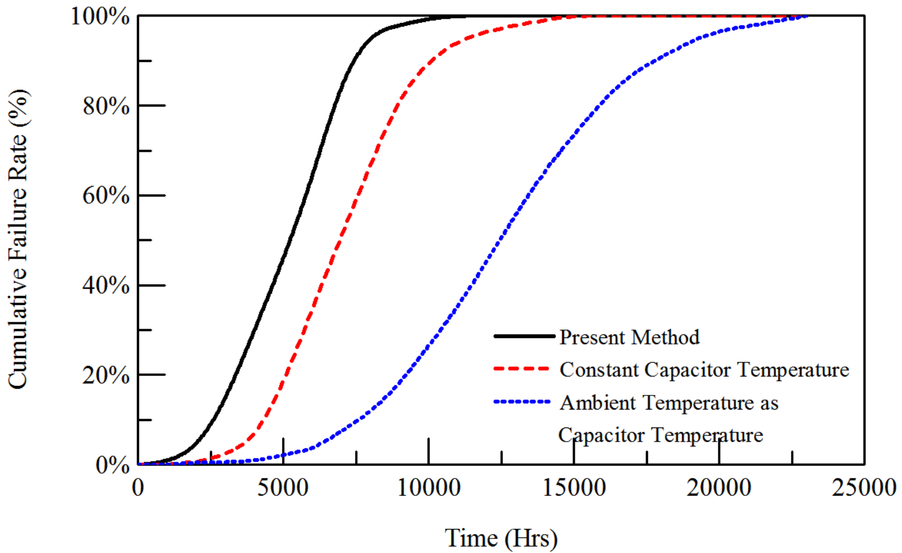

Figure 2.15: Simulated Cumulative Failure Rate of the Electrolytic Capacitors.

prediction has been developed. A combined experimental-numerical approach, using multi-physics modeling techniques to extract relevant physics-based parameters, at the component level, is proposed for lifetime prediction. The models have been supported and validated by actual tests, incorporating time-/temperature-dependent component models. The validated models have been used to provide a long-term reliability prediction with improved confidence and tolerance. As a demonstration example, this chapter focuses on a representative failure mode of an electrolytic capacitor in LED drivers.

Through parametric study, it clearly shows that the temperature of electrolytic capacitor continually rises during operation in a constant ambient condition. As a result, the degradation predicted by the present study is faster than conventional models. Results also show that the mean output current increases about 20% of its initial value; and ripple current increases about 82% within 10,000 hours for the given parameters in this study in a single inductor buck-boost converter. Compared with the output current, the ripple current is more sensitive to degradation of electrolytic capacitors. The method developed in this chapter can be extended to investigate other failure modes and other components in an LED driver system.

REFERENCES

[1] B. Sun, X. J. Fan, C. Qian, and G. Q. Zhang, *PoF-simulation-assisted reliability prediction for electrolytic capacitor in LED drivers,* IEEE Transactions on Industrial Electronics **63**, 6726 (2016).

[2] W. D. van Driel and X. J. Fan, *Solid state lighting reliability: components to systems* (Springer Science & Business Media, 2012).

[3] *LED luminaire lifetime: recommendations for testing and reporting, Third Edition* (Department of Energy (DoE), United States, 2014).

[4] J. Huang, D. S. Golubović, S. W. Koh, D. Yang, X. Li, X. J. Fan, and G. Q. Zhang, *Degradation modeling of mid-power white-light LEDs by using wiener process,* Optics Express **23**, A966 (2015).

[5] G. Lu, W. D. van Driel, X. J. Fan, M. Y. Mehr, J. Fan, K. Jansen, and G. Q. Zhang, *Degradation of microcellular PET reflective materials used in LED-based products,* Optical Materials **49**, 79 (2015).

[6] J. Huang, D. S. Golubovic, S. Koh, D. Yang, X. Li, X. J. Fan, and G. Q. Zhang, *Degradation mechanisms of mid-power white-light LEDs under high-temperature-humidity conditions,* IEEE Transactions on Device and Materials Reliability **15**, 220 (2015).

[7] C. Qian, X. J. Fan, J. Fan, C. Yuan, and G. Q. Zhang, *An accelerated test method of luminous flux depreciation for LED luminaires and lamps,* Reliability Engineering & System Safety **147**, 84 (2016).

[8] *Hammer Testing Findings for Solid-State Lighting Luminaires* (Department of Energy (DoE), United States, 2013).

[9] R. A. Pinto, M. R. Cosetin, A. Campos, M. A. D. Costa, and R. N. do Prado, *Compact emergency lamp using power LEDs,* IEEE Transactions on Industrial Electronics **59**, 1728 (2012).

[10] S. Y. Hui, S. N. Li, X. H. Tao, W. Chen, and W. M. Ng, *A novel passive offline LED driver with long lifetime,* IEEE Transactions on Power Electronics, **25**, 2665 (2010).

[11] D. G. Lamar, M. Arias, A. Rodriguez, A. Fernandez, M. M. Hernando, and J. Sebastian, *Design-oriented analysis and performance evaluation of a low-cost high-brightness LED driver based on flyback power factor corrector,* IEEE Transactions on Industrial Electronics **60**, 2614 (2013).

2

[12] X. Qu, S. C. Wong, and C. K. Tse, *Resonance-assisted buck converter for offline driving of power LED replacement lamps,* Power Electronics, IEEE Transactions on **26**, 532 (2011).

[13] X. Wu, J. Yang, J. Zhang, and Z. Qian, *Variable on-time (VOT)-controlled critical conduction mode buck PFC converter for high-input AC/DC hb-LED lighting applications,* Power Electronics, IEEE Transactions on **27**, 4530 (2012).

[14] P. S. Almeida, D. Camponogara, M. D. Costa, H. Braga, and J. M. Alonso, *Matching LED and driver life spans: A review of different techniques,* Industrial Electronics Magazine, IEEE **9**, 36 (2015).

[15] C. Branas, F. J. Azcondo, and J. M. Alonso, *Solid-state lighting: a system review,* Industrial Electronics Magazine, IEEE **7**, 6 (2013).

[16] L. Han and N. Narendran, *An accelerated test method for predicting the useful life of an LED driver,* Power Electronics, IEEE Transactions on **26**, 2249 (2011).

[17] P. Lall, P. Sakalaukus, and L. Davis, *Reliability and failure modes of solid-state lighting electrical drivers subjected to accelerated aging,* IEEE Access **3**, 531 (2015).

[18] B. Wang, X. Ruan, K. Yao, and M. Xu, *A method of reducing the peak-to-average ratio of LED current for electrolytic capacitor-less AC-DC drivers,* Power Electronics, IEEE Transactions on **25**, 592 (2010).

[19] S. Wang, X. Ruan, K. Yao, S. C. Tan, Y. Yang, and Z. Ye, *A flicker-free electrolytic capacitor-less AC-DC LED driver,* Power Electronics, IEEE Transactions on **27**, 4540 (2012).

[20] W. Chen and S. Y. R. Hui, *Elimination of an electrolytic capacitor in AC/DC light-emitting diode (LED) driver with high input power factor and constant output current,* Power Electronics, IEEE Transactions on **27**, 1598 (2012).

[21] S. Dietrich, S. Strache, R. Wunderlich, and S. Heinen, *Get the LED out: Experimental validation of a capacitor-free single-inductor, multiple-output LED driver topology,* Industrial Electronics Magazine, IEEE **9**, 24 (2015).

[22] H. Ma, J. S. Lai, Q. Feng, W. Yu, C. Zheng, and Z. Zhao, *A novel valley-fill SEPIC-derived power supply without electrolytic capacitor for LED lighting application,* Power Electronics, IEEE Transactions on **27**, 3057 (2012).

[23] A. Lazaro, A. Barrado, M. Sanz, V. Salas, and E. Olias, *New power factor correction AC-DC converter with reduced storage capacitor voltage,* Industrial Electronics, IEEE Transactions on **54**, 384 (2007).

[24] A. Lahyani, P. Venet, G. Grellet, and P. J. Viverge, *Failure prediction of electrolytic capacitors during operation of a switchmode power supply,* Power Electronics, IEEE Transactions on **13**, 1199 (1998).

[25] M. L. Gasperi, *Life prediction modeling of bus capacitors in ac variable-frequency drives,* Industry Applications, IEEE Transactions on **41**, 1430 (2005).

[26] Y. M. Chen, H. C. Wu, M. W. Chou, and K. Y. Lee, *Online failure prediction of the electrolytic capacitor for LC filter of switching-mode power converters,* Industrial Electronics, IEEE Transactions on **55**, 400 (2008).

[27] K. Abdennadher, P. Venet, G. Rojat, J. M. Retif, and C. Rosset, *A real-time predictive-maintenance system of aluminum electrolytic capacitors used in uninterrupted power supplies,* Industry Applications, IEEE Transactions on **46**, 1644 (2010).

[28] B. Sun, X. J. Fan, C. Yuan, C. Qian, and G. Q. Zhang, *A degradation model of aluminum electrolytic capacitors for LED drivers,* in *Thermal, Mechanical and Multi-Physics Simulation and Experiments in Microelectronics and Microsystems (EuroSimE), 2015 16th International Conference on* (IEEE, 2015) pp. 1–4.

[29] S. Tarashioon, W. van Driel, and G. Zhang, *Multi-physics reliability simulation for solid state lighting drivers,* Microelectronics Reliability **54**, 1212 (2014).

[30] S. Tarashioon, A. Baiano, H. van Zeijl, C. Guo, S. Koh, W. van Driel, and G. Zhang, *An approach to "design for reliability" in solid state lighting systems at high temperatures,* Microelectronics Reliability **52**, 783 (2012).

[31] P. Fang and Y. F. Liu, *An electrolytic capacitor-free single stage buck-boost LED driver and its integrated solution,* in *2014 IEEE Applied Power Electronics Conference and Exposition - APEC 2014* (IEEE, 2014) pp. 1394–1401.

[32] *LTwiki,* (Linear Technology Corporation, 2014).

[33] *LTC3783 PWM LED Driver and Boost, Flyback and SEPIC Controller* (Linear Technology Corporation, 2008).

[34] X. J. Fan, *Development, validation, and application of thermal modeling for a MCM power package,* in *Semiconductor Thermal Measurement and Management Symposium, 2003. Ninteenth Annual IEEE* (2003) pp. 144–150.

[35] S. Westerlund and L. Ekstam, *Capacitor theory,* Dielectrics and Electrical Insulation, IEEE Transactions on **1**, 826 (1994).

[36] M. Ward, *Electrical Engineering Science* (McGraw-Hill, 1971).

[37] P. Wang and A. Anderko, *Computation of dielectric constants of solvent mixtures and electrolyte solutions,* Fluid Phase Equilibria **186**, 103 (2001).

[38] W. M. Haynes, *CRC handbook of chemistry and physics* (CRC press, 2014).

[39] A. Høyland and M. Rausand, *System reliability theory: models and statistical methods*, Vol. 420 (John Wiley & Sons, 2009).

[40] E. Zio, *The Monte Carlo simulation method for system reliability and risk analysis* (Springer, 2013).

[41] C. Dubilier, *Application guide, aluminum electrolytic capacitors* (2002).

3

A Novel Lifetime Prediction for Integrated LED Lamps by Electro-Thermal Simulation

In this chapter, an integrated LED lamp with an electrolytic capacitor-free driver is considered to study the coupling effects of both LED and driver's degradations on lamp's lifetime. An electrolytic capacitor-less buck-boost driver is used. The physics of failure based electronic thermal simulation is carried out to simulate the lamp's lifetime in three different scenarios: Scenario 1 considers LED degradation only, Scenario 2 considers the driver degradation only, and Scenario 3 considers both degradations from LED and driver simultaneously. When these two degradations are both considered, the lamp's lifetime is reduced by about 22% compared to the initial target of 25,000 hours. The results of Scenario 1 and 3 are close to each other. Scenario 2 gives erroneous results in terms of luminous flux as the LED's degradation over time is not taken into consideration. This implies that LED's degradation must be taken into considerations when LED and driver's lifetimes are comparable.

Parts of this chapter have been published in Reliability Engineering & System Safety, **163**, pp.14-21,(2017) [1].

3

3.1. Introduction

Light Emitting Diode (LED) has been regarded as one of the most promising lighting solutions due to its energy efficiency, flexible controllability and long lifetime [2–4]. An LED lamp is a complex system which is mainly comprised of an LED light source, a driver, control gears, secondary optical parts and heat dissipation components [4]. The LED light source often has a lifetime as long as 25,000 - 100,000 hours [2–4]. However, the LED driver has a much shorter life, in particular, when electrolytic capacitors are utilized [5–7]. Many studies have focused on the degradation analysis of LEDs only, without taking consideration of the LED driver's degradation [3, 8–12]. For example, a test method has been developed to accelerate of luminous flux depreciation of LED lamps or luminaires by an elevated temperature [3]. Degradations of LEDs in the high temperature-humidity environment have been studied [8, 9]. The LED color shift by optical materials has been investigated [10, 11]. A life prediction method for LED considering real mission profiles has been developed [13].

For the driver's degradation, if the driver's lifetime is much shorter than LED's life, LEDs' degradation may not be significant for prediction the system's lifetime, as the eventual lifetime of the entire system is determined by driver's lifetime. With such an assumption, a physics-of-failure (PoF) based lifetime prediction methodology for LED drivers has been developed [5]. However, little research considers both degradations of the driver and LEDs in an integrated LED lamp.

Numerous reliability assessment methodologies have been developed to consider the degradations of a complex system. For instance, the general path models have been well established and widely used in reliability assessment [14–17], owing to their ease of use. As the requirement of reality, many stochastic process approaches have been developed in recent years [18–22]. For LED systems, the Gamma process and copula function have been applied to model the reliability [23]. The Wiener process has been used to predict the LEDs' lumen depreciation and color shift [24]. Moreover, the reliability block diagram method is developed for degradation analysis of complex systems [25]. A stochastic modeling framework has been investigated for interactions among degradations of components of a system [26]. These statistical reliability models and methods need to collect large amounts of data experimentally. Recently, using the Physics of Failure (PoF) simulations as virtual tests to collect data for reliability assessment have attracted increasing research attention. For instance, the degradation distribution models, degradation path models and SPICE simulations have been integrated for a tolerance design [16]. A multi-physics simulation method has been used to predict the performance of an LED driver during degradations of semiconductor devices [27].

For an integrated lamp, in which the LED light source and driver are assembled together, both degradations of the LEDs and the driver will affect each other through the ever-changing of temperature distributions and current during operation. Therefore, it is necessary to use the electronic thermal simulation to determine the electronic and thermal characteristics as a function of time. In this paper, an integrated LED lamp with an electrolytic capacitor-free driver is considered to study the coupling effects of both LEDs and driver's degradations on lamp's lifetime. An electrolytic capacitor-less buck-boost driver is used as it has a comparable lifetime with LEDs. Such a driver is integrated with a commercial LED light bulb for lifetime study. Circuit simulations are carried out to obtain the power distributions and current to LEDs. Thermal simulations are performed subsequently based on power distribution to obtain the temperature distribution of the LED lamp, in particular, the LED junction temperature and driver's overall temperature. The lumen flux depreciation as a function of time can then be obtained. The interaction of these two degradations is studied with several scenarios.

This paper is organized as follows. Section 3.2 describes the degradation models used for LEDs and driver respectively. In Section 3.3, a selected driver circuit and the thermal simulation for the selected LED lamp is introduced. Section 3.4 describes parameter extraction experiments. In Section 3.5, several scenarios are analyzed to predict the lifetime of the lamp and the effects of both degradations. Section 3.6 concludes this work finally.

3.2. DEGRADATION MODELS

3.2.1. LED LIGHT SOURCE

The exponential model is applied to describe lumen depreciation in the constant junction temperature T_j and the constant driving current I as follows [3]:

$$\phi_{lm}(t) = \Phi(I) \cdot e^{-\beta(T_j)\cdot t} \tag{3.1}$$

where t is time, Φ_{lm} is the absolute luminous flux at time t, $\phi(I)$ is the luminous flux factor that is a function of current I, and the depreciation rate β follows the Arrhenius Equation [7]:

$$\beta(T_j) = A_\beta \cdot e^{\frac{E_{a,\beta}}{\kappa T_j}} \tag{3.2}$$

where, A_β is the pre-exponential factor, $E_{a,\beta}$ is the activation energy of LED.

If the junction temperature $T_j(t)$ and driving current $I(t)$ change as functions of time, the deviation of lumen depreciation from time t to time $t+\Delta t$ can be described by:

$$ln\Delta\frac{\Phi_{lm}[T_j(t),\Delta t]}{\Phi[I(t)]} = -\beta[T_j(t)]\cdot\Delta t \tag{3.3}$$

Thus, when t is from time 0 to time x, the accumulated lumen depreciation can be described by:

$$ln\Delta\frac{\Phi_{lm}[T_j(t),x]}{\Phi[I(t)]} = \sum_{0}^{x} ln\Delta\frac{\Phi_{lm}[T_j(t),\Delta t]}{\Phi[I(t)]} = \sum_{0}^{x} -\beta[T_j(t)]\cdot\Delta t \tag{3.4}$$

In the integral form, the accumulated lumen depreciation can be described by:

$$ln\frac{\Phi_{lm}[T_j(t),x]}{\Phi[I(t)]} = -\int_0^x \beta[T_j(t)]\cdot dt + C_{lm} \tag{3.5}$$

Thus:

$$\frac{\Phi_{lm}[T_j(t),x]}{\Phi[I(t)]} = e^{-\int_0^x \beta[T_j(t)]\cdot dt + C_{lm}} \tag{3.6}$$

The boundary condition is:

$$\frac{\Phi_{lm}[T_j(0),0]}{\Phi[I(0)]} = 1 \tag{3.7}$$

Thus, C_{lm}=0, as a result from time 0 to time x:

$$\phi_{lm}(t) = \Phi(I)\cdot e^{-\int_0^x \beta[T_j(t)]\cdot dt} \tag{3.8}$$

$\phi(I)$ in Equation 3.1 can be described by the following function [28]:

$$\Phi(I) = \eta(I)\cdot I\cdot V_f \tag{3.9}$$

where $\eta(I)$ is LED's efficacy at current I and V_f is the forward voltage which is a function of junction temperature T_j and current I.

The efficacy η is affected by both temperature droop (T-droop) and current droop (J-droop) [29, 30]. However, in high current status, the T-droop becomes negligible in comparison with the J-droop. Thus, η can be assumed approximately as a function of

the J-droop [30]:

$$\eta = \eta_0 \cdot \frac{bn^2}{an + bn^2 + cn^3} \tag{3.10}$$

where η_0 is the efficacy factor, a and c are the linear and the 3rd-order non-radiative recombination rates, b is the radiative recombination rate, and n is the average carrier density of LED, which is proportional to the current I, hence the efficacy can be described the following function:

$$\eta(I) = \eta_0 \cdot \frac{B_e I}{A_e + B_e I + C_e I^2} \tag{3.11}$$

where η_0, A_e, B_e and C_e are dependent on the LED's properties dependent materials and structure.

Combine Equation 3.1, 3.3 and 3.5, the luminous flux in the ever-changing junction temperature $T_j(t)$ and current $I(t)$ can be described by the following function [31]:

$$\Phi_{lm}(t) = \eta_0 \cdot \frac{B_e I^2(t)}{A_e + B_e I(t) + C_e I^2(t)} \cdot V_f \cdot e^{-\int_0^t \beta[T_j(x)] \cdot dx} \tag{3.12}$$

System conditions, $I(t)$, V_f, and $T_j(t)$, depend on structure and materials' properties of the lamp and circuit, and can be determined by the electronic-thermal simulations. The physical characteristics of the selected LED, η_0, A_e, B_e, C_e, A_β and $E_{a,\beta}$, are invariables, and can be extracted by experiments. In this chapter, η_0, A_e, B_e, and C_e were determined experimentally for the selected LED, and their values are shown in Table 3.2. A_β and $E_{a,\beta}$ will be adjusted through a parametric study in Section 3.5.

3.2.2. LED DRIVER

Literature [32, 33] has shown that the on-state resistance of a MOSFET of an LED driver increases with aging process, leading to the degradation of output current. The study in [34] also indicates that the transistor declines during operation, and brings a decreasing output current of the driver. In the present chapter, the driver's degradation in terms of the output current is considered. The effective value of the output current I can be represented by the following equation:

$$I(t) = \frac{V_{ref}}{R_{ref}} \tag{3.13}$$

where V_{ref} is a constant reference voltage, and R_{ref} is the overall current control resistance. Research in [27] has shown that the resistance of current control device degrades linearly with time. Thus, a linear degradation model for the overall current control resistance R_{ref} is assumed:

$$R_{ref}(t) = R_0 \cdot [1 + A(T_D) \cdot t] \tag{3.14}$$

where R_0 is the initial resistance, T_D is the overall driver temperature and the degradation rate A follows the Arrhenius Equation:

$$A(T_D) = A_0 \cdot e^{\frac{E_{a,D}}{\kappa \cdot T_D}} \tag{3.15}$$

where, A_0 is the basic degradation rate and $E_{a,D}$ is the overall activation energy of LED driver. If the driver temperature T_D changes continuously in time t, Equation 3.8 can be deduced to an integration form, as follows:

$$R_{ref}[t, T_D(t)] = R_0 \cdot \int_0^t 1 + A[T_D(x) \cdot x] \cdot dx \tag{3.16}$$

where, the driver temperature $T_D(t)$ is a system condition, and can be determined by electronic thermal simulations. Among the physical characteristics of the selected driver, R_0 can be determined by the initial output current of the driver, $E_{a,D}$ and A_0, which control the driver degradation, will be adjusted through the parametric study in Section 3.5.

3.3. Simulation Methodology

3.3.1. Electronic Simulations

An electrolytic capacitor-free buck-boost converter, as shown in Figure 3.1, is selected as the LED driver. This type of LED driver is one of the most commonly used drivers in lighting applications [35]. In this work, the driver's switching frequency is 300 kHz, the input voltage range is 9 to 20 Vdc, the rated output current is 400 mA, the duty cycle is 25%, and the rated output power is 6.0W. Device models in the driver, which are provided by a public database [36], have been validated and verified.

A temperature-dependent LED degradation model is considered in circuit simulations. The LED's forward voltage V_f can be described by [28]:

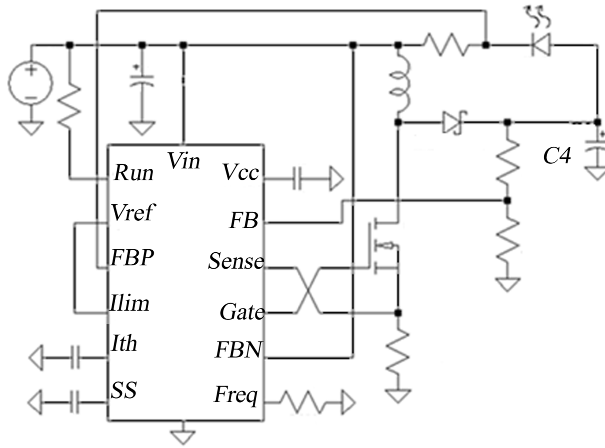

Figure 3.1: The Electrolytic Capacitor-Free Buck-Boost LED Driver [37].

$$V_f[I(t),T_j(t)] = N\cdot\kappa\cdot T_j(t)\cdot ln[\frac{I(t)}{I_S}+1]+R_S\cdot I(t) \tag{3.17}$$

where, N is the ideality factor, I_s is the saturation current, R_s is the equivalent series resistance. Literature [38] suggests that the electronic characteristics of LEDs after seasoning is not affected by aging time, but strongly affected by junction temperature T_j. Thus, the R_s, I_s and N, are considered as the functions of junction temperature T_j as following, according to literature [28, 39, 40]:

$$R_S[T_j(t)] = R_{S0}\cdot[1+A_S\cdot T_j(t)] \tag{3.18}$$

$$I_S[T_j(t)] = I_{S0}\cdot T_j^2(t)\cdot e^{-\frac{A_I}{T_j(t)}} \tag{3.19}$$

$$N[T_j(t)] = \frac{T_j(t)}{A_N\cdot T_j(t)+B_N} \tag{3.20}$$

The power distribution of the entire circuit can be obtained by circuit simulations. The thermal power of the LED light source P_L is the difference between input power and optical power of the LED light source:

$$P_L(t) = I(t)\cdot V_f[I(t),T_j(t)] - C\cdot\Phi_{lm}(t) \tag{3.21}$$

where C is the ratio of optical power and luminous flux.

The thermal power of the driver P_D is the sum of heat from all components in the driver. Thus, P_D equals to the difference between total input power and total output power of the driver:

$$P_D(t) = P_{in}(t) - I(t) \cdot V_f[I(t), T_j(t)] \tag{3.22}$$

where P_{in} is the total input power.

3.3.2. THERMAL SIMULATIONS

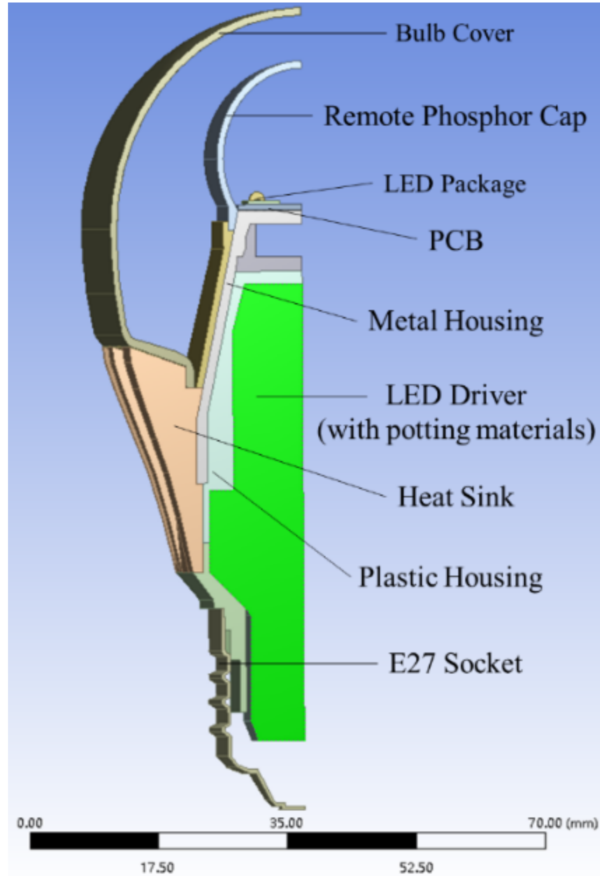

Figure 3.2: The Model of The selected LED Lamp.

This chapter selects a commercial LED light bulb as the carrier. Figure 3.2 displays

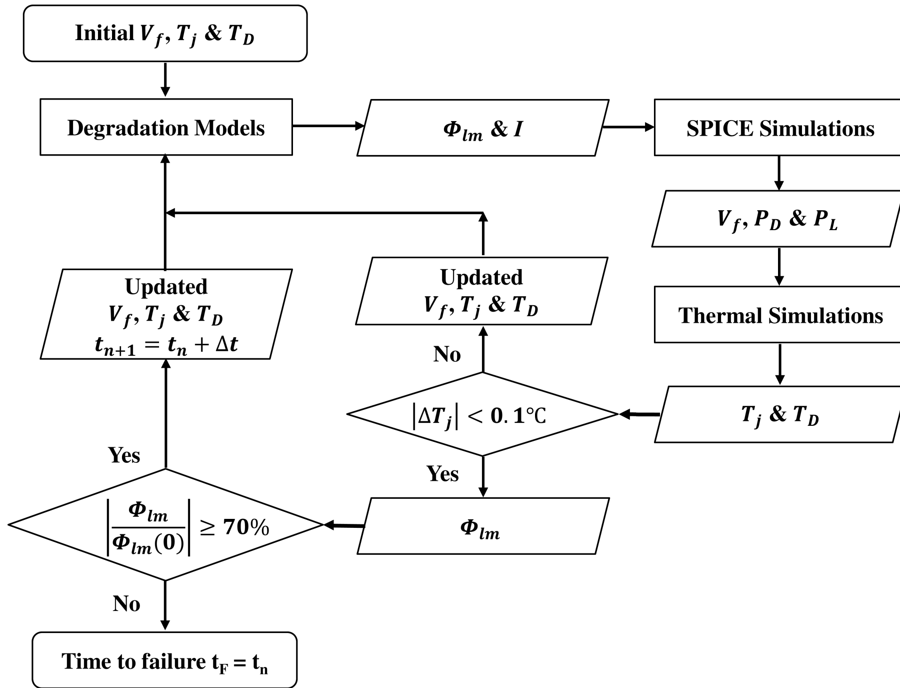

Figure 3.3: Flowchart of the Electronic-Thermal Simulation Methodology.

the lamp's structure, in which the geometrical information and material properties can refer to the literature [41–44]. An electrolytic capacitor-free buck-boost converter, as shown in Figure 3.1, is used as the driver to replace the original one. The heat generated by both LEDs and the driver determine the junction temperature of LED as well as the driver's temperature. Therefore, system-level finite element analysis is conducted to obtain the temperature distributions.

In this thermal finite element model, the driver and its potting materials as a whole are considered as a volume (green portion in Figure 3.2). All thermal power dissipated by each individual component in Figure 3.1 is summed together and uniformly distributed over the surface. The driver's temperature, T_D, is taken from the maximum temperature of the surface.

3.3.3. SIMULATION METHODOLOGY

Figure 3.3 illustrates the flowchart of the electronic thermal simulation in the present study. The simulation process begins with the initial guess of T_j and T_D and the initial LED's forward voltage V_f, from which the degradation models in Equation 3.6 and 3.10

can be applied to obtain the luminous flux Φ_{lm}, and the current I. Then the electronic simulations are performed to update V_f and obtain the power dissipations by Equation 3.11, 3.15 and 3.16. Subsequently, the thermal simulations are performed to update T_j and T_D. Such a simulation process loop is performed iteratively until the error between values of T_j in two consecutive steps is less than 0.1K, as shown in Figure 3.3. Then light output can be calculated using Equation 3.6.

Generally, the useful lifetime of LED lighting products is typically given in terms of the expected operating hours until light output has depreciated to 70% of initial levels [3]. If this threshold is not reached, the aging time t advances to a small increment Δt. Since the temperatures update T_j and T_D are not known at $t+\Delta t$, the above iteration process repeats. The time increment Δt in this work is assumed to be 1000 hours. When time $t = t_F$, and the Φ_{lm} has depreciated to 70% of the initial value, the simulation stops, and t_F is considered as the lifetime of the LED lamp.

3.4. Parameter Extraction of LED Models

The physical parameters of the lumen depreciation model and the electronic model of the LED light source, C, η_0, A_e, B_e, C_e, R_{s0}, A_s, I_{s0}, A_I, A_n and B_n, need to be determined experimentally. Hence, ten selected high power LED packages were tested in eight junction temperature levels, from 293K to 363K. Each sample was placed on a thermal plate inside a 50cm integrating sphere system. Then, the transient electronic and optical characteristics of each sample, including current, forward voltage, luminous flux, and efficacy, are measured at different junction temperature levels. For each junction temperature, the transient current of each sample sweeps from 200mA to 350mA. As shown in Figure 3.4, the measured I-V characteristics were fitted by Equation 3.11 to 3.14, whereas the efficacy was fitted by Equation 3.5 by the least square method, obtaining these physical parameters of the LED models. Table 3.1 summarizes the averaged values of the model parameters. The details of tests and parameter extractions can refer to the Literature [31].

3.5. Result and Discussions

3.5.1. Lamp's Initial Temperature Distributions

Firstly, considering the lamp's operation conditions with an ambient room temperature of 298K and a natural convective heat transfer coefficient of $5W \cdot m^{-2}K^{-1}$, the electronic-thermal simulation is performed to obtain the initial LED junction temperature $T_j(0)$ and the driver temperature $T_D(0)$. As shown in Table 3.1. The simulation results agree

Figure 3.4: The LED Sample and the Integrating Sphere System.

Table 3.1: Physical Parameters of The LED Light Source

Parameter	Value	Parameter	Value
R_{s0}	5.914×10^{-1}	A_s	6.699×10^{-4}
I_{s0}	4.786×10^{5}	A_I	1.274×10^{-1}
A_n	1.240	B_n	-2.882×10^{2}
C	4.087×10^{-3}	η_0	1.456×10^{2}
A_e	0.999	B_e	1.406×10^{3}
C_e	2.138×10^{3}		

well with the experimental data [42, 43]. Table 3.1 also gives the targeted temperatures of T_j and T_D for this lamp design. It can be seen that initial temperatures of both LEDs and driver are within the design requirement.

Table 3.2: Temperature Distributions

Temperature	Predicted Value	Targeted Value
T_j	351.8 K	358 K
T_D	318.4 K	328 K

3.5.2. DEFINITION OF DIFFERENT SCENARIOS

LED is usually selected to have a desired lifetime at the initial temperature of operation. In the present study, the LED with a lifetime of 25,000 hours at the initial LED junction temperature is selected. The driver is also selected to have a 25,000 hours lifetime at the initial temperature T_D. Table 3.2 lists the parameters to be used to satisfy the selection requirement.

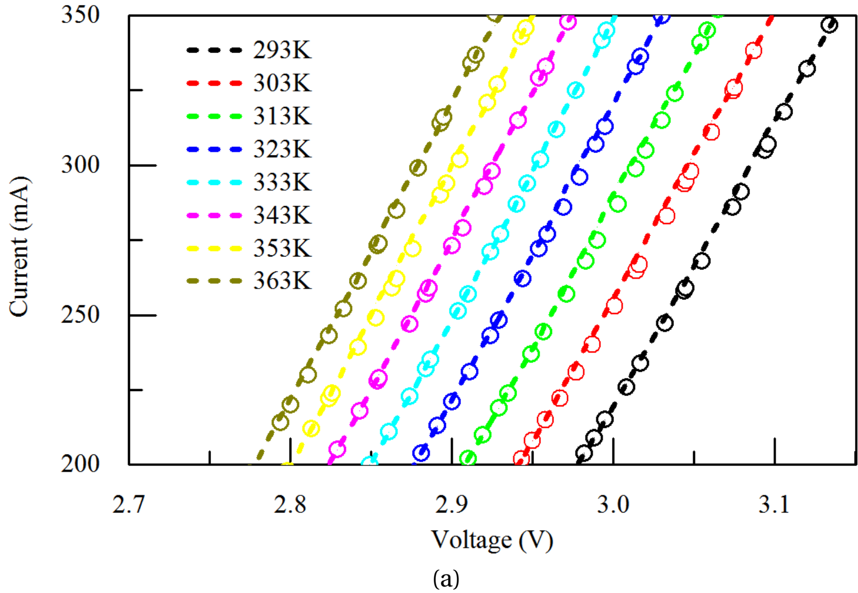

(a)

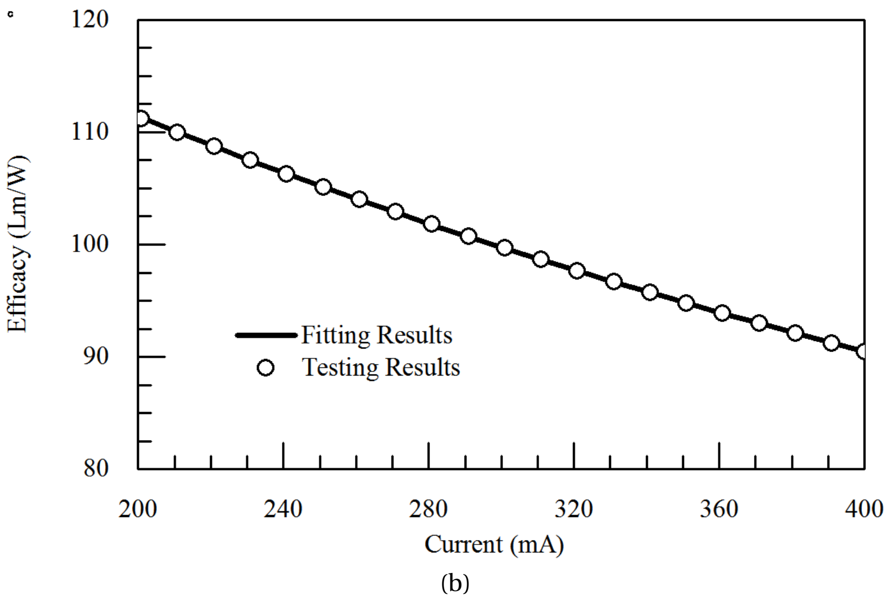

(b)

Figure 3.5: The (a) I-V Curves and (b) Efficacy Curve of the Selected LED.

For LED, this means that the selected LED will have luminous flux above 70% of initial levels before 25,000hours if the LED's junction temperature and current remain unchanged during operation. For LED driver, it implies that the output current from the

Table 3.3: Designed Parameters

Parameter	Value	Parameter	Value
A_β	2.834×10^{-1}	$E_{a,\beta}$	0.3eV
A_0	3.591×10^{-1}	$E_{a,D}$	0.7eV

driver will not decrease by 10% of the initial value at the constant initial driver temperature $T_D(0)$. However, the LED junction temperature, and the driver temperature will change continuously with time, due to the simultaneous degradations of both LEDs and driver. Ultimately, this will affect the actual lifetime of the lamp.

Three scenarios are therefore defined. Scenario 1 considers the LED depreciation only, Scenario 2 considers the driver degradation only, while Scenario 3 considers both degradations from LEDs and driver simultaneously, as summarized in Table 3.3.

Table 3.4: DESIGNED SCENARIOS

Case	LED	Driver
Scenario 1	25,000hrs lifetime at the constant initial T_j (L25K)	No degradation
Scenario 2	No degradation	25,000hrs lifetime at the constant initial T_D (D25K)
Scenario 1	25,000hrs lifetime at the constant initial T_j (L25K)	25,000hrs lifetime at the constant initial T_D (D25K)

3.5.3. RESULTS AND DISCUSSIONS

LED CURRENT

Figure 3.4 shows the relative LED current with respect to the initial value in each scenario as a function of operation time. For Scenario 1, as the driver's degradation is not considered, the LED current maintains at its initial value (the driver is a constant current converter with no degradation). For Scenario 2 the LED current drops 10% at 25000 hours. When two degradations co-exist simultaneously, the LED current drops a little more, about 11% at 25,000 hours.

LED JUNCTION TEMPERATURE

Figure 3.5 displays the LED junction temperature in each scenario. The LED junction temperature increases with time for Scenarios 1, but decreases for Scenario 2. However,

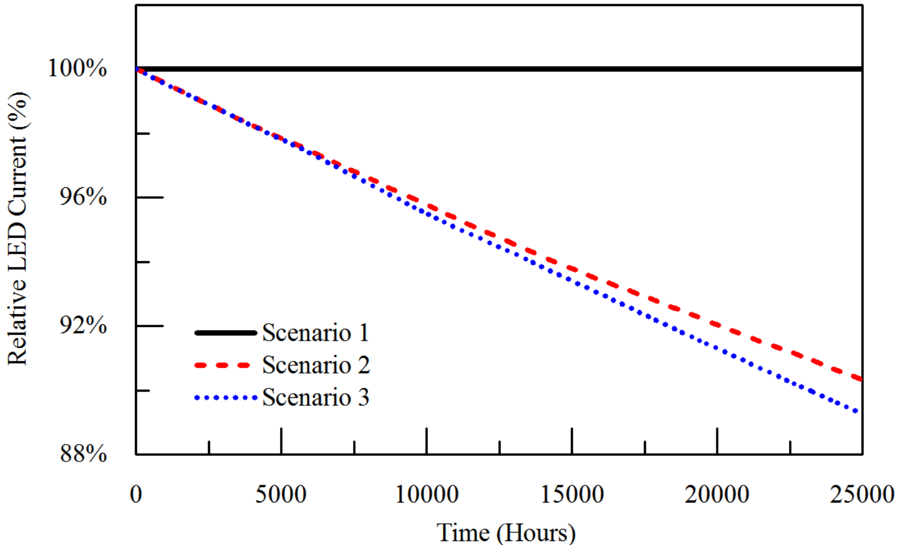

Figure 3.6: The LED Current of Each Scenario.

the LED's junction temperature does not change much for Scenario 3 with both degradations considered. This is because that driver's current decreases over time (in Figure 3.4), thus less power is provided to LEDs. On the other hands, when LED's degradation is considered, more thermal power is generated as the efficacy of LED decreases. These two effects eventually cancel out the impact on LED's junction temperature.

Driver's Temperature

Figure 3.6 indicates the driver's temperatures for three scenarios. Similarly, the driver's temperature increases with time in Scenarios 1, but decreases in Scenario 2, and does not change much for Scenario 3.

Lumen Maintenance and lifetime

Figure 3.7 shows the lumen maintenance over time for three scenarios. The lumen maintenance drops significantly with time for Scenario 1. As the driver does not degrade in this scenario, the luminous flux depreciation is due to the LEDs' degradation over time, and is further accelerated by the increase of the LED junction temperature over operation process. For Scenario 2, the lumen depreciation is not significant even though the driver may be near the end of its lifetime at 25,000 hours. It can be seen, from Figure 3.4 and Figure 3.5, that under Scenario 2, both LED current and LED junction temperature drops significantly. However, the lumen output does not change as much as tempera-

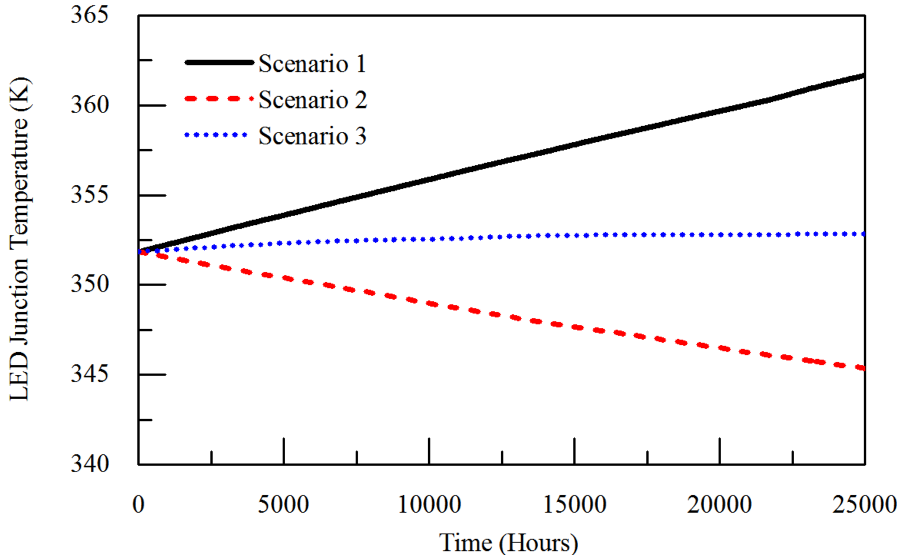

Figure 3.7: The LED Junction Temperature of Each Scenario.

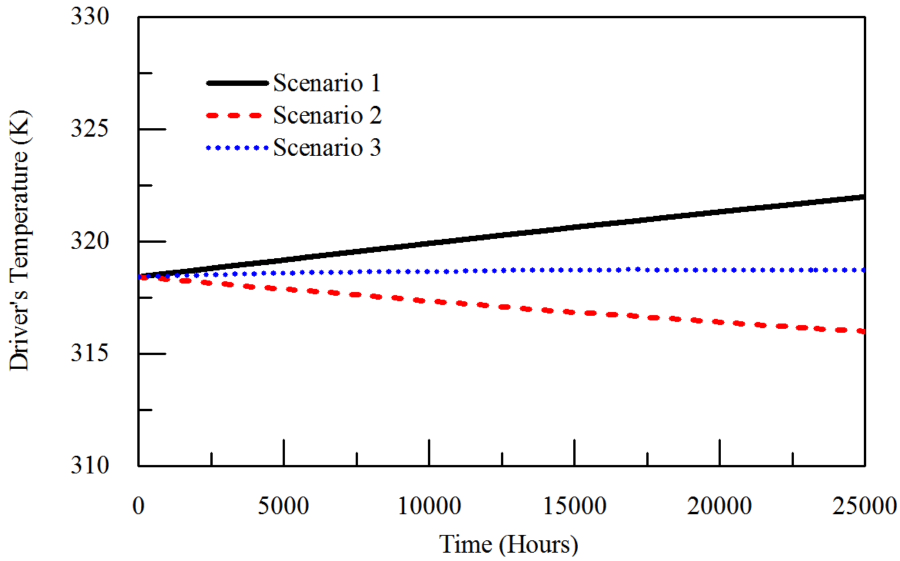

Figure 3.8: The Driver's Temperature of Each Scenario.

ture and current, as Scenario 2 does not consider the LED degradation over time. For Scenarios 3, when both degradations are considered, the lumen output decreases with time significantly, in spite of the little change in the LED junction temperature, shown in

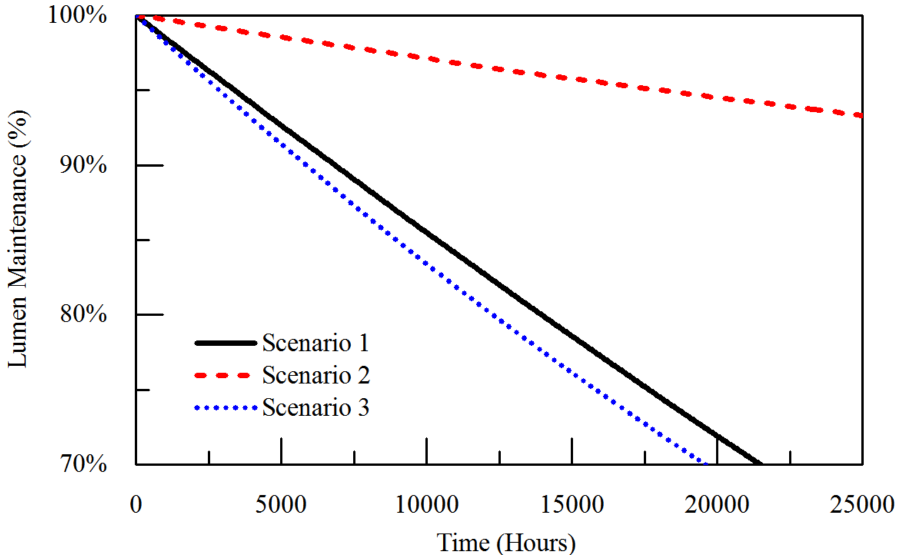

Figure 3.9: The Lumen Maintenance and for Each Scenario.

Figure 3.5 The lumen depreciation in Scenario 3 is attributed to the combined effects of the reduced current in LED, due to driver degradation, and the lumen depreciation on time, due to LEDs' degradation.

Table 3.4 summarizes the lifetime prediction for these three scenarios. It can be seen that when driver and LED's degradations are considered, the LED lamp's lifetime is reduced by about 22% compared to the initial target of 25,000hours. From this table, it can be found that the results of Scenario 1 and 3 are close to each other. This implies that without considering driver's degradation (Scenario 1), the predicted lamp lifetime may just underestimate a bit. The underlying mechanism is that the driver's degradation will reduce the LED's junction temperature so that LED's temperature does not rise as much as that LED degradation only. For Scenario 2, a lifetime of 25,000 hours is taken since the LED current would drop by 10% of its initial value at that time. This indicates that the driver's failure will occur, even though LEDs' degradation is not considered. It implies that LEDs' degradation should be taken into account when driver's lifetime is comparable to LED's lifetime. Otherwise, the luminous flux depreciation prediction would be inaccurate using Scenario 2, as shown in Figure 3.7.

Table 3.5: Lifetime of Each Combination

Scenario	Lifetime
Scenario 1	21500 Hrs
Scenario 2	19600 Hrs
Scenario 3	19600 Hrs

3.6. CONCLUSIONS

IN this chapter, an integrated LED lamp with an electrolytic capacitor-free driver is considered to study the coupling effects of both LED and driver's degradations on LED lamp's lifetime. An electrolytic capacitor-less buck-boost LED driver is used. as it has a comparable lifetime with the LED. Circuit simulations are carried out to obtain the power distributions and output current and the voltage to LEDs. Thermal simulations are subsequently performed based on power distribution to obtain the temperature distributions of the LED lamp, in particular, LED junction temperature and driver's overall temperature. The lumen flux depreciation as a function of time can then be obtained. Three scenarios are considered: Scenario 1 considers LED degradation only, Scenario 2 considers the driver degradation only, and Scenario 3 considers both degradations from LED and driver simultaneously.

In Scenario 1, the LED current stays at its initial value as the driver does not degrade. As a result, the LED junction temperature and the driver's temperature increase with operation time, which would accelerate the LED's degradation, and thus reduce the lumen maintenance further.

In Scenario 2, the LED current decreases over time due to the driver's degradation. As a result, the LED junction temperature and the driver's temperature decrease with operation time. However, Scenario 2 gives erroneous results in terms of luminous flux as the LED's degradation over time is not taken into consideration. This implies that LED's degradation must be taken into considerations when both LED and driver's lifetimes are comparable.

In Scenario 3, the LED current decrease with operation time, but the LED junction temperature and the driver's temperature do not change much. This is because that driver's output current decreases over time, thus less power is provided to LED. On the other hands, when LED's degradation is considered, more thermal power is generated as the efficacy of LED decreases. These two effects eventually cancel out the impact on the LED junction temperature. Nonetheless, because of the combined effects of the reduced current in LEDs and the lumen dependence on time, the LED lamp's lifetime is reduced

significantly.

REFERENCES

[1] B. Sun, X. Fan, W. van Driel, H. Ye, J. Fan, C. Qian, and G. Zhang, *A novel lifetime prediction for integrated LED lamps by electronic-thermal simulation,* Reliability Engineering & System Safety, Accepted **163**, 14 (2017).

3

[2] J. Fan, K. C. Yunga, and M. Pecht, *Prognostics of lumen maintenance for high power white light emitting diodes using a nonlinear filter-based approach,* Reliability Engineering and System Safety (2013).

[3] C. Qian, X. J. Fan, J. Fan, C. Yuan, and G. Q. Zhang, *An accelerated test method of luminous flux depreciation for LED luminaires and lamps,* Reliability Engineering & System Safety **147**, 84 (2016).

[4] W. D. van Driel and X. J. Fan, *Solid state lighting reliability: components to systems* (Springer Science & Business Media, 2012).

[5] B. Sun, X. J. Fan, C. Qian, and G. Q. Zhang, *PoF-simulation-assisted reliability prediction for electrolytic capacitor in LED drivers,* IEEE Transactions on Industrial Electronics **63**, 6726 (2016).

[6] B. Sun, X. J. Fan, C. Yuan, C. Qian, and G. Q. Zhang, *A degradation model of aluminum electrolytic capacitors for LED drivers,* in *Thermal, Mechanical and Multi-Physics Simulation and Experiments in Microelectronics and Microsystems (EuroSimE), 2015 16th International Conference on* (IEEE, 2015) pp. 1–4.

[7] S. Koh, C. Yuan, B. Sun, B. Li, X. J. Fan, and G. Q. Zhang, *Product level accelerated lifetime test for indoor LED luminaires,* in *2013 14th International Conference on Thermal, Mechanical and Multi-Physics Simulation and Experiments in Microelectronics and Microsystems (EuroSimE)* (IEEE, 2013).

[8] J. Huang, D. S. Golubovic, S. Koh, D. Yang, X. Li, X. J. Fan, and G. Q. Zhang, *Degradation mechanisms of mid-power white-light LEDs under high-temperature-humidity conditions,* IEEE Transactions on Device and Materials Reliability **15**, 220 (2015).

[9] J. Huang, D. S. Golubović, S. Koh, D. Yang, X. Li, X. J. Fan, and G. Q. Zhang, *Rapid degradation of mid-power white-light LEDs in saturated moisture conditions,* IEEE Transactions on Device and Materials Reliability (2015).

[10] G. Lu, W. van Driel, X. J. Fan, M. Yazdan Mehrb, J. Fan, K. Jansenf, and G. Q. Zhang, *Degradation of micro-cellular pet reflective materials used in LED-based products,* Optical Materials (2015).

[11] G. Lu, W. van Driel, X. J. Fan, M. Yazdan Mehrb, J. Fan, K. Jansenf, and G. Q. Zhang, *Color shift investigations for LED secondary optical designs: Comparison between bpa-pc and pmma,* Optical Materials (2015).

[12] J. Fan, C. Qian, K. C. Yung, X. J. Fan, G. Q. Zhang, and M. Pecht, *Optimal design of life testing for high-brightness white LEDs using the six sigma DMAIC approach,* IEEE Transactions on Device and Materials Reliability (2015).

[13] X. Qu, H. Wang, X. Zhan, F. Blaabjerg, and H. S. H. Chung, *A lifetime prediction method for LEDs considering real mission profiles,* IEEE Transactions on Power Electronics **PP**, 1 (2016).

[14] F. Haghighi and S. J. Bae, *Reliability estimation from linear degradation and failure time data with competing risks under a step-stress accelerated degradation test,* IEEE Transactions On Reliability **64**, 960 (2015).

[15] Z. Wang, H. Fu, and Y. Zhang, *Analyzing degradation by an independent increment process,* Quality and Reliability Engineering International **30**, 1275 (2014).

[16] G. Zhai, Y. Zhou, and X. Ye, *A tolerance design method for electronic circuits based on performance degradation,* Quality and Reliability Engineering International **31**, 635 (2015).

[17] Z.-S. Ye and M. Xie, *Stochastic modelling and analysis of degradation for highly reliable products,* Applied Stochastic Models in Business and Industry **31**, 16 (2015).

[18] C. Zhang, X. Lu, Y. Tan, and Y. Wang, *Reliability demonstration methodology for products with gamma process by optimal accelerated degradation testing,* Reliability Engineering & System Safety **142**, 369 (2015).

[19] J.-Y. Chiang, Y. Lio, and T.-R. Tsai, *Degradation tests using geometric brownian motion process for lumen degradation data,* Quality and Reliability Engineering International **31**, 1797 (2015).

[20] Z.-S. Ye, N. Chen, and Y. Shen, *A new class of wiener process models for degradation analysis,* Reliability Engineering & System Safety **139**, 58 (2015).

[21] W. Peng, Y.-F. Li, Y.-J. Yang, H.-Z. Huang, and M. J. Zuo, *Inverse gaussian process models for degradation analysis: A bayesian perspective,* Reliability Engineering & System Safety **130**, 175 (2014).

[22] Z. Ye, M. Revie, and L. Walls, *A load sharing system reliability model with managed component degradation,* IEEE Transactions on Reliability **63**, 721 (2014).

[23] H. Hao, C. Su, and C. Li, *LED lighting system reliability modeling and inference via random effects gamma process and copula function,* International Journal of Photoenergy (2015).

[24] J. Huang, D. S. Golubović, S. W. Koh, D. Yang, X. Li, X. J. Fan, and G. Q. Zhang, *Degradation modeling of mid-power white-light LEDs by using wiener process,* Optics Express **23**, A966 (2015).

[25] L. Ding, H. Wang, K. Kang, and K. Wang, *A novel method for SIL verification based on system degradation using reliability block diagram,* Reliability Engineering & System Safety **132**, 36 (2014).

[26] L. Bian and N. Gebraeel, *Stochastic modeling and real-time prognostics for multi-component systems with degradation rate interactions,* IIE Transactions **46**, 470 (2014).

[27] S. Tarashioon, W. van Driel, and G. Zhang, *Multi-physics reliability simulation for solid state lighting drivers,* Microelectronics Reliability **54**, 1212 (2014).

[28] E. F. Schubert, T. Gessmann, and J. K. Kim, *Light emitting diodes* (Wiley Online Library, 2005).

[29] D. S. Meyaard, Q. Shan, J. Cho, E. F. Schubert, S. H. Han, M. H. Kim, C. Sone, S. J. Oh, and J. K. Kim, *Temperature dependent efficiency droop in gainn light-emitting diodes with different current densities,* Applied Physics Letters (2012).

[30] J. Piprek, *Efficiency droop in nitride-based light-emitting diodes,* physica status solidi (a) (2010).

[31] B. Sun, X. J. Fan, W. v. Driel, T. Michel, J. Zhou, and G. Q. Zhang, *Lumen decay prediction in LED lamps,* in *IEEE International Conference on Thermal, Mechanical and Multi-Physics Simulation and Experiments in Microelectronics and Microsystems (EuroSIME)* (2015).

[32] S. Lan, C. M. Tan, and K. Wu, *Reliability study of LED driver–a case study of black box testing,* Microelectronics Reliability (2012).

[33] S. Lan, C. M. Tan, and K. Wu, *Methodology of reliability enhancement for high power LED driver,* Microelectronics Reliability **54**, 1150 (2014).

[34] X. Shao, *Research on Reliability Assessment Method of The LED Driver Power Supply,* Thesis (2012).

[35] P. Fang and Y. F. Liu, *An electrolytic capacitor-free single stage buck-boost LED driver and its integrated solution,* in *2014 IEEE Applied Power Electronics Conference and Exposition - APEC 2014* (IEEE, 2014) pp. 1394–1401.

[36] *LTwiki,* (Linear Technology Corporation, 2014).

[37] *LTC3783 PWM LED Driver and Boost, Flyback and SEPIC Controller* (Linear Technology Corporation, 2008).

[38] B. Hamon, B. Bataillou, A. Gasse, and G. Feuillet, *N-contacts degradation analysis of white flip chip LEDs during reliability tests,* in *2014 IEEE International Reliability Physics Symposium* (IEEE).

[39] M. Hudait and S. Krupanidhi, *Doping dependence of the barrier height and ideality factor of au/n-gaas schottky diodes at low temperatures,* Physica B: Condensed Matter (2001).

[40] E. F. Schubert, T. Gessmann, and J. K. Kim, *Light emitting diodes* (Wiley Online Library, 2005).

[41] Y. Huaiyu, K. S. Wee, W. Jia, and H. W. Van Zeijl, *Dynamic thermal simulation of high brightness LEDs with unsteady driver power output,* in *2012 13th International Conference on Thermal, Mechanical and Multi-Physics Simulation and Experiments in Microelectronics and Microsystems (EuroSimE)* (2012).

[42] X. Perpina, R. Werkhoven, M. Vellvehi, X. Jorda, J. Kunen, J. Jakovenk, P. Bancken, and P. Bolt, *LED driver thermal design considerations for solid-state lighting technologies,* in *2012 13th International Conference on Thermal, Mechanical and Multi-Physics Simulation and Experiments in Microelectronics and Microsystems (EuroSimE)* (IEEE, 2013).

[43] J. Jakovenko, R. Werkhoven, J. Formanek, and J. Kunen, *Thermal simulation and validation of 8w LED lamp,* in *2011 12th International Conference on Thermal, Mechanical and Multi-Physics Simulation and Experiments in Microelectronics and Microsystems (EuroSimE)* (2011).

[44] J. Jakovenko, J. Formanek, V. Janicek, M. Huask, and R. Werkhoven, *High power solid state retrofit lamp thermal characterization and modeling,* Radio Engineering (2012).

3

4

A Reliability Prediction for The LED Lamp with An Electrolytic Capacitor Free Driver

This chapter studies the interaction of catastrophic failure of the driver and LED luminous flux decay for an integrated LED lamp with an electrolytic capacitor-free LED driver. Electronic thermal simulations are utilized to obtain the lamp's dynamic history of temperature and current for two distinct operation modes: constant current mode (CCM), and constant light output (CLO) mode, respectively. Driver's mean time to failure (MTTF), and the LED's lifetime in term of luminous flux are calculated. Under CLO mode, the LED's current increases exponentially to maintain the constant light output. As a result, the junction temperatures of LEDs, MOSFETs and power diodes in driver rise significantly, leading to a much shorter MTTF, and faster luminous flux depreciation. However, under the CCM mode, the junction temperatures of LEDs, MOSFETs and diodes change modestly, therefore, the driver's MTTF and LED's luminous flux decay are not affected much by the variation of temperatures during LED's degradation process.

Parts of this chapter have been published by IEEE Transactions on Components, Packaging and Manufacturing Technology [1].

4.1. Introduction

An LED lighting system (lamp or luminaire) is mainly comprised of an LED light source module, a driver, control gears, secondary optical parts, and heat dissipation components [2]. In the past decades, numerous studies have been focusing on the performance and reliability of LED itself [3–12]. A typical LED light source now has a lifetime as long as 25,000 - 100,000 hours in terms of luminous flux maintenance [2, 13]. However, the driver's life is usually much shorter than the light source's, in particular, if electrolytic capacitors are utilized [14–16]. A physics-of-failure (PoF) based reliability prediction methodology has been developed to estimate the failure rate distribution of electrolytic capacitors in LED drivers [14]. In recent years, many electrolytic capacitor-free topologies have been developed with more reliable components [17–19], including thin film capacitors [20] and LC filters [19]. In addition, several new control technologies can also improve the lifetime of electrolytic capacitors, for instance, the resonance-assisted filter [21] and the variable on-time control method [22]. The lifetime of the LED driver may be extended to match the LED light source lifetime [23].

Generally, the lifetime of an LED is given in terms of the expected operating hours until light output has depreciated to 70% of the initial level. The catastrophic failure of an LED driver depends on its critical components and their operation conditions, such as the MOSFETs and power diodes [24–26]. The total rate of catastrophic failures determines the mean time to failure (MTTF) for the driver. There are two distinct concepts of lifetimes involved in an LED system: mean time to failure (e.g. driver), and LED's lifetime in terms of luminous flux depreciation. When these two lifetimes are far different, it is obvious that they do not interact with each other. For example, if driver's MTTF is much less than LED's lifetime, the eventual LED lamp's lifetime is determined by driver's MTTF since the catastrophic failure of the driver will result in the complete light out. However, few study has been conducted to investigate the reliability of LED lamp when the driver's MTTF is comparable to the LED's lifetime.

This chapter studies the interaction of driver's catastrophic failure and LED's luminous flux decay for an integrated LED lamp with an electrolytic capacitor-free LED driver. A fly-back converter with an LC filter is used in the present study. The overall catastrophic failure rate of the critical components in the driver are considered as functions of temperature and current. Electronic thermal simulations are utilized for a commercial LED bulb to obtain the lamp's dynamic history of temperature and current. Two distinct operation modes are considered: constant current mode (CCM), and the constant light output (CLO) mode[27], respectively. The LED's lifetime in terms of luminous flux is calculated using LED's degradation model. A fault tree is applied to calculate the driver's

MTTF.

This chapter is organized as follows. Section 4.2 describes the general methodology. In Section 4.3 to 4.5, the circuit models, LED's degradation model, the thermal models and the failure rate models are introduced respectively. Section 4.6 defines different modes and discusses the results. Section 4.7 concludes this work finally.

4.2. General Methodology

Figure 4.1 displays the general methodology which integrates the electronic thermal simulation with the fault tree method to obtain both the LED's luminous flux decay and driver's probability of catastrophic failures and MTTF. For a given LED system, such as an LED lamp with an integrated driver, electronic simulations are applied to obtain the power distribution of each component in driver and also input power to LEDs. Based on the system's structure and material properties, thermal simulations, which combine both system-level thermal modeling and compact models, are conducted. An iteration process is necessary at each operation time point to determine the state of temperature under operating conditions. Details of the electronic thermal simulation can be found in our previous [14, 28]. Through the electronic thermal simulation, the junction temperature of the LED light source, the current of the driver, and the lumen output can be obtained. LED's luminous flux decay can be calculated based on the calculated results of current and junction temperature using LED's degradation model. The driver's probability of failure and MTTF can also be calculated according to the the failure rate models of critical components. In the following, the details of electronic simulation, the LED's degradation model, the thermal simulation, as well as the MOSFET and diode's failure rate model in driver, are described.

4.3. Electronic Models

4.3.1. Driver Circuit

Figure 4.2 displays a fly-back driver with an LC filter. The LC filter can store energy as capacitors, thus, it is considered as one of the most cost-effective electrolytic capacitor elimination approaches [19, 29]. In this circuit, the models of all components are well validated and verified by manufacturers [30]. The rated input power of the entire driver is 6.3W, and the rated input power is about 5.2W. Ideal feedback units and a current control unit are added, making this driver have two operation modes: the constant current mode (CCM) and the constant light output mode (CLO). In the constant current mode, the current from the driver to the LED light source remains unchanged. The current can be

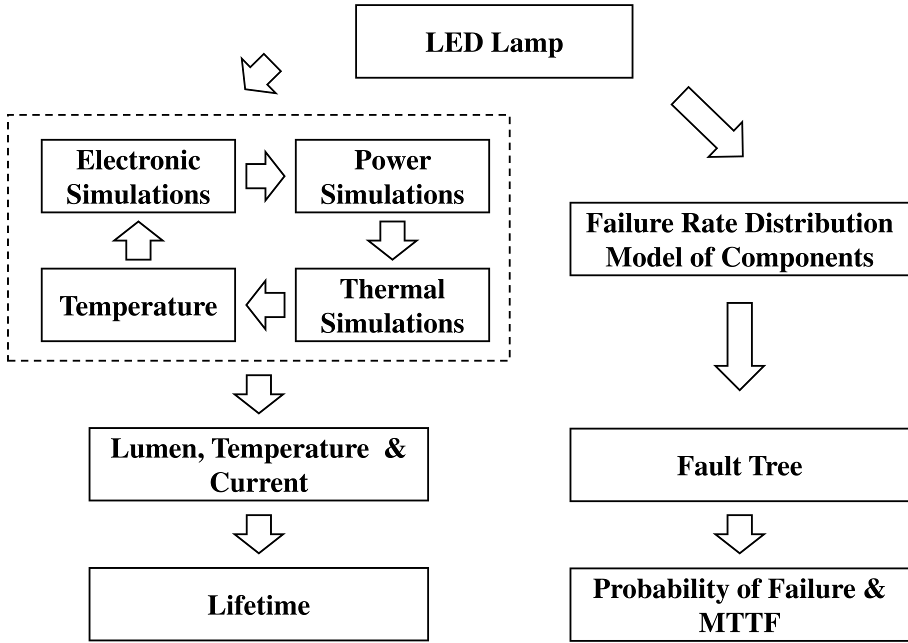

Figure 4.1: General Methodology of The Proposed Approach.

adjusted to achieve invariant light output in CLO mode.

4.3.2. LED LIGHT SOURCE

A temperature-dependent model for LED light source is considered in the circuit model in Figure 4.2. The luminous flux is a function of the ever-changing junction temperature $T_j(t)$ and current $I_{LED}(t)$. Thus, the luminous flux $\Phi_{lm}(t)$ can be described by the following function:

$$\Phi_{lm}(t) = \begin{cases} \eta_0 \cdot \dfrac{B_e I_{LED}^2(t)}{A_e + B_e I_{LED}(t) + C_e I_{LED}^2(t)} \cdot V_f \cdot e^{-\int_0^t \beta[T_j(x)] \cdot dx} & (T_j < T_{MAX}) \\ 0 & (T_j \geq T_{MAX}) \end{cases} \tag{4.1}$$

where η_0 is the basic efficacy, A_e and C_e are the linear and the 3rd-order non-radiative recombination rates, B_e is the radiative recombination rate, V_f is the forward voltage, this work supposes the maximum junction temperature T_{MAX}=423K and β is the depreciation rate which follows the Arrhenius Equation [16]:

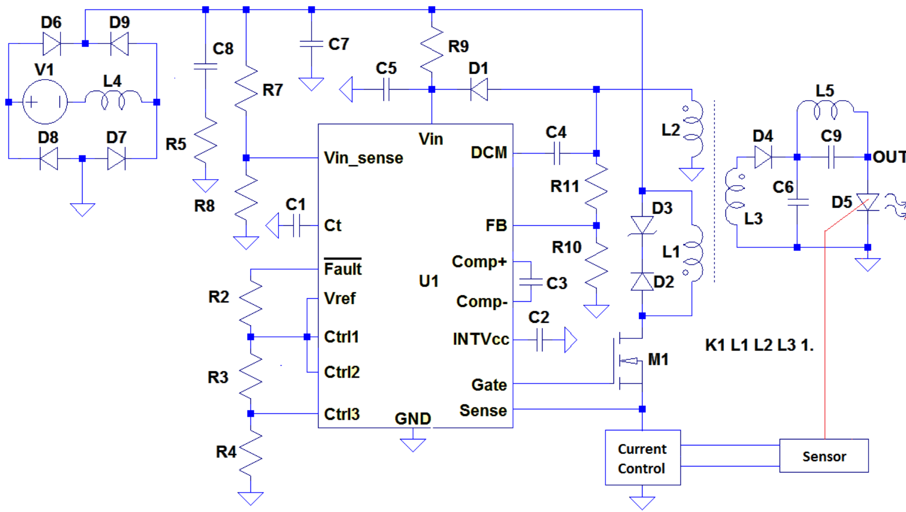

(a)

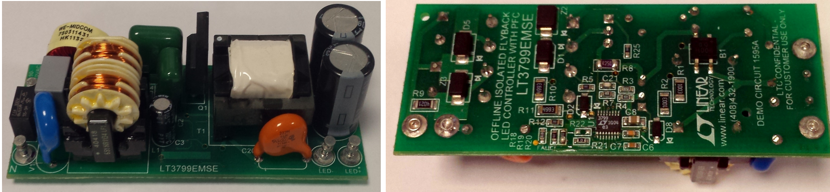

(b)

Figure 4.2: The (a) Circuit and (b) Layout of the Fly-Back LED Driver [31].

$$\beta(T_j) = A_\beta \cdot e^{-\frac{E_{a,\beta}}{\kappa \cdot T_j}} \tag{4.2}$$

The performance of an LED light source can be described by the following function [32]:

$$V_f[I(t), T_j(t)] = N \cdot \kappa \cdot T_j(t) \cdot ln[\frac{I(t)}{I_S} + 1] + R_S \cdot I(t) \tag{4.3}$$

where, N is the ideality factor, κ is the Boltzmann constant, I_s is the saturation current, R_s is the equivalent series resistance of the LED. The R_s, I_s and N can be described by

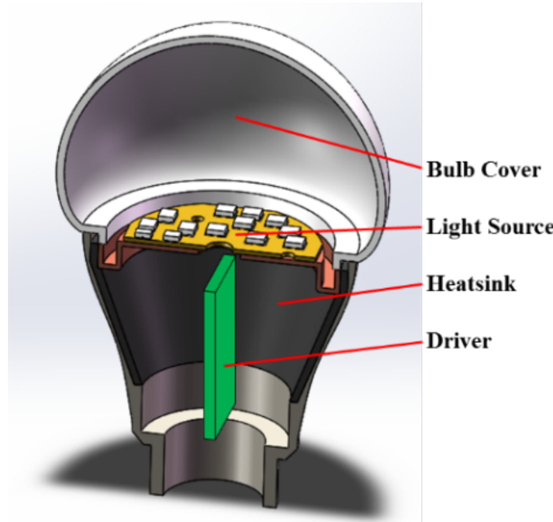

Figure 4.3: The Model of the selected LED Lamp.

the following functions [32–34]:

$$R_S[T_j(t)] = R_{S0} \cdot [1 + A_S \cdot T_j(t)] \tag{4.4}$$

$$I_S[T_j(t)] = I_{S0} \cdot T_j^2(t) \cdot e^{-\frac{A_I}{T_j(t)}} \tag{4.5}$$

$$N[T_j(t)] = \frac{T_j(t)}{A_N \cdot T_j(t) + B_N} \tag{4.6}$$

The details of the LED models mentioned above can be found in the literature [28, 35].

4.4. Thermal Simulation

A commercial LED bulb is selected as the carrier of the present study. As shown in Figure 4.3, it consists of a bulb cover, LED light source, heat sinks, a driver and other relevant parts [36]. The light source of this lamp includes 24 LED packages mounted on a metal board. The original driver in this lamp is replaced by the electrolytic capacitor free driver shown in Figure 4.2 for the purpose of the study in this chapter.

The heat sources come from the LEDs and the driver's components. System level thermal simulations are conducted to calculate the LEDs' junction temperature T_{LED} and air temperature around the driver T_D. The driver (the green part in Figure 4.3) is considered as homogeneous material with heat from the driver distributed evenly on

surface. In the system level thermal model, the thermal power densities of LEDs and the driver are $8.45\times10^5 W\cdot m^{-2}$ and $1.9\times10^6 W\cdot m^{-3}$ respectively. The lamp operates in room temperature (296K) with a natural convection condition $(10.5W\cdot(m^2\cdot K)^{-1})$. Table 4.1 lists thermal conductivity used in system level thermal simulations.

Table 4.1: Thermal Material Properties

Part	Thermal Conductivity
Bulb Cover	$2.0\times10^{-1} W\cdot(m\cdot K)^{-1}$
LED Board	$1.2\times10^{1} W\cdot(m\cdot K)^{-1}$
Heat Sink	$1.1\times10^{2} W\cdot(m\cdot K)^{-1}$
Driver	$1.5\times10^{-1} W\cdot(m\cdot K)^{-1}$
LED Chip	$4.5\times10^{1} W\cdot(m\cdot K)^{-1}$
LED Package	$5.0W\cdot(m\cdot K)^{-1}$
Welding Layer	$2.5\times10^{1} W\cdot(m\cdot K)^{-1}$
Lamp Shell	$1.0\times10^{1} W\cdot(m\cdot K)^{-1}$

The thermal compact model of each critical component in the driver is applied to find their junction temperature:

$$T_{j,i} = T_D + R_{th,i}\cdot P_{th,i} \tag{4.7}$$

where $T_{j,i}$ is the the junction temperature of the component, $R_{th,i}$ is the thermal resistance from junction to surface of the component which is usually provided by components' data-sheets [37], $P_{th,i}$ is the thermal power of the component.

To validate the system level thermal simulation, temperature distribution of the lamp is measured. The lamp is place in the room temperature (296K) and natural convection condition. The temperature at each point is measured by a thermocouple pyrometer system. Figure 4.4 displays the simulation results, and Table 4.2 compares the test and simulation results. Errors between the simulation and test results are less than 1K.

Table 4.2: Thermal Material Properties

Position	Simulation Result	Test Result	Error
Light Source	379.7K 106.7°C	379.4K	0.290K
Heatsink 1	367.4K 94.4°C	367.1K	0.264K
Heatsink 2	366.3K 93.3°C	366.0K	0.268K
Heatsink 3	364.9K 91.9°C	365.5K	0.596K
Driver	398.5K 125.5°C	398.6K	0.103K

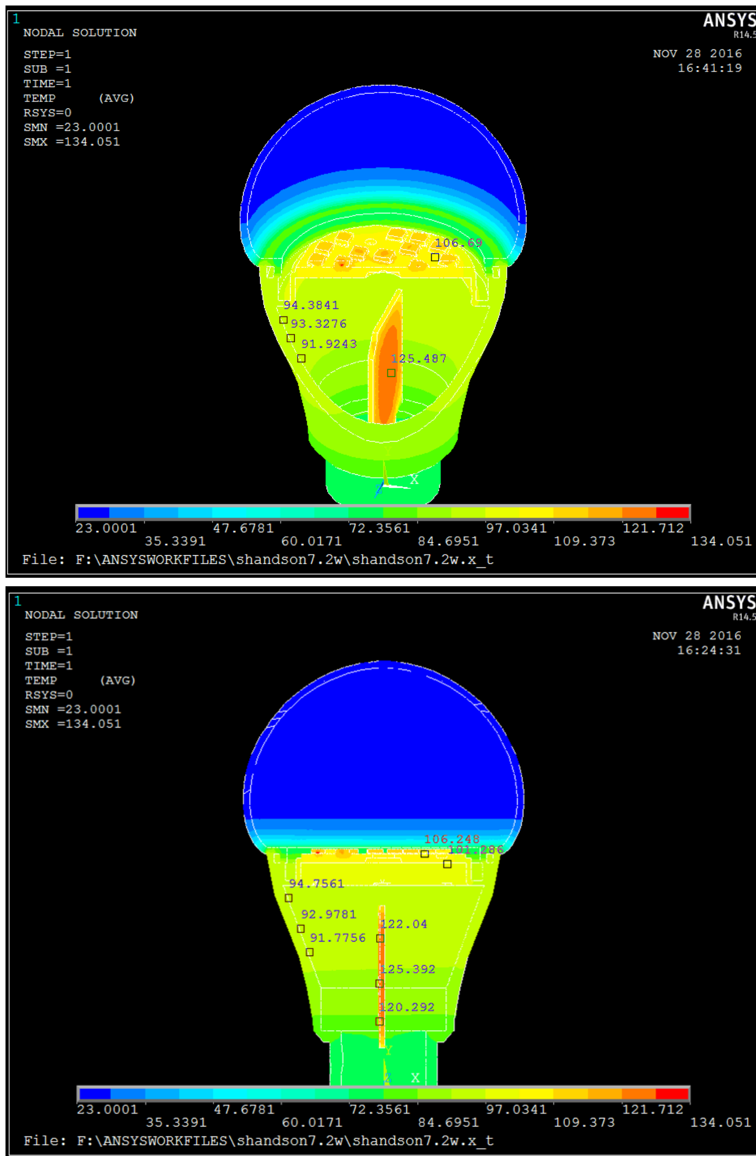

Figure 4.4: The Model of The selected LED Lamp.

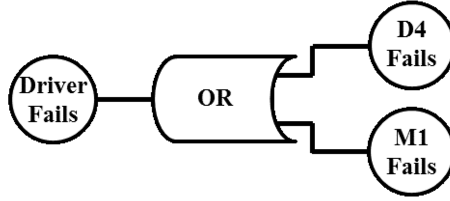

Figure 4.5: The Fault Tree of The LED Driver.

4.5. FAULT TREE AND THE MODEL OF FAILURE PROBABILITY

THE catastrophic failures of the MOSFET M1 and the Diode D4 in the circuit shown in Figure 4.2 are considered. Assuming that the failures of M1 and D4 are independent to each other, the probability density of the catastrophic failure of the driver can be described by the following function:

$$f_{Driver}(t) = f_M(t) + f_D(t) - f_M(t) \cdot f_D(t) \tag{4.8}$$

where f_{Driver} is the failure probability density of the LED driver at time t, f_M is the failure probability density of the MOSFET, f_D is the failure probability density of the diode. Equation 4.8 is described by a fault tree shown in Figure 4.5.

The failure probability density of a MOSFET can be described by the inverse power law [38]:

$$f_M(t) = f_M[I_M(t), T_M(t)] = f_{M0} \cdot [\frac{I_M(t)}{I_{rate}}]^p \cdot e^{-\frac{E_{a,M}}{\kappa}[\frac{1}{T_M(t)} - \frac{1}{T_A}]} \tag{4.9}$$

where $I_M(t)$ is the average current of the MOSFET at time t, $T_M(t)$ is junction temperature of the MOSFET at time t, f_{M0} is the failure probability density of the MOSFET in rated current I_{rated} and typical ambient temperature T_A=298K, p is the current accelerated coefficient and $E_{a,M}$ is the activation energy of the MOSFET.

The failure probability density of a diode can be described by the [38]:

$$f_D(t) = f_D[T_D(t)] = f_{D0} \cdot e^{-\frac{E_{a,D}}{\kappa}[\frac{1}{T_D(t)} - \frac{1}{T_A}]} \tag{4.10}$$

where, f_D is the failure probability density of the diode, T_{Di} (t) is junction temperature of the diode at time t, f_{D0} is the rated failure probability density of the diode in typical ambient temperature T_A=298K, $E_{a,D}$ is the activation energy of the diode.

The conditions $I_M(t)$, $T_M(t)$ and $T_{Di}(t)$ at each operation time point can be obtained by the electronic-thermal simulations, and thus, the failure probability densities f_M, f_D

and f_{Driver} at each time point can be calculated by Equation 4.8 to 4.10. Then, the mean time to failure (MTTF) of the LED driver can be calculated by the following equation:

$$MTTF = \frac{t_{MAX}}{\int_0^{t_{MAX}} f_{Driver}(t) \cdot dt} \tag{4.11}$$

where t_{MAX} is the total operation duration. In order to simply the calculation, this work selects 1000 hours as the time increment. Between two time points, the integrating region is assumed to be a trapezoid.

4

4.6. Case Studies and Results

4.6.1. Selection of LED and Driver

The LED light source is preselected with the activation energy and pre-factor of $E_{a,\beta}$= 0.3eV and A_β= 0.2829, according to our previous test results [35]. The other parameters that appear in Equation 4.1 to 4.6 are listed in Table 4.3. Those data were extracted experimentally from our previous study [28, 35].

Table 4.3: Physical Parameters of The LED Light Source

Parameter	Value	Parameter	Value
R_{s0}	5.914×10^{-1}	A_s	6.699×10^{-4}
I_{s0}	4.786×10^{5}	A_I	1.274×10^{-1}
A_n	1.240	B_n	-2.882×10^{2}
C	4.087×10^{-3}	η_0	1.456×10^{2}
A_e	0.999	B_e	1.406×10^{3}
C_e	2.138×10^{3}		

According to the electronic thermal simulation at the initial state during operation, the LED's junction temperature is about 340K. Based on the parameters defined above, the LED's lifetime in terms of luminous flux decay is about 25000 hours at the constant temperature 340K and with a current of 400mA, by Equation 4.1 and 4.2.

For the driver, the empirical values [39] of model parameters for the MOSFET M1 and Diode D4 shown Equation 4.9 and 4.10 are selected as p of 2.0, $E_{a,M}$ and $E_{a,D}$ as 0.7eV respectively. According to the simulation results, the initial junction temperature values of $T_M(0)$ for M1 and $T_{Di}(0)$ for D4, are about 357K and 344K respectively. Assume that the driver's MTTF at the initial state equals to 25,000hours, $f_{M0} = 4.12 \times 10^(- 7)$, $f_{D0} = 2.74 \times 10^(- 7)$. Since temperatures in the lamp and the current during operation will change over time, the actual LED's lifetime in terms of luminous flux decay and the

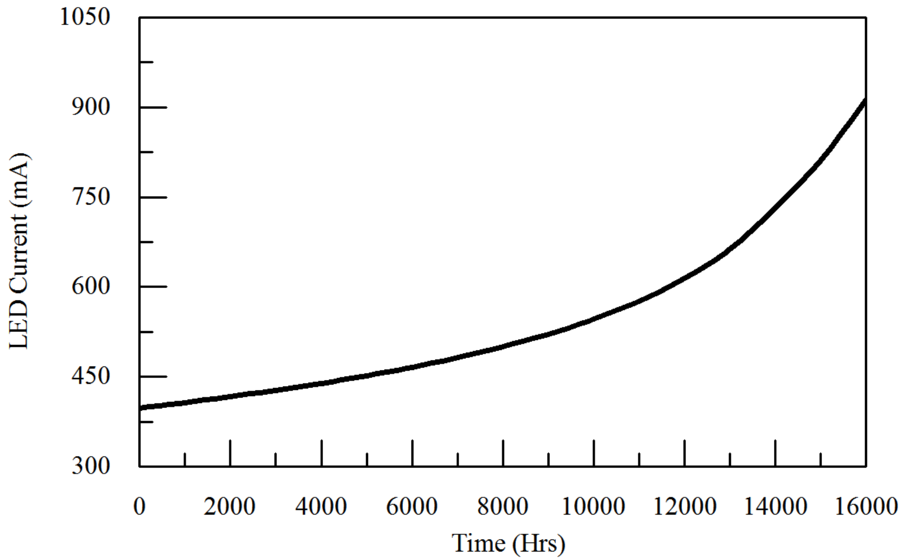

Figure 4.6: The LED Current Curve of The CLO Mode.

MTTF for driver will be different from the pre-selected values. The details of the results will be discussed below.

4.6.2. Results and Discussions

Constant Light Output (CLO) Mode

Figure 4.6 displays the LED current curve at the CLO mode. The LED's current increases exponentially, e.g. from the initial 400mA to 910mA in 16000 hours. Such an increase in current mainly compensates the luminous efficacy degradation of the LED to maintain the constant light output.

Figure 4.7 displays the LED junction temperature as a function of time. Due to the elevated current, the LED's temperature increases greatly. At 16000 hours, the junction temperature of the LED light source increases by about 84K and exceeds 423K.

Figure 4.8 shows the history of the junction temperatures of M1 and D4 at the CLO mode. In 16,000 hours, the junction temperatures of M1 increases from 357K to 452K, and the junction temperatures of D4 rises from 344K to 432K. Figure 4.9 shows the cumulative failure rate of M1 in different conditions of the CLO mode. In the constant temperature and current of the M1, the cumulative failure rate is about 47% at 16000 hours. If M1's junction temperature increase only is considered, the failure rate accumulates to 100% around 12000 hours. If M1's current increase only is considered, the cumulative

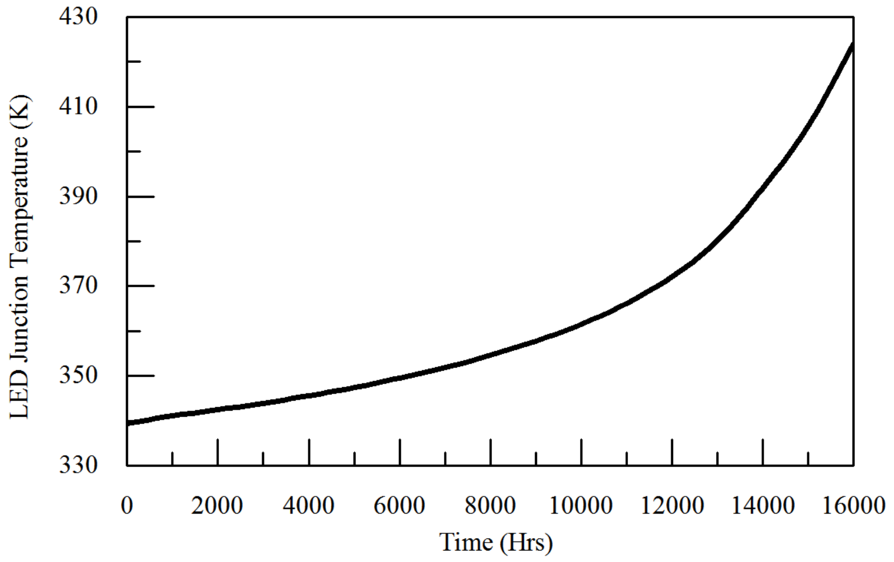

Figure 4.7: The LED Junction Temperature of The CLO Mode.

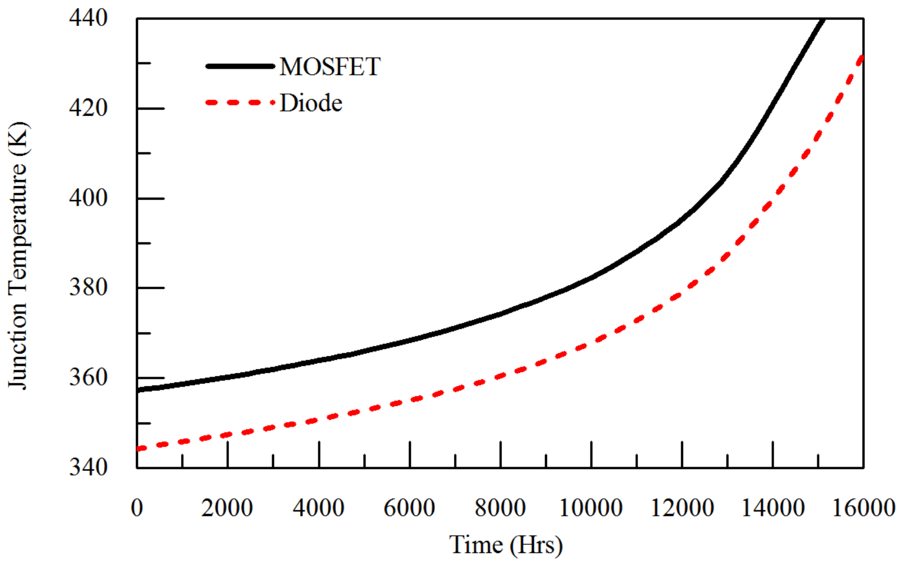

Figure 4.8: The Junction Temperature of M1 and D4 of The CLO Mode.

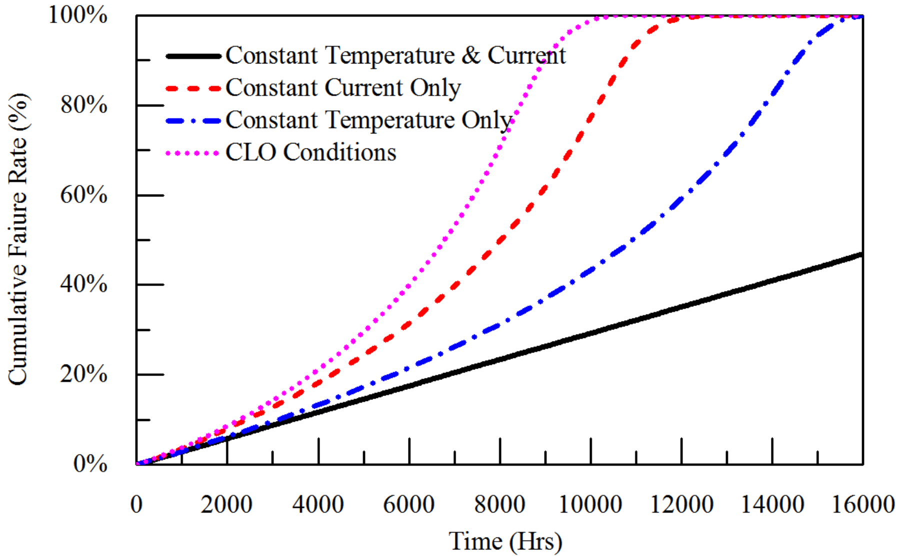

Figure 4.9: Cumulative Failure Rates of M1 in The CLO Mode.

failure rate is about 98% at 16000 hours. If both of junction temperature and current of M1 in CLO mode are considered, the failure rate of M1 accumulates to 100% in about 10000 hours. The increased junction temperature has larger effects on the failure rate.

Figure 4.10 displays cumulative failure rate of the driver for the CLO mode in comparison with a constant temperature and a constant current, same as the initial ones. In the ever-changing temperature and current operation condition, the driver's failure rate accumulates to 100% in about 8700 hours. In the constant temperature and current condition, the failure rate accumulates about 64% in 16000 hours. As discussed above, the driver's failure rates are greatly increased due to the significant increase of driver's temperature and current. Thus, the driver in the CLO mode has a much shorter MTTF than in constant condition.

CONSTANT CURRENT MODE (CCM)

Figure 4.11 displays the LED junction temperature in CCM mode. After 25000 hours, the junction temperature of the LED light source increases by only about 6K. As the LED degrades, more thermal power is generated, leading temperature increase for the entire lamp modestly. However, such rise is much less than that in CLO mode.

Figure 4.12 displays the normalized luminous flux maintenance under CCM mode. The LED's lifetime is reduced to about 20000 hours, 20% shorter than in the constant temperature and current.

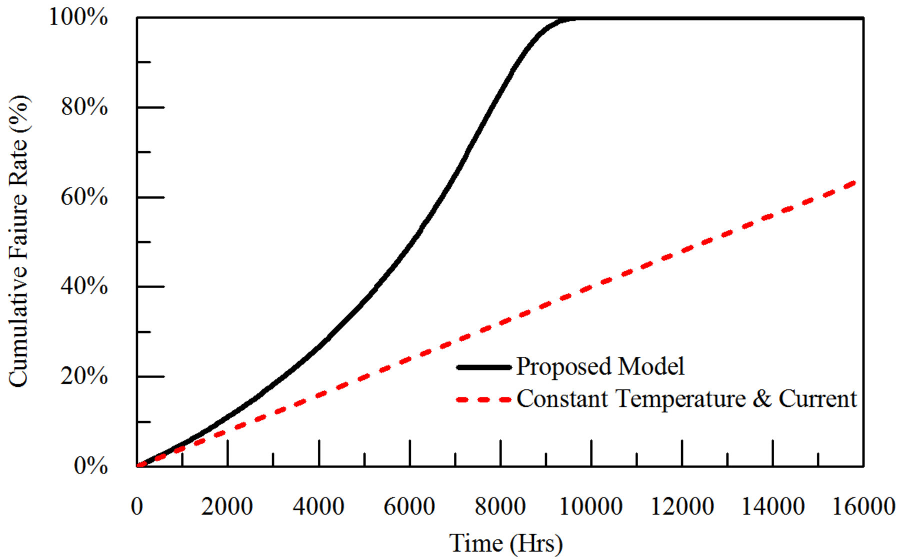

Figure 4.10: Cumulative Failure Rates of The Driver in CLO Mode.

Figure 4.13 shows the history of the junction temperatures of M1 and D4 in the CCM mode. The junction temperature of M1 increases from 357K to 364K, and D4's junction temperature rises from 344K to 349K in 25000 hours. Compared with the CLO mode, the junction temperature of M1 and D4 increase slightly.

Figure 4.14 displays cumulative failure rate of the driver in different conditions of CCM mode. The LED driver's failure rate accumulates to 100% in about 22500 hours, compared to 25,000hours at the constant temperature and current. This implies that the driver's failure rate in CCM mode does not change dramatically, as seen in CLO mode.

Table 4.4 summarizes LED's lifetimes in terms of lumen output and the driver's MTTFs for CLO and CCM modes. It is seen that even the preselected driver and LED both have a lifetime of 25,000 hours at the initial respective junction temperatures and operating current conditions, the actual lamp's lifetime can be significantly shorter in CLO mode. This is because that the current continually increases in LEDs for the CLO mode, which will increase the LED's junction temperature greatly. Since the driver is integrated together with LED, the driver's M1 and D4 junction temperatures also increase significantly, leading to a much early failure. In the CLO mode for the lamp studied here, since the LED's lifetime in terms of luminous decay is 16,000 hours, the catastrophic failure will occur first. It means that the whole lamp will have a lifetime of 8,700 hours.

In the CCM mode, the luminous flux decay lifetime is slightly shorter than the driver's

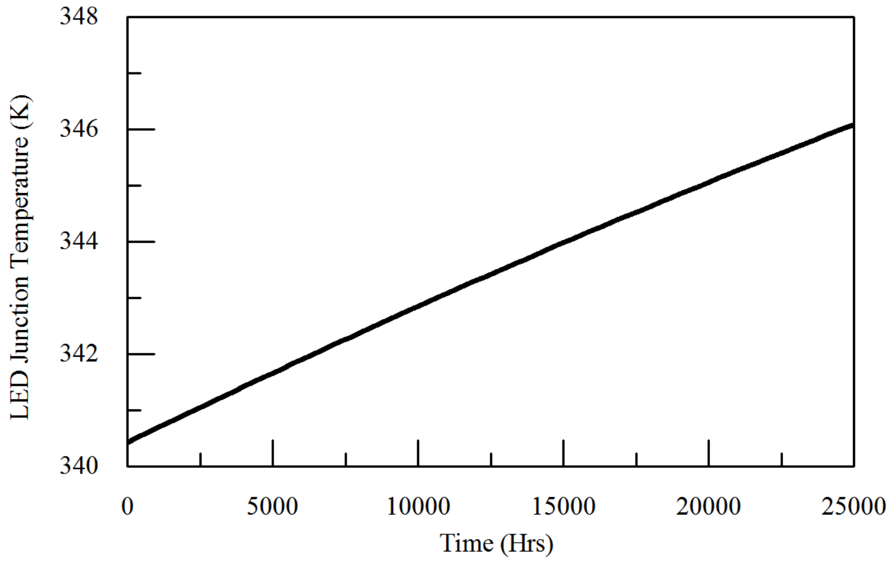

Figure 4.11: The LED Junction Temperature of The CCM Mode.

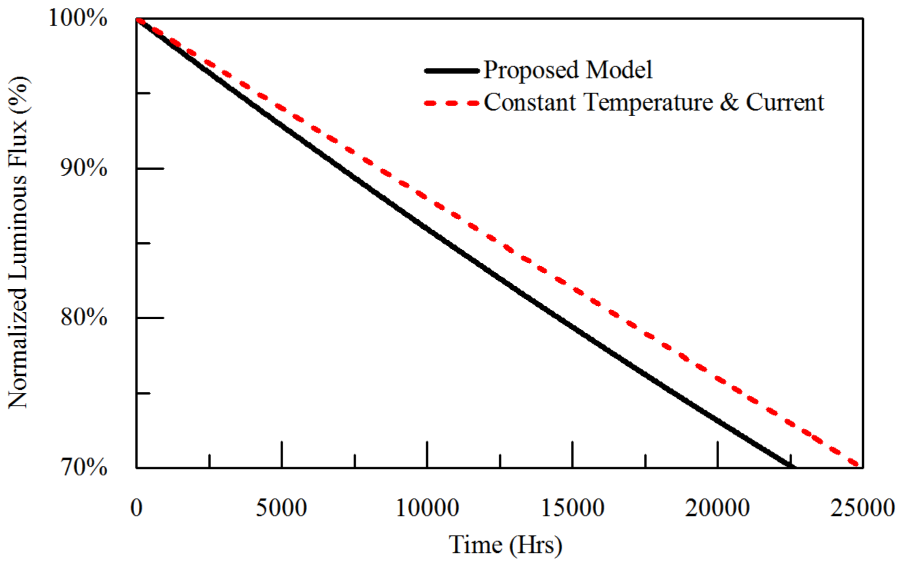

Figure 4.12: Normalized Luminous Flux of The CCM Mode.

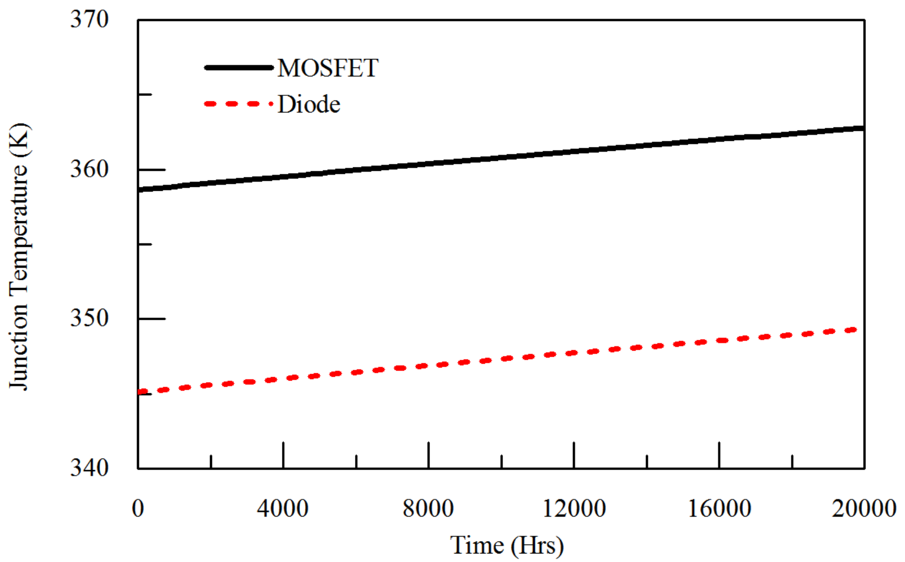

Figure 4.13: The Junction Temperatures of M1 and D4 in The CCM Mode.

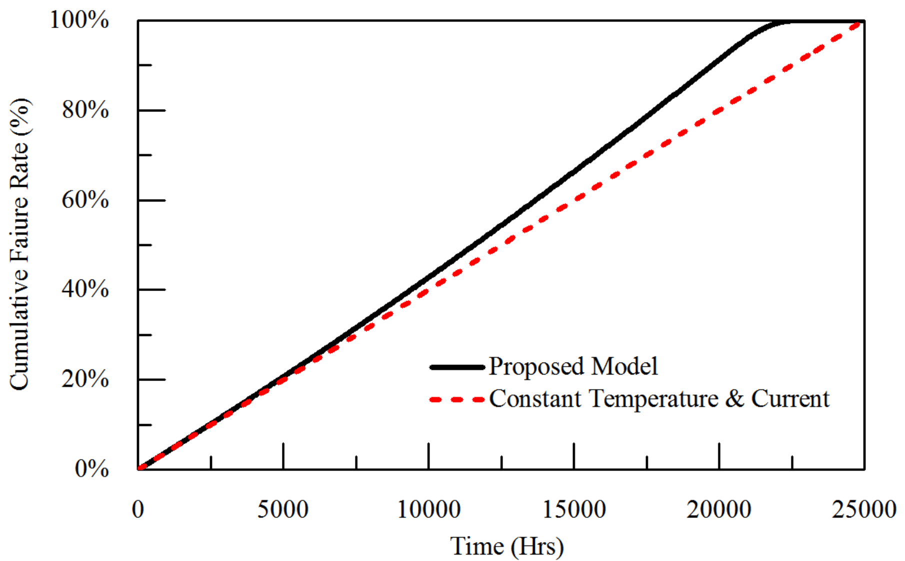

Figure 4.14: Cumulative Failure Rates of The Driver in The CCM Mode.

MTTF, thus, the lamp will fail first due to the unacceptable luminous flux output. However, since both MTTF and luminous flux decay time are very close, it is also possible that the lamp will fail first by catastrophic failure. In either case, the lamp's actual lifetime is still less than the designed target of 25,000 hours.

Table 4.4: Lifetime and MTTF

Case	Lifetime (Hrs)	T_j(K)	MTTF (Hrs)	T_D(K)
Initial Status	25'000	340	25'000	336
CLO	16'000	Varying	8'700	Varying
CCM	20'000	Varying	22'500	Varying

4.7. CONCLUSIONS

THIS chapter studies the interaction of catastrophic failures of a driver and the LED light source on the actual lifetime of the lamp. There are two distinct concepts of lifetimes involved in an LED lamp: driver's MTTF in terms of catastrophic failure, and LED's lifetime in terms of luminous flux output. The actual LED's lifetime is taken from the smaller one of these two values. LED's lifetime in terms of luminous flux decay depends on the history of LED's junction temperature and current. Driver's MTTF depends on the history of junction temperatures of key components, such as MOSFET and diodes in the driver. Electronic simulations were conducted first to obtain the power distributions among components and the current passing through LEDs. Then system-level thermal simulation and compact model were applied to obtain the temperature distributions. Since the LED's degradation is a continuous process, such electronic and thermal simulations need to be carried out throughout whole time domain.

In the present study, a fly-back converter with an LC filter is used. Two distinct operation modes are considered: the constant current mode (CCM), and the constant light output (CLO) mode, respectively. Under the CLO mode, LED's current increases exponentially. As a result, the junction temperatures of LEDs, MOSFET and diode rise by about 84K, 95K and 88K respectively in about 16,000 hours. The constant light output mode eliminates lumen depreciation at the expense of the LED lamp's reliability. Since the MTTF of the driver in the CLO mode is much shorter than the LED's luminous flux decay lifetime, the catastrophic failure of the driver will occur first.

For the CCM mode, since the current is forced to remain unchanged, the junction temperatures of the LED, the MOSFET and the diode rise modestly about 6K, 7K and 5K respectively, leading the lifetime drops to about 20000 hours, and the MTTF drops to

about 22500 hours. Since the LED's lifetime and driver's MTTF in this mode are comparable, either catastrophic failure or the excessive lumen depreciation may occur first.

4

REFERENCES

[1] *A reliability prediction for integrated LED lamp with electrolytic capacitor-free driver,* IEEE Transactions on Components, Packaging and Manufacturing Technology **7**, 1081 (2017).

[2] W. D. van Driel and X. J. Fan, *Solid state lighting reliability: components to systems* (Springer Science & Business Media, 2012).

[3] J. P. Kim and S. W. Jeon, *Investigation of light extraction by refractive index of an encapsulant, a package structure, and phosphor,* IEEE Transactions on Components, Packaging and Manufacturing Technology **6**, 1815 (2016).

[4] X. Yu, B. Xie, Q. Chen, Y. Ma, R. Wu, and X. Luo, *Thermal remote phosphor coating for phosphor-converted white-light-emitting diodes,* IEEE Transactions on Components, Packaging and Manufacturing Technology **5**, 1253 (2015).

[5] X. Liu, Z. Lv, and S. Liu, *Low thermal-resistance silicon-based substrate for light-emitting diode packaging,* IEEE Transactions on Components, Packaging and Manufacturing Technology **5**, 1387 (2015).

[6] Y. Liu, Z. Lin, X. Zhao, C. C. Tuan, K. S. Moon, S. Yoo, M. G. Jang, and C. p. Wong, *High refractive index and transparent nanocomposites as encapsulant for high brightness LED packaging,* IEEE Transactions on Components, Packaging and Manufacturing Technology **4**, 1125 (2014).

[7] Z. Chen, Q. Zhang, F. Jiao, R. Chen, K. Wang, M. Chen, and S. Liu, *Study on the reliability of application-specific LED package by thermal shock testing, failure analysis, and fluid-solid coupling thermo-mechanical simulation,* IEEE Transactions on Components, Packaging and Manufacturing Technology **2**, 1135 (2012).

[8] C. Qian, X. J. Fan, J. Fan, C. Yuan, and G. Q. Zhang, *An accelerated test method of luminous flux depreciation for LED luminaires and lamps,* Reliability Engineering & System Safety **147**, 84 (2016).

[9] J. Huang, D. S. Golubovic, S. Koh, D. Yang, X. Li, X. J. Fan, and G. Q. Zhang, *Degradation mechanisms of mid-power white-light LEDs under high-temperature-humidity conditions,* IEEE Transactions on Device and Materials Reliability **15**, 220 (2015).

[10] J. Huang, D. S. Golubović, S. Koh, D. Yang, X. Li, X. J. Fan, and G. Q. Zhang, *Rapid degradation of mid-power white-light LEDs in saturated moisture conditions,* IEEE Transactions on Device and Materials Reliability (2015).

[11] J. Fan, C. Qian, K. C. Yung, X. J. Fan, G. Q. Zhang, and M. Pecht, *Optimal design of life testing for high-brightness white LEDs using the six sigma DMAIC approach,* IEEE Transactions on Device and Materials Reliability (2015).

[12] Y. Zhao, J. Liu, A. Wei, and J. Li, *High-power light-emitting diodes package with phase change material,* IEEE Transactions on Components, Packaging and Manufacturing Technology **4**, 1747 (2014).

[13] *Hammer Testing Findings for Solid-State Lighting Luminaires* (Department of Energy (DoE), United States, 2013).

[14] B. Sun, X. J. Fan, C. Qian, and G. Q. Zhang, *PoF-simulation-assisted reliability prediction for electrolytic capacitor in LED drivers,* IEEE Transactions on Industrial Electronics **63**, 6726 (2016).

[15] B. Sun, X. J. Fan, C. Yuan, C. Qian, and G. Q. Zhang, *A degradation model of aluminum electrolytic capacitors for LED drivers,* in *Thermal, Mechanical and Multi-Physics Simulation and Experiments in Microelectronics and Microsystems (EuroSimE), 2015 16th International Conference on* (IEEE, 2015) pp. 1–4.

[16] S. Koh, C. Yuan, B. Sun, B. Li, X. J. Fan, and G. Q. Zhang, *Product level accelerated lifetime test for indoor LED luminaires,* in *2013 14th International Conference on Thermal, Mechanical and Multi-Physics Simulation and Experiments in Microelectronics and Microsystems (EuroSimE)* (IEEE, 2013).

[17] L. Gu, X. Ruan, M. Xu, and K. Yao, *Means of eliminating electrolytic capacitor in AC/DC power supplies for LED lightings,* IEEE Transactions on Power Electronics (2009).

[18] J. C. Lam and P. K. Jain, *A high power factor, electrolytic capacitor-less AC-input LED driver topology with high frequency pulsating output current,* IEEE Transactions on Power Electronics (2015).

[19] L. Gu, X. Ruan, M. Xu, and K. Yao, *Means of eliminating electrolytic capacitor in AC/DC power supplies for LED lightings,* IEEE Transactions on Power Electronics (2009).

[20] S. Gandhi, M. R. Pulugurtha, H. Sharma, P. Chakraborti, and R. R. Tummala, *High-k thin-film capacitors with conducting oxide electrodes on glass substrates for power-supply applications,* IEEE Transactions on Components, Packaging and Manufacturing Technology **6**, 1561 (2016).

[21] X. Qu, S. C. Wong, and C. K. Tse, *Resonance-assisted buck converter for offline driving of power LED replacement lamps,* Power Electronics, IEEE Transactions on **26**, 532 (2011).

[22] X. Wu, J. Yang, J. Zhang, and Z. Qian, *Variable on-time (VOT)-controlled critical conduction mode buck PFC converter for high-input AC/DC hb-LED lighting applications,* Power Electronics, IEEE Transactions on **27**, 4530 (2012).

[23] S. Dietrich, S. Strache, R. Wunderlich, and S. Heinen, *Get the LED out: Experimental validation of a capacitor-free single-inductor, multiple-output LED driver topology,* Industrial Electronics Magazine, IEEE **9**, 24 (2015).

[24] S. Lan, C. M. Tan, and K. Wu, *Methodology of reliability enhancement for high power LED driver,* Microelectronics Reliability **54**, 1150 (2014).

[25] R. Wu, F. Blaabjerg, H. Wang, and M. Liserre, *Overview of catastrophic failures of freewheeling diodes in power electronic circuits,* Microelectronics Reliability **53**, 1788 (2013).

[26] A. Scandurra, G. F. Indelli, R. Zafarana, A. Cavallaro, E. Scrofani, J. P. Giry, S. Russo, and M. Bakowski, *Molding compounds adhesion and influence on reliability of plastic packages for SiC-based power MOS devices,* IEEE Transactions on Components, Packaging and Manufacturing Technology **3**, 1094 (2013).

[27] Philips, *Constant Light Output (CLO)* (2014).

[28] B. Sun, X. Fan, W. van Driel, H. Ye, J. Fan, C. Qian, and G. Zhang, *A novel lifetime prediction for integrated LED lamps by electronic-thermal simulation,* Reliability Engineering & System Safety, Accepted **163**, 14 (2017).

[29] B. Wang, X. Ruan, K. Yao, and M. Xu, *A method of reducing the peak-to-average ratio of LED current for electrolytic capacitor-less AC-DC drivers,* Power Electronics, IEEE Transactions on **25**, 592 (2010).

[30] *LTwiki,* (Linear Technology Corporation, 2014).

4

[31] *LT3799 Offline Isolated Flyback LED Controller with Active PFC* (Linear Technology Corporation, 2011).

[32] E. F. Schubert, T. Gessmann, and J. K. Kim, *Light emitting diodes* (Wiley Online Library, 2005).

[33] H. T. Chen, S. C. Tan, and S. Hui, *Color variation reduction of GaN-based white light-emitting diodes via peak-wavelength stabilization,* IEEE Transactions on Power Electronics (2014).

[34] M. Hudait and S. Krupanidhi, *Doping dependence of the barrier height and ideality factor of au/n-gaas schottky diodes at low temperatures,* Physica B: Condensed Matter (2001).

[35] B. Sun, X. J. Fan, W. v. Driel, T. Michel, J. Zhou, and G. Q. Zhang, *Lumen decay prediction in LED lamps,* in *IEEE International Conference on Thermal, Mechanical and Multi-Physics Simulation and Experiments in Microelectronics and Microsystems (EuroSIME)* (2015).

[36] Y. Huaiyu, K. S. Wee, W. Jia, and H. W. Van Zeijl, *Dynamic thermal simulation of high brightness LEDs with unsteady driver power output,* in *2012 13th International Conference on Thermal, Mechanical and Multi-Physics Simulation and Experiments in Microelectronics and Microsystems (EuroSimE)* (2012).

[37] *ES1A-ES1J Surface Mount Rectifiers* (Technology, Lu Guang Electronic, 2012).

[38] T. Santini, S. Morand, M. Fouladirad, L. Phung, F. Miller, B. Foucher, A. Grall, and B. Allard, *Accelerated degradation data of SiC MOSFETs for lifetime and remaining useful life assessment,* Microelectronics Reliability **54**, 1718 (2014).

[39] *MIL-HDBK-217F: Reliability Prediction of Electronic Equipment* (Department of Defense (DoD), United States, 1995).

5

A Physics and Statistics Combined Reliability Prediction Methodology for LED Drivers

In this chapter, stochastic properties of LEDs degradation are taken into consideration to investigate the reliability of the LED driver in an integrated LED lamp. The lumen depreciation process leads to the increase of the air temperature surrounding the driver, thus affecting driver's reliability. The Wiener process is introduced to describe the randomness of lumen depreciation process. The compact thermal model of the LED lamp is developed to obtain the relationship between LED's thermal dissipation and junction temperatures of critical components in the driver. The driver's survival probability is then obtained using the Markov Chain method. The effect of the lumen depreciation to the driver is studied with two scenarios. It has been found that the statistical properties of LEDs life data will lead to a large range of the driver's survival probability. The stochastic analysis of LEDs life data from accelerated degradation testing can improve the accuracy of the prediction of the LED driver and LED lamp.

Parts of this chapter have been submitted to IEEE Transactions on Industrial Electronics, 2017 [1].

5.1. Introduction

Light emitting diode (LED) lamps have been rapidly developed in recent years due to the wide applications of commercial blue LEDs [2, 3]. The market share of LED lighting products will increase to about 60% to 75% before 2020 [2]. An LED lamp mainly comprises an LED light source, a driver, control gear, secondary optical parts, and heat dissipation components [2]. Compared to the conventional lamps, LED lamps have many unique advantages such as its superior energy efficiency, environmental friendliness, and long lifetime [2, 4]. Numerous studies have been focusing on the reliability of LED itself [5–10]. For example, the relationship between LED structure and thermal resistance has been studied [11]. A control methodology for nonlinear photo-electro-thermal dynamics of LEDs has been developed [12]. An accelerated test method has been developed to shorten lumen depreciation process of LED lamps or luminaires [5]. The LED color shift by optical materials has been investigated [8, 9]. The impact of high temperature-humidity environment to LEDs' degradation have been studied [6, 7]. Although it claims an LED's lifetime up to 25,000 to 100,000 hours [2, 4], the customer experiences may be different, and some of the LED lamps can fail for a considerable time ahead of the claimed lifetime [4, 13]. One of the reasons for such a discrepancy between the claimed lifetime and the practical lifetime of an LED lamp could be due to the mismatch in the lifetime of the LEDs and the driver [14].

The driver is considered as one of the major reliability bottlenecks of LED lamps. To investigate the primary causes of failures in drivers, various critical components and materials including electrolytic capacitors [15, 16], ceramic capacitors [17], molding compounds [18] and power transistors [19] have been studied. Usually, the electrolytic capacitor is considered as the weakest link in mainstream LED drivers [20, 21]. Thus, many new technologies have been developed to avoid failures of electrolytic capacitors [22], for instance, input current shaping [23], power decoupling [24], harmonic injection [25], LC filtering [26], resonance-assisted filtering [27] and variable on-time control [28]. Further, numerous reliability assessment methods have been developed for drivers. For instance, empirical models have been adopted to predict the probability of failures of critical components [29]. The Markov Chain model has been applied for the reliability modeling of boost converters [30]. Physics-of-failure (PoF) based reliability simulations have been developed to study the interaction between the lumen depreciation and driver's failure [31, 32].

For an integrated LED lamp, the driver's operating temperature interacts with LED's lumen depreciation. With the decay of luminous flux, the LED light source will generate more heat, which causes the driver's operation temperature to rise. It has been found

that high operating temperature can accelerate degradation of the driver [31] and lead to catastrophic failures [32]. However, conventional lifetime prediction methods for LED lamps assume that the drive operates at a constant temperature condition.

The randomness of the LED's lumen depreciation has been well studied for LED itself. For instance, reliability models based on Gamma process [33] and Wiener process [14] have been developed to predict the luminous decay and color shift of LEDs. A Six sigma DMAIC approach is used for life test for white LEDs [10]. The real operation conditions have been considered by an LED life prediction method [34]. However, few studies consider the effect of randomness lumen depreciation on LED driver's reliability.

This chapter studies the effect of statistical property of LED's lumen depreciation on LED driver's reliability. An integrated LED light bulb is selected for the purpose of study. The Wiener process based model is introduced to describe the lumen depreciation process. The compact thermal model is developed to obtain the relationship between LEDs' thermal dissipation and junction temperatures of the critical components in the driver. The probability of catastrophic failures in the driver can then be obtained by the Markov Chain method by considering the increase of driver's temperature. The effect of the lumen depreciation to the driver is studied with two scenarios.

This chapter is organized as follows. Section 5.2 introduces the methodology. Section 5.3 describes the lumen depreciation model of the LED light source based on the Wiener process. Section 5.4 explains the reliability model of selected LED driver. Section 5.5 introduces the compact thermal model of the LED lamp. Section 5.6 defines various scenarios of case studies and discusses the results. Section 5.7 concludes this work.

5.2. METHODOLOGY

THIS considers the lumen depreciation process as a stochastic process. At each time point, the lumen maintenance of the LED light source follows a certain distribution. Meanwhile, the lumen maintenance determines power distribution of an integrated LED lamp, including thermal power and optical power. With different lumen maintenance, an integrated LED lamp will have a different thermal power distribution and thus a different temperature distribution. Since the light source and the driver are assembled together, the air temperature surrounding the driver will increase with the lumen depreciation process and has a certain randomness at each time point.

As shown in Figure 5.1, the proposed methodology contains the lumen depreciation model, thermal model, reliability models.

The lumen depreciation model uses the Wiener process to describe the lumen depre-

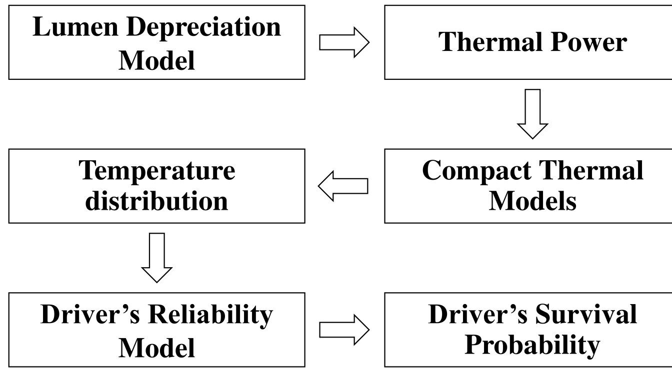

Figure 5.1: General Methodology of The Proposed Approach.

ciation process [14]. The thermal power of the LED light source for each lumen maintenance value can be obtained. Then, a compact thermal model of the LED lamps is utilized to calculate the temperature distribution of the LED lamp, in particular, the air temperature surrounding the driver and junction temperatures of driver's critical components. With known temperatures, the survival probability of the driver can be calculated by a Markov Chain based reliability model [30]. The details of each model will be introduced in Section 5.3 to 5.5.

5.3. LUMEN DEPRECIATION MODEL

ACCORDING to work presented in [2, 5, 14], the exponential model [5] and the Wiener Process [14] can be used to describe the lumen depreciation process. Thus, the lumen maintenance at time t, the ratio of luminous flux remaining at time t to its initial value, can be described by:

$$\Phi(t) = e^{-\beta t} + W(t) \tag{5.1}$$

where, $\Phi(t)$ is the lumen maintenance at time t, β is the depreciation rate, $W(t)$ is the stochastic distribution of the lumen depreciation at time t, which follows the normal distribution [35]:

$$W(t) \sim N(0, \alpha t) \tag{5.2}$$

Hence, at any given time t, the lumen maintenance also follows the normal distribution:

$$\Phi(t) \sim N(e^{-\beta t}, \alpha t) \tag{5.3}$$

In this model, the mean values of the lumen maintenance degrade exponentially, and the standard deviations increase linearly with a rate of α. This work defines the three variances, $\pm 3\alpha t$, as the lower and upper bound of the lumen maintenance. As the boundary condition, $\Phi(0) = 1$. Moreover, the probability density function at time t is [35]:

$$p[\Phi(t)] = \frac{1}{\sqrt{2\pi}} e^{-[\frac{\Phi(t)-e^{-\beta t}}{\sqrt{2}\alpha t}]^2} \tag{5.4}$$

To determine the parameters in the lumen depreciation model by Equation 5.3, 30 LED light sources, as shown in Figure 5.2, were tested at 328K and the rated input current for a period of 2000 hours. The input power and lumen maintenance of each sample were tested by an integrating sphere system.

Figure 5.2: The Selected LED Light Source.

At time t=0, total power $P_{LED} = 6.65W$ and optical power $P_{Opt} = 2.51W$. The tested lumen maintenance distributions as functions of time are shown in Figure 5.3. The normality tests were carried out on the results to check the normality of the lumen maintenance distribution.

The P-value from a normality test is a statistical indicator representing the probabil-

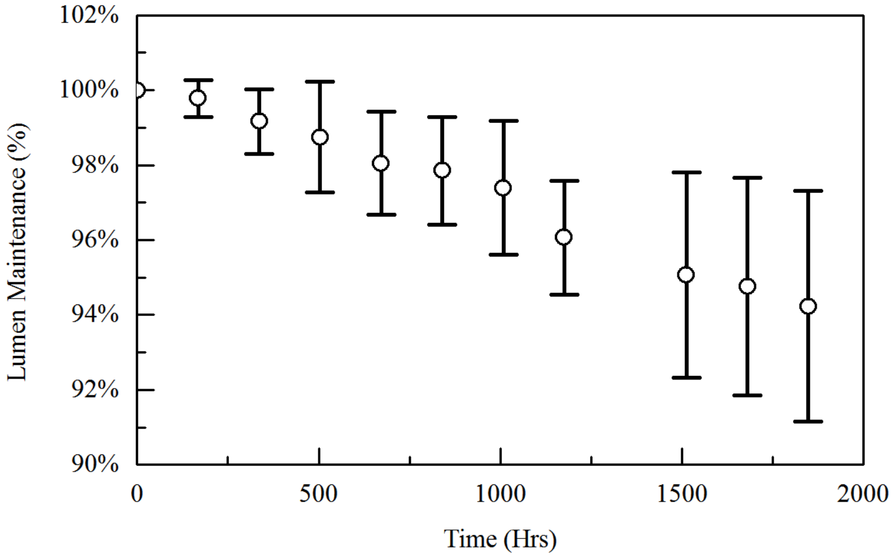

Figure 5.3: Lumen Maintenance Distributions.

5

ity of the observed sample to follow the assumed distribution. A larger P value indicates that the obtained distribution follows the assumed distribution. $P = 0.05$ is the threshold value for the normality test in statistics. The obtained P-values are shown in Figure 5.5. It can be seen from the results that the P values of lumen maintenance distribution are much higher than 0.05. Thus, the normal distributions in Equation 5.3 are confirmed.

The mean values and standard deviations of lumen maintenance distribution are displayed in Figure 5.6. The obtained test results are fitted by functions given by Equation 5.3. The parameter of curve fitting α and β are 5.7558×10^{-6} and 3.1371×10^{-5} respectively. The maximum errors of the predicted mean values and standard deviations are 1.64% and 0.32% respectively. Hence, the test results show a good agreement with the proposed models.

With known parameter α and β, the lumen depreciation distribution curves of the LED light source can be extrapolated by Equation 5.1. Figure 5.7 displays the mean value, upper bound (MAX) and lower bound (MIN) curves of the lumen maintenance. In 20,000 hours, the mean value drops about 47%. Meanwhile, the upper bound and lower bound drop about 12% and 88% respectively.

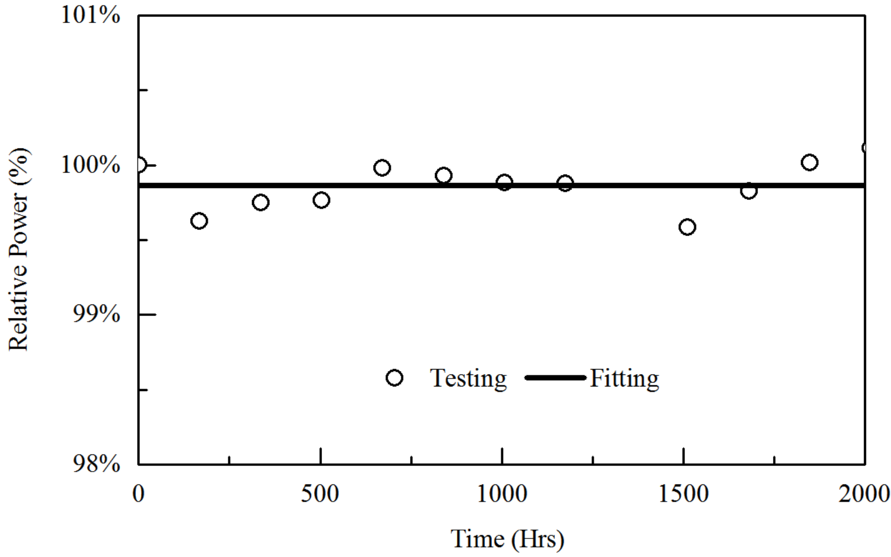

Figure 5.4: Relative Input Power of LEDs.

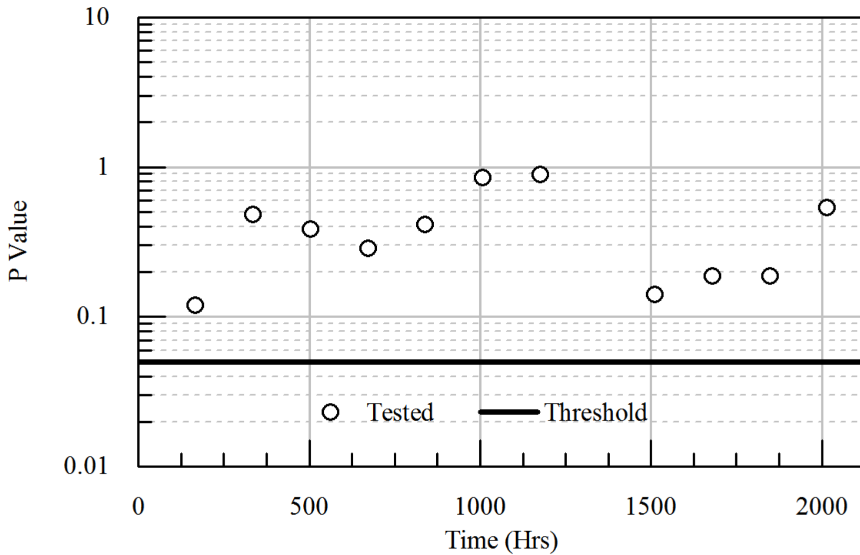

Figure 5.5: Normality Test Results.

5.4. RELIABILITY MODEL OF THE DRIVER

As a carrier of the proposed method, a commercial LED bulb lamp shown in Figure 5.8 is selected for the present study. In the body of the lamp, a quasi-resonance

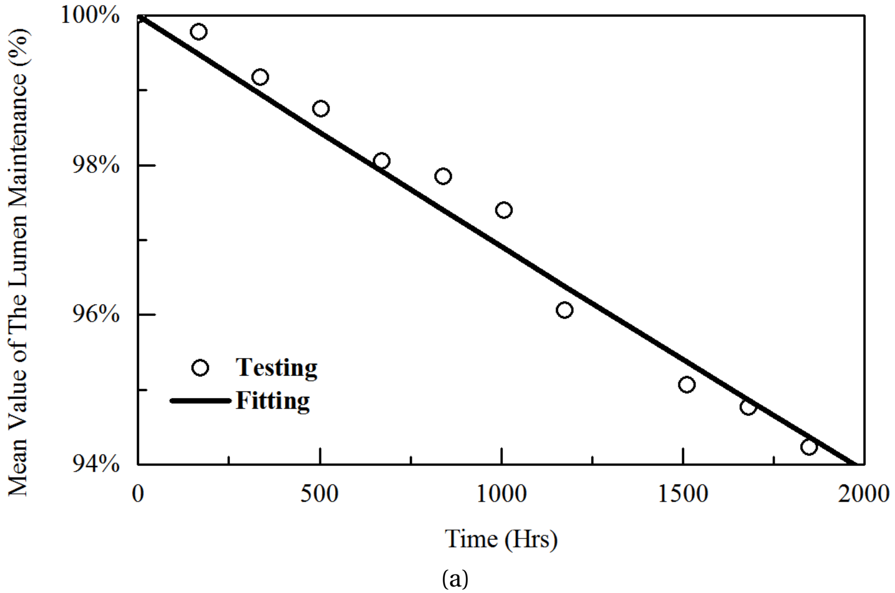

(a)

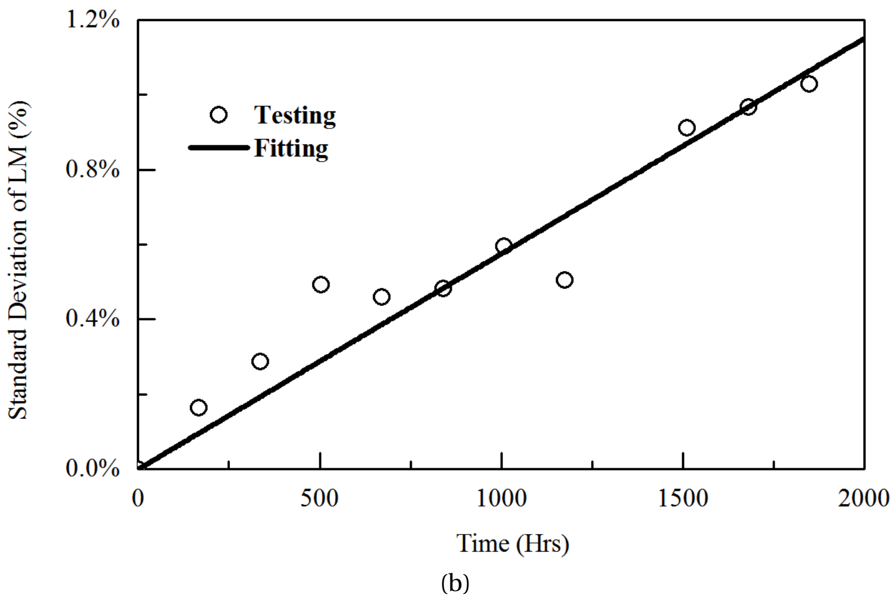

(b)

Figure 5.6: (a) Mean values and (b) Standard Deviations of The Lumen Deprecation.

converter shown in Figure 5.9 is used to drive the LED light source. Due the absence of the potting material, there is an air gap between the driver and the lamp's body. For the purpose of study, the driver assumes two critical components: the power diode $D1$ and

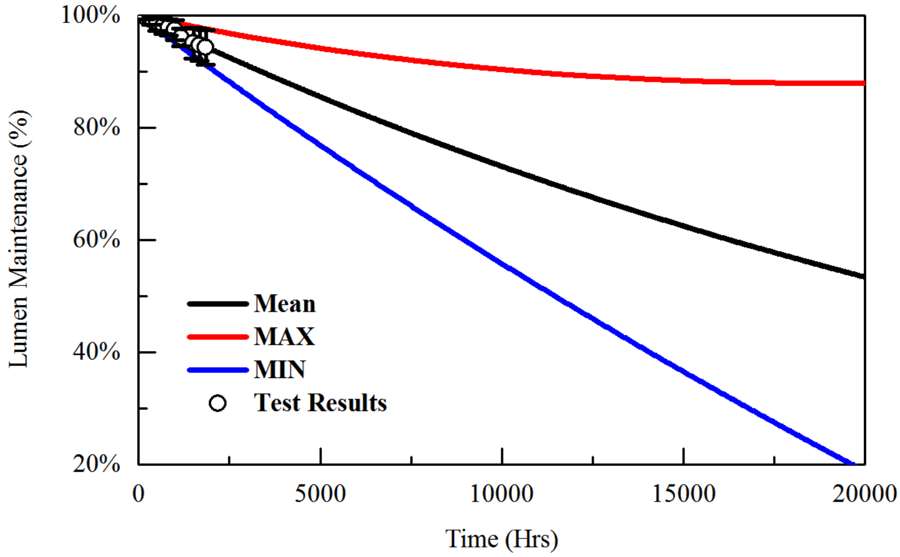

Figure 5.7: Extrapolated Lumen Maintenance Curves.

the control IC $U1$.

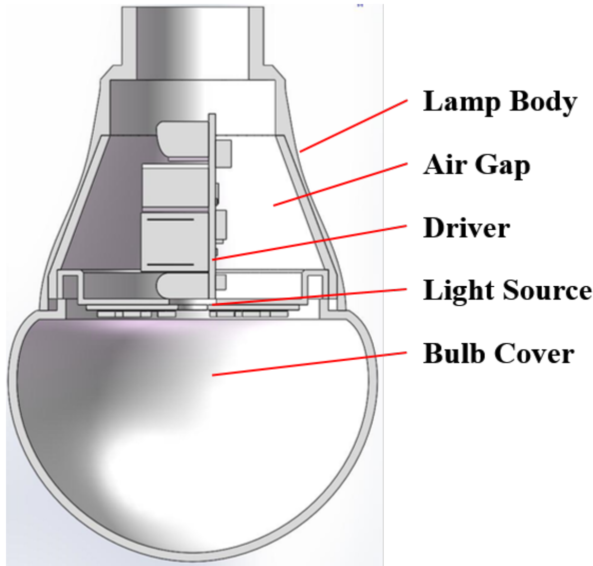

Figure 5.8: The Model of The selected LED Lamp.

This work focuses catastrophic failures of critical components of the driver. The failure of the driver distributes randomly during operation. As a result, the reliability can

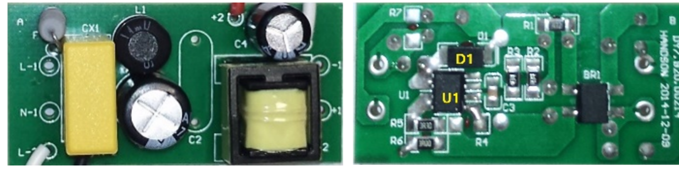

(a)

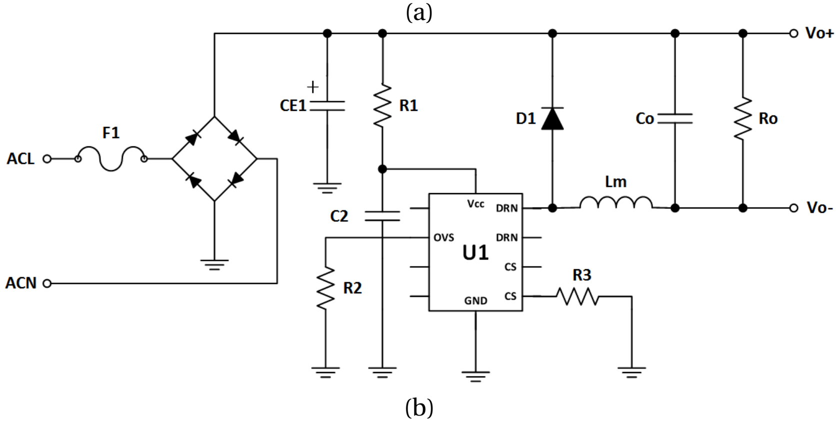

(b)

Figure 5.9: (a) Layout and (b) Circuit of the Selected LED Driver [36].

be obtained by Markov Chain [30]. Expressed by the differential equation, the driver's survival probability can be obtained by [37]:

$$\frac{dR_D(t)}{dt} = -f_D(t) \cdot R_D(t) \tag{5.5}$$

where, $R_D(t)$ is the driver's survival probability at time t, $f_D(t)$ is the probability density function of the driver's failures. If $f_D(t)$ stays unchanged with operation time, $R_D(t)$ is [30]:

$$R_D(t) = e^{-f_D(t) \cdot t} \tag{5.6}$$

If $f_D(t)$ changes with operation time, $R_D(t)$ is given by [37]:

$$R_D(t) = e^{-\int_0^t f_D(x) \cdot dx} \tag{5.7}$$

Suppose the failure of each critical component is independent of each other, the $f_D(t)$ is a function of failure probability densities of critical components [30]:

$$f_D(t) = f_{Di}(t) + f_{IC}(t) - f_{Di}(t) \cdot f_{IC}(t) \tag{5.8}$$

where $f_{Di}(t)$ and $f_{IC}(t)$ are failure probability densities of the power diode $D1$ and the control IC $U1$ respectively. $f_{Di}(t)$ and $f_{IC}(t)$ can be obtained by [29]:

$$f_{Di}(t) = \lambda_{Di} \cdot e^{-\frac{E_{a,Di}}{\kappa \cdot T_{j,Di}}} \tag{5.9}$$

$$f_{IC}(t) = \lambda_{IC} \cdot e^{-\frac{E_{a,IC}}{\kappa \cdot T_{j,IC}}} \tag{5.10}$$

where, $T_{j,Di}$ and $T_{j,IC}$ are junction temperatures, λ_{Di} and λ_{IC} are basic failure probability densities, $E_{a,Di}$ and $E_{a,IC}$ are the activation energy of the power diode and the control IC. In this work, λ_{Di}, λ_{IC}, $E_{a,Di}$ and $E_{a,IC}$ are obtained from the empirical models [29], and $T_{j,Di}$ and $T_{j,IC}$ can be calculated by the compact thermal model of the selected LED lamp. As a result, the MTTF of the driver is a function of $f_D(t)$:

$$MTTF = \int_0^{\infty} t \cdot f_D(t) \cdot dt \tag{5.11}$$

5.5. THERMAL MODEL OF THE LED LAMP

THE temperature distributions for an LED lamp, in principle, can be obtained through system-level computational fluid dynamics (CFD) or finite element analysis (FEA), provided that the power dissipation on each component, the thermal properties of materials, and the geometrical information are known. On the other hand, compact thermal model is quite exact and fast in calculations of temperature distributions when information of geometry and materials are incomplete. As shown in Figure 5.10, this work develops the compact thermal model of the LED lamp to obtain the relationship between LED's thermal dissipation and junction temperatures of critical components in the driver.

For the considered lamp, there are several heat sources: the LEDs and driver components. The thermal energy from LEDs and driver heat the air gap inside the lamp, increasing the junction temperature of driver's components. In Figure 5.10, $T_{A,in}$ is the air temperature inside the lamp, T_A is the ambient temperature, $T_{C,Di}$ and $T_{C,IC}$ are the case temperatures of power diode and IC respectively, $T_{j,Di}$ and $T_{C,IC}$ are the junction

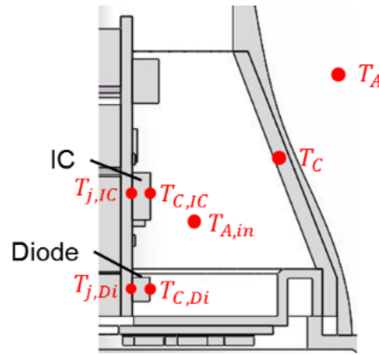

(a)

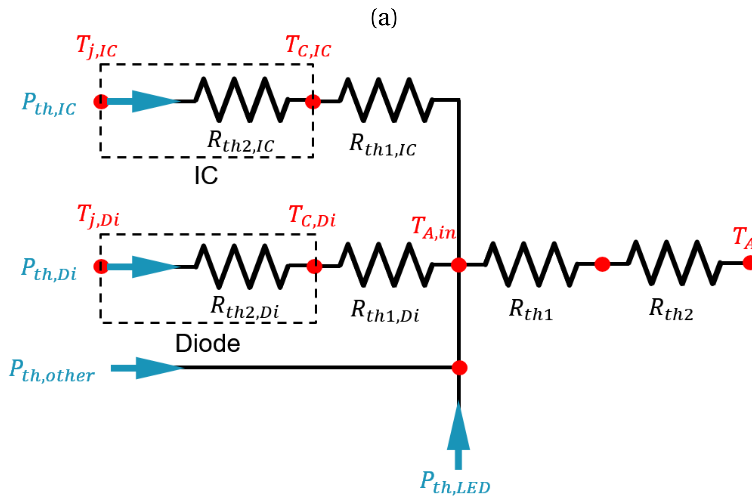

(b)

Figure 5.10: (a) The Selected Lamp Structure with (b) the Compact Thermal Model.

temperatures of the diode and IC respectively. R_{th1} is the thermal resistance between the air surrounding the driver and the lamp's case, R_{th2} is the thermal resistance between the lamp's case and the ambient, $R_{th1,Di}$ and $R_{th1,IC}$ are convective thermal resistances, $R_{th2,Di}$ and $R_{th2,IC}$ are conductive thermal resistances. $P_{th,LED}$ is the thermal power of the LED light source, $P_{th,Di}$ and $P_{th,IC}$ are thermal powers of the diode and the IC respectively. The heat from other components of the driver is considered in the total thermal power of the driver.

Once the lamp reaches thermal equilibrium point, the case temperatures $T_{C,Di}$ and $T_{C,IC}$, junction temperatures $T_{j,Di}$ and $T_{C,IC}$ are functions of the components' thermal power $P_{th,Di}$ and $P_{th,IC}$:

$$T_{C,Di} = P_{th,Di} \cdot (R_{th1,Di} + R_{th2,Di}) + T_{A,in} \tag{5.12}$$

$$T_{C,IC} = P_{th,IC} \cdot (R_{th1,IC} + R_{th2,IC}) + T_{A,in} \tag{5.13}$$

In this work, $R_{th1,Di}$ and $R_{th1,IC}$ are obtained experimentally, and $R_{th2,Di}$ and $R_{th2,IC}$ are obtained from datasheets[36, 38]. The air temperature inside the lamp $T_{A,in}$ is a function of total thermal power of the lamp:

$$T_{A,in} = (R_{th1} + R_{th2}) \cdot (P_{th,LED} + P_{th,D}) + T_A \tag{5.14}$$

where, $P_{th,D}$ is the driver's total thermal power. As thermal resistances of the lamp, R_{th1}+R_{th2} can be measured experimentally. Since the electronic characteristics of LEDs after seasoning is not affected by lumen depreciation [39], $P_{th,LED}$ can be obtained by:

$$P_{th,LED} = P_{LED} - P_{Opt} \cdot \Phi(t) \tag{5.15}$$

where, P_{LED} is the total power and P_{Opt} is the initial optical power of the LED light source.

The electronic-optical tests were carried out on the driver to measure its power consumption. The driver was tested in room temperature (298K). The root mean square values of operation voltages and current of the IC and the power diode were measured by a power meter. Meanwhile, the total thermal power of the driver was measured as well. Table 5.1 lists the electronic-optical test results.

Table 5.1: Electronic Test Results

	Voltage	Current	Failure Mode
IC	0.756V	0.095A	$P_{th,IC}$=0.072W
Diode	1.109V	0.121A	$P_{th,Di}$=0.133W
LEDs	-	-	P_{LED}=6.650W
Total	-	-	$P_{th,D}$=0.640W

The thermal tests were carried out to measure the thermal resistances R_{th1}+R_{th2} and validate the compact thermal models and. Firstly, the lamp was placed at room temperature (298K) and natural convection, and the air temperature inside the lamp was

measured by thermocouples. By adjusting the total thermal power of the lamp, the thermal resistance R_{th1}+R_{th2} can be calculated using Equation 5.14. The temperature difference between the air surrounding the driver and the ambient as a function of the lamp's total thermal power $P_{th,LED}$+$P_{th,D}$ is shown in Figure 5.11. The air temperature inside the lamp increases linearly with the total thermal power. Fitted by Equation 5.14, the thermal resistance R_{th1}+R_{th2} is about 8.62KW^{-1}

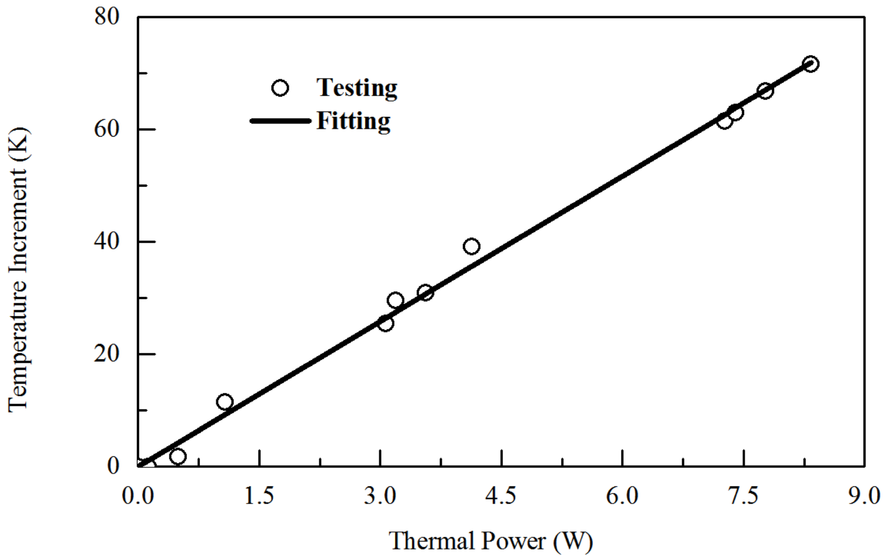

Figure 5.11: Air Temperature Increment Curve Inside The Lamp.

Secondly, the driver was tested at room temperature (298K) and convection-free condition to obtain the condition as inside the LED lamp. Case temperatures of the IC and the power diode are measured by an IR camera. As shown in Figure 5.12, the temperature differences between the cases of IC and power diode, and IC and ambient are 14.52K and 15.79K respectively. Fitted by Equation 5.12 and 5.13, $R_{th1,IC}$=200KW^{-1} and $R_{th1,Di}$=120KW^{-1}.

5.6. Case Studies and Results

5.6.1. Definition of Scenarios

As listed in Table 5.2, two different scenarios are considered in this work. In Scenario S1, the driver's operation temperature remains at a constant value before the lumen depreciation; whereas in Scenario S2, the temperature inside the lamp increase with the

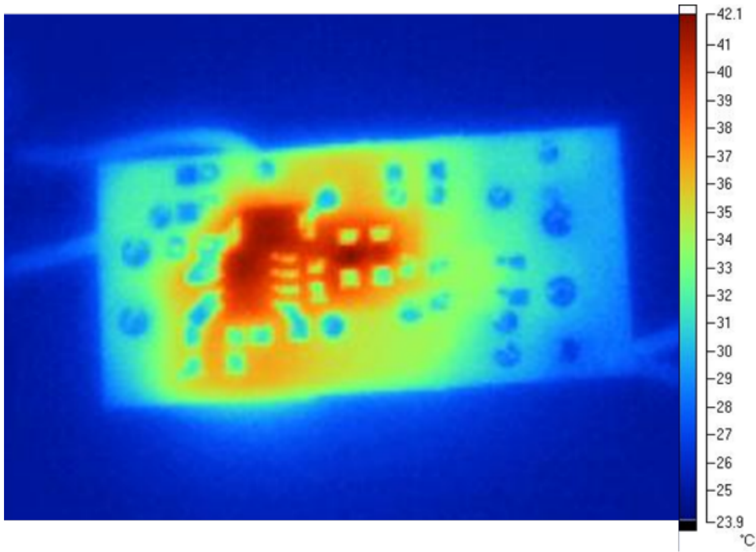

Figure 5.12: Case Temperature of The Driver.

5

lumen depreciation process.

Table 5.2: Scenario Designs

Scenario	Condition
S1	$T_{A,in}(t) = T_{A,in}(0)$=339K
S2	$T_{A,in}(t)$ rises with the lumen depreciation Mean: $\Phi(t) = e^{-\beta \cdot t}$ Min : $\Phi(t) = e^{-\beta \cdot t} + 3\alpha t$ Max : $\Phi(t) = e^{-\beta \cdot t} - 3\alpha t$

As obtained from empirical models [29], tests and data-sheets of critical components [36, 38], Table 5.3 summarizes the model parameters used in the proposed method.

5.6.2. RESULTS AND DISCUSSIONS

THE temperature difference between the air surrounding the driver and the ambient in Scenario S2 obtained by Equation 5.14 is shown in Figure 5.13. With the lumen depreciation process, the mean value of the air temperature surrounding the driver in Scenario S2 increases about 10K in 20,000 hours. In the same time period, the upper bound and lower bound rise about 3K and 18K respectively. It can be seen that the air temperature inside the LED lamp increases with time and has a wide spread due to the

Table 5.3: Parameters of Proposed Models

Parameter	Value	Parameter	Value
α	5.7558×10^{-6}	β	3.1371×10^{-5}
P_{Opt}	$2.560W$	P_{LED}	$6.650W$
$P_{th,D}$	$0.640W$	R_{th}	$8.62KW^{-1}$
$R_{th1,IC}$	$200KW^{-1}$	$R_{th1,Di}$	$120KW^{-1}$
$R_{th2,IC}$	$50KW^{-1}$	$R_{th2,Di}$	$34KW^{-1}$
$E_{a,IC}$	$0.70eV$	$E_{a,Di}$	$0.23eV$
λ_{IC}	0.48	λ_{Di}	0.0038
T_A	$298K$		

LED random properties.

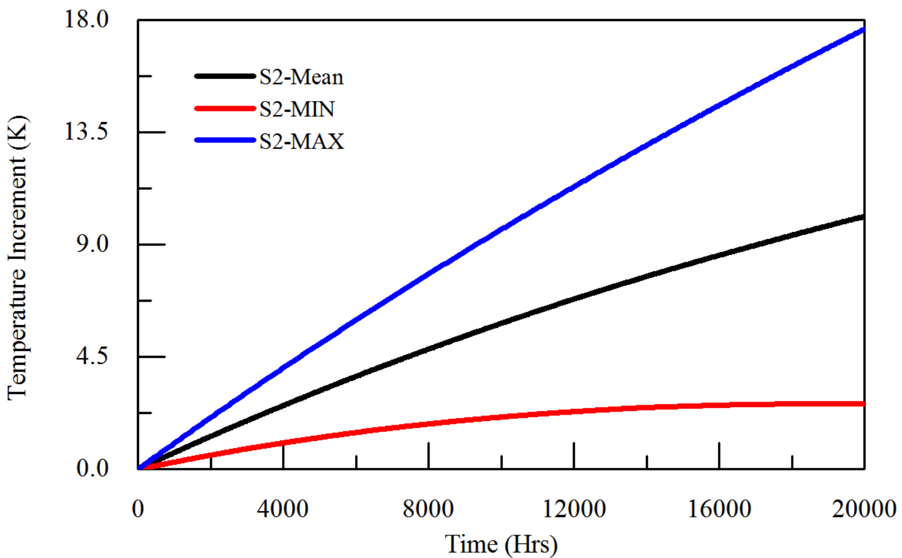

Figure 5.13: Air Temperature Increment Curves.

Then, the failure probability density of the driver can be obtained by Equation 5.8, 5.9 and 5.10. As shown in Figure 5.14, the mean value of the failure probability density increases from 5.5691×10^{-5} to 1.0800×10^{-4}. Further, the upper bound and lower bound have changed to 1.7241×10^{-4} and 6.6347×10^{-5} respectively, after 20,000 hours aging.

The survival probability of driver can be obtained by Equation 5.7. The survival probability curve of the driver for each scenario is displayed in Figure 5.15. For Scenario S1, the driver's survival probability degrades to about 32.8% at 20,000 hours. For Scenario

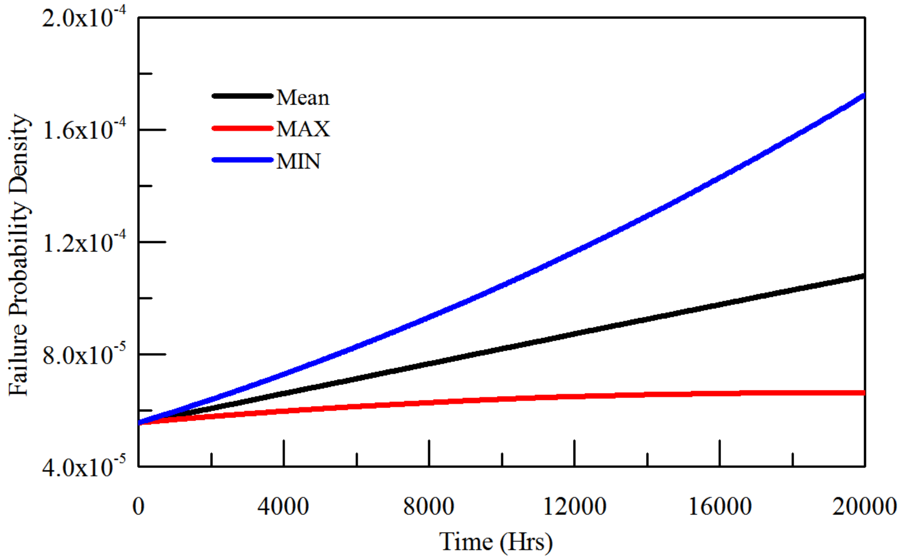

Figure 5.14: Failure Probability Density Curves of The Driver.

5

S2, the mean value, upper bound and lower bound of the driver's survival probability drop to about 19.4%, 28.3%, and 11.6% respectively in the same period. Table 5.4 lists the MTTF of the driver, the LED light source and the lamp calculated using Equation 5.11. The MTTF of Scenario S1 is about 17,300 hours. The mean value, upper bound and lower bound of MTTFs of Scenario S2 are 12,600, 15,600 and 10,900 hours respectively. Compared to the mean value of Scenario S2, MTTFs of Scenario S1 is about 37.9% longer. Therefore, constant temperature assumptions will bring significant errors to reliability prediction.

Table 5.4: Mean Time to Failure of The Driver

Scenario	Mean Time to Failure
S1	17,300 hours
S2-Mean	12,600 hours
S2-Min	10,900 hours
S2-Max	15,600 hours

Compared to the conventional methods, the proposed model predicts the distributions of driver's reliability degradation process considering the influence of the lumen depreciation. Scenario S1 overestimates the reliability of the driver. The driver's reliability is significantly influenced by its operation temperature. The statistical properties

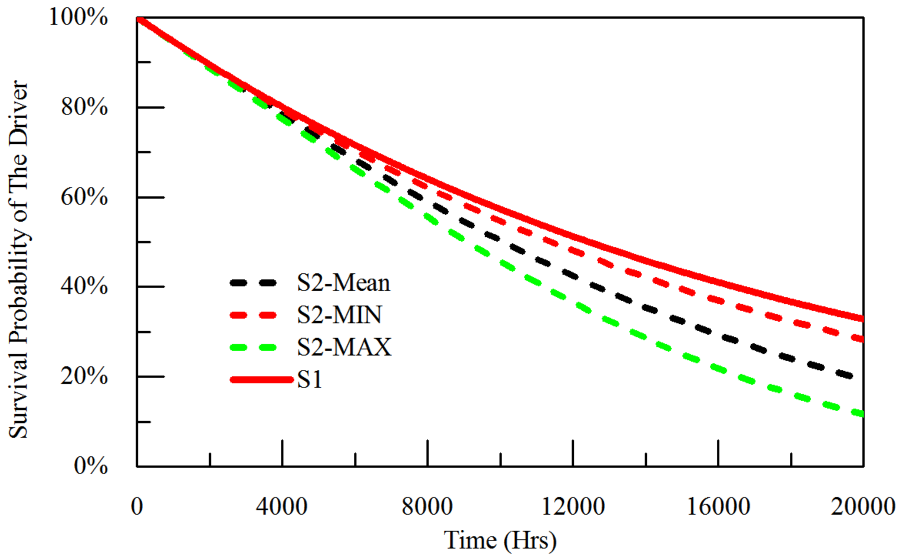

Figure 5.15: Survival Probability Curves of The Driver.

of LEDs life data lead to a wide range of the driver's survival probability and MTTF. For accurate reliability prediction at every time, it is necessary to consider the ever-changing operation temperature during the lumen depreciation process.

5.7. Conclusions

In this chapter, stochastic properties of LEDs degradation are considered to investigate the reliability of integrated LED driver. The Wiener process is used to describe the lumen depreciation process, and the compact thermal model is utilized to obtain the temperature distribution. The driver's survival probability as a function of time is obtained by the Markov Chain. An integrated lamp is selected for case study. Thermal measurement and electronic-optical tests are conducted to calibrate the model parameters. Two scenarios are studied: Scenario S1 considers constant operation temperatures of the driver and Scenario S2 considers that the operating temperature of driver increases with the lumen depreciation process.

For Scenario S1, the operation temperature of the driver is considered as 339K. After 20,000 hours aging, the driver's survival probability degrades to about 32.8%. As a result, the driver's MTTFs in Scenario S1 is about 17,300 hours.

For Scenario S2, the operation temperature of the driver is considered to increase with the lumen depreciation process. The mean value, upper bound and lower bound of

air temperature surrounding the driver rise to about 10K, 3K and 18K in 20,000 hours. As a result, the mean value, upper bound and lower bound of the driver's survival probability decrease to about 19.4%, 28.3%, and 11.6% respectively in the same period.

It has been found that the statistical properties of LEDs life data will lead to a large range of the driver's survival probability. The stochastic analysis of LEDs life data from accelerated degradation testing can improve the accuracy of the prediction of the LED driver and LED lamp.

The approach developed in this paper provides a general methodology, and it is applicable for other types of LED drivers. Moreover, in the future study, the stochastic process of LED's degradation can be integrated with electronic-thermal simulation to obtain the power dissipation directly.

REFERENCES

[1] B. Sun, X. J. Fan, C. Q. Chui, and G. Q. Zhang, *A stochastic process based reliability prediction method for LED driver,* Reliability Engineering & System Safety **submitted**.

[2] W. D. van Driel and X. J. Fan, *Solid state lighting reliability: components to systems* (Springer Science & Business Media, 2012).

[3] Y. Wang, J. M. Alonso, and X. Ruan, *A review of LED drivers and related technologies,* IEEE Transactions on Industrial Electronics **PP**, 1 (2017).

[4] *Hammer Testing Findings for Solid-State Lighting Luminaires* (Department of Energy (DoE), United States, 2013).

[5] C. Qian, X. J. Fan, J. Fan, C. Yuan, and G. Q. Zhang, *An accelerated test method of luminous flux depreciation for LED luminaires and lamps,* Reliability Engineering & System Safety **147**, 84 (2016).

[6] J. Huang, D. S. Golubovic, S. Koh, D. Yang, X. Li, X. J. Fan, and G. Q. Zhang, *Degradation mechanisms of mid-power white-light LEDs under high-temperature-humidity conditions,* IEEE Transactions on Device and Materials Reliability **15**, 220 (2015).

[7] J. Huang, D. S. Golubović, S. Koh, D. Yang, X. Li, X. J. Fan, and G. Q. Zhang, *Rapid degradation of mid-power white-light LEDs in saturated moisture conditions,* IEEE Transactions on Device and Materials Reliability (2015).

[8] G. Lu, W. D. van Driel, X. J. Fan, M. Y. Mehr, J. Fan, K. Jansen, and G. Q. Zhang, *Degradation of microcellular PET reflective materials used in LED-based products,* Optical Materials **49**, 79 (2015).

[9] G. Lu, W. van Driel, X. J. Fan, M. Yazdan Mehrb, J. Fan, K. Jansenf, and G. Q. Zhang, *Color shift investigations for LED secondary optical designs: Comparison between bpa-pc and pmma,* Optical Materials (2015).

[10] J. Fan, C. Qian, K. C. Yung, X. J. Fan, G. Q. Zhang, and M. Pecht, *Optimal design of life testing for high-brightness white LEDs using the six sigma DMAIC approach,* IEEE Transactions on Device and Materials Reliability (2015).

[11] H. T. Chen, Y. F. Cheung, H. W. Choi, S. C. Tan, and S. Y. Hui, *Reduction of thermal resistance and optical power loss using thin-film light-emitting diode (LED) structure,* IEEE Transactions on Industrial Electronics **62**, 6925 (2015).

[12] J. Dong and G. Zhang, *Identification and robust control of the nonlinear photoelectrothermal dynamics of LED systems,* IEEE Transactions on Industrial Electronics **64**, 2215 (2017).

[13] *LED luminaire lifetime: recommendations for testing and reporting, Third Edition* (Department of Energy (DoE), United States, 2014).

[14] J. Huang, D. S. Golubović, S. W. Koh, D. Yang, X. Li, X. J. Fan, and G. Q. Zhang, *Degradation modeling of mid-power white-light LEDs by using wiener process,* Optics Express **23**, A966 (2015).

[15] B. Sun, X. J. Fan, C. Qian, and G. Q. Zhang, *PoF-simulation-assisted reliability prediction for electrolytic capacitor in LED drivers,* IEEE Transactions on Industrial Electronics **63**, 6726 (2016).

[16] S. Y. Hui, S. N. Li, X. H. Tao, W. Chen, and W. M. Ng, *A novel passive offline LED driver with long lifetime,* IEEE Transactions on Power Electronics, **25**, 2665 (2010).

[17] X. Xu, A. S. Gurav, P. M. Lessner, and C. A. Randall, *Robust BME class-i MLCCs for harsh-environment applications,* IEEE Transactions on Industrial Electronics **58**, 2636 (2011).

[18] A. Garcia, N. Warner, N. A. D'Souza, E. Tuncer, L. Nguyen, M. Denison, and J. T. Fong, *Reliability of high-voltage molding compounds: Particle size, curing time, sample thickness, and voltage impact on polarization,* IEEE Transactions on Industrial Electronics **63**, 7104 (2016).

[19] H. Chen and S. Lu, *Fault diagnosis digital method for power transistors in power converters of switched reluctance motors,* IEEE Transactions on Industrial Electronics **60**, 749 (2013).

[20] P. S. Almeida, D. Camponogara, M. D. Costa, H. Braga, and J. M. Alonso, *Matching LED and driver life spans: A review of different techniques,* Industrial Electronics Magazine, IEEE **9**, 36 (2015).

[21] C. Branas, F. J. Azcondo, and J. M. Alonso, *Solid-state lighting: a system review,* Industrial Electronics Magazine, IEEE **7**, 6 (2013).

[22] S. Dietrich, S. Strache, R. Wunderlich, and S. Heinen, *Get the LED out: Experimental validation of a capacitor-free single-inductor, multiple-output LED driver topology,* Industrial Electronics Magazine, IEEE **9**, 24 (2015).

[23] G. G. Pereira, M. A. D. Costa, J. M. Alonso, M. F. de Melo, and C. H. Barriquello, *LED driver based on input current shaper without electrolytic capacitor,* IEEE Transactions on Industrial Electronics **PP**, 1 (2017).

[24] D. Camponogara, D. Ribeiro Vargas, M. Dalla Costa, J. M. Alonso, J. Garcia, and T. Marchesan, *Capacitance reduction with an optimized converter connection applied to LED drivers,* IEEE Transactions on Industrial Electronics (2015).

[25] L. Gu, X. Ruan, M. Xu, and K. Yao, *Means of eliminating electrolytic capacitor in AC/DC power supplies for LED lightings,* IEEE Transactions on Power Electronics (2009).

[26] X. Ruan, B. Wang, K. Yao, and S. Wang, *Optimum injected current harmonics to minimize peak-to-average ratio of LED current for electrolytic capacitor-less AC–DC drivers,* IEEE Transactions on Power Electronics (2011).

[27] X. Qu, S. C. Wong, and C. K. Tse, *Resonance-assisted buck converter for offline driving of power LED replacement lamps,* Power Electronics, IEEE Transactions on **26**, 532 (2011).

[28] X. Wu, J. Yang, J. Zhang, and Z. Qian, *Variable on-time (VOT)-controlled critical conduction mode buck PFC converter for high-input AC/DC hb-LED lighting applications,* Power Electronics, IEEE Transactions on **27**, 4530 (2012).

[29] *MIL-HDBK-217F: Reliability Prediction of Electronic Equipment* (Department of Defense (DoD), United States, 1995).

[30] A. Khosroshahi, M. Abapour, and M. Sabahi, *Reliability evaluation of conventional and interleaved DC-DC boost converters,* IEEE Transactions on Power Electronics **30**, 5821 (2015).

[31] B. Sun, X. Fan, W. van Driel, H. Ye, J. Fan, C. Qian, and G. Zhang, *A novel lifetime prediction for integrated LED lamps by electronic-thermal simulation,* Reliability Engineering & System Safety, Accepted **163**, 14 (2017).

[32] *A reliability prediction for integrated LED lamp with electrolytic capacitor-free driver,* IEEE Transactions on Components, Packaging and Manufacturing Technology **7**, 1081 (2017).

[33] H. Hao, C. Su, and C. Li, *LED lighting system reliability modeling and inference via random effects gamma process and copula function,* International Journal of Photoenergy (2015).

[34] X. Qu, H. Wang, X. Zhan, F. Blaabjerg, and H. S. H. Chung, *A lifetime prediction method for LEDs considering real mission profiles,* IEEE Transactions on Power Electronics **PP**, 1 (2016).

[35] K. Ito, *Diffusion Processes* (Wiley Online Library, 1974).

[36] *DU8671 Constant Current LED Driver in QS Mode* (Top-Cycle Semiconductor., People's Republic, 2015).

[37] C. W. Gardiner, *Handbook of stochastic methods* (Springer Berlin, 1985).

[38] *ES1A-ES1J Surface Mount Rectifiers* (Technology, Lu Guang Electronic, 2012).

[39] B. Hamon, B. Bataillou, A. Gasse, and G. Feuillet, *N-contacts degradation analysis of white flip chip LEDs during reliability tests,* in *2014 IEEE International Reliability Physics Symposium* (IEEE).

6

Concluding Remarks and Recommendations

In this dissertation, the lifetime predictions of LED drivers and LED lamps are conducted for various failure modes including LED's depreciation, driver's degradation and driver's catastrophic failures. Different types of LED drivers: driver with electrolytic capacitors and electrolytic capacitor-free driver, are investigated. Different operation modes: constant current mode (CCM) and constant optical output (CLO) mode are studied. Electronic-thermal simulation is applied throughout the dissertation for different drivers and lamps under various operation conditions. The electronic simulation uses validated SPICE models of LED drivers. Thermal simulation is based either on finite element analysis or compact thermal models. Various reliability and statistical methods, such as the Monte Carlo method, the fault-tree method, the Markov Chain method, and the Wiener process, are applied and integrated with the physics of failure (PoF) method, i.e., electronic-thermal simulation in this dissertation for various problems. Specifically, the major conclusions are summarized as following,

1. ***Reliability of electrolytic capacitor in LED drivers.***[1] In this study, a single inductor buck-boost DC-DC converter is simulated to understand the degradation behavior of electrolytic capacitor. The simulation results agree well with the accelerated test results. It has been observed that the temperature of an output stage capacitor increases significantly during operation time. Therefore, electrolytic capacitors degrade faster than

that with constant temperature assumption. The capacitor's performance without taking temperature change into account results in an overestimated lifetime of a driver.

The proposed simulation methodology developed in this research can be extended to investigate other failure modes and other components in an LED driver system.

2. *Coupling effect of LED and driver's degradations on LED lamp's lifetime.* [2] In this study, an integrated LED lamp with an electrolytic capacitor-free driver is considered to investigate the coupling effects of both LED and driver's degradations on lamp's lifetime. An electrolytic capacitor-less buck-boost driver is used, in which its life is comparable to the LED's one. It has been found that the erroneous results will be obtained if LED's degradation is not taken into considerations. Furthermore, it can be seen that when driver degrades, the output current decreases over time, thus less power is provided to LED. On the other hand, when LED degrades, more thermal power is generated as the efficacy of LED decreases. These two effects eventually cancel out the impact on the LED junction temperature. Nonetheless, because of the combined effects of the reduced current in LEDs and the lumen dependence over time, the LED lamp's lifetime is reduced significantly.

The method developed in this research will be very useful in designing LED product with desired lifetime by selecting different drivers and LED light sources. The proposed method can also be extended to the small signal analysis of an LED lamp, to study the interaction between LEDs and the driver via current ripple.

3. *Interaction of LED driver's catastrophic failure and LED degradation.* [3] In this study, the interaction of catastrophic failure of the driver and LED luminous flux decay for an integrated LED lamp with an electrolytic capacitor-free LED driver is investigated for two distinct operation modes: constant current mode (CCM), and constant optical output (CLO) mode, respectively. It has been found that under CLO mode, the LED's current increases exponentially to maintain the constant light output. As a result, the junction temperatures of LEDs, MOSFETs and power diodes in driver rise significantly, leading to a much shorter MTTF, and faster luminous flux depreciation. However, under the CCM mode, the junction temperatures of LEDs, MOSFETs and diodes change modestly. Therefore, the driver's MTTF and LED's luminous flux decay are not affected much by the variation of temperatures during LED's degradation process under CCM mode.

The proposed method in this research can be extended to investigate other control methodologies in an LED driver system.

4. *Effect of LED's stochastic lumen degradation on LED driver's reliability.* [4] In this study, a quasi-resonance LED driver is integrated with a commercial LED light bulb for reliability investigation. Stochastic properties of LEDs degradation are taken into

consideration. It has been found that the statistical properties of LEDs life data will lead to a large range of the driver's survival probability. The stochastic analysis of LEDs life data from accelerated degradation testing can improve the accuracy of the prediction of the LED driver and LED lamp.

The stochastic process of LED's degradation can be integrated with electronic-thermal simulation to more accurately predict the lifetime of LED driver and LED lamp.

REFERENCES

[1] B. Sun, X. J. Fan, C. Qian, and G. Q. Zhang, *PoF-simulation-assisted reliability prediction for electrolytic capacitor in LED drivers,* IEEE Transactions on Industrial Electronics **63**, 6726 (2016).

[2] B. Sun, X. Fan, W. van Driel, H. Ye, J. Fan, C. Qian, and G. Zhang, *A novel lifetime prediction for integrated LED lamps by electronic-thermal simulation,* Reliability Engineering & System Safety, Accepted **163**, 14 (2017).

[3] *A reliability prediction for integrated LED lamp with electrolytic capacitor-free driver,* IEEE Transactions on Components, Packaging and Manufacturing Technology **7**, 1081 (2017).

[4] B. Sun, X. J. Fan, C. Q. Chui, and G. Q. Zhang, *A stochastic process based reliability prediction method for LED driver,* Reliability Engineering & System Safety **submitted**.

A

APPENDIX A

A.1. AN ACCELERATED TEST METHOD FOR OUTDOOR LED DRIVER

BASE on the understanding of failure modes [3–7], an accelerated test method for LED driver is developed [1, 2]. As shown in Figure A.1, this method contains four major procedures: sampling method, suitability test, accelerated method and failure criteria.

A.1.1. SAMPLING METHOD

Industry experiences suggest that mass product failures follow the Poisson distribution. Therefore, the minimum sample size N is a function of confidence level CL and reliability level R:

$$N = \frac{In(1-CL)}{InR} \tag{A.1}$$

Table A.1 gives minimum sample size requirements for different confidence levels and reliability levels.

Parts of this section have been published by 10th China International Forum on Solid State Lighting (ChinaSSL 2013) [1] and China Solid State Lighting Alliance [2].

A

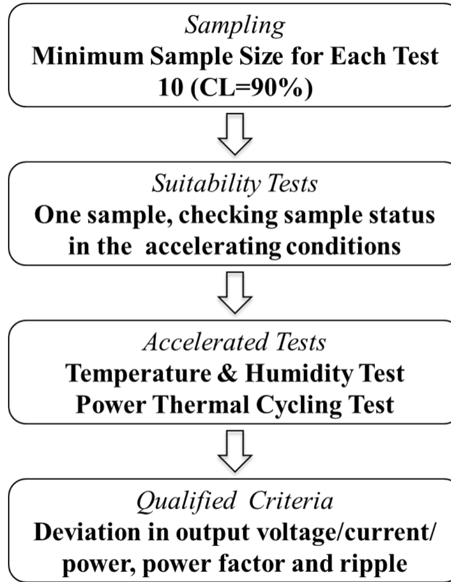

Figure A.1: Test procedures of the proposed test method for LED driver.

Table A.1: Minimum Sample Size

Confidence Level	Reliability Level	Minimum Sample Size
60%	80%	4
60%	90%	9
60%	90%	18
90%	80%	10
90%	90%	22
90%	90%	45
95%	80%	13
95%	90%	28
95%	90%	58

A.1.2. SUITABILITY TEST METHOD

If the test stresses exceed limitations of a LED driver's operation conditions, a new failure mode may be brought to the driver. Meanwhile, some LED drivers have the over-temperature perfection function. The output power of the driver may be reduced or switched off when the driver's temperature exceeds its safety threshold. Thus, suitability test should be carried out before the accelerated test.

The suitability test has three steps:

1. Place an LED driver in the room condition, measure the performance of the driver;
2. Place the driver in the condition of 358K and 85% RH, and then, measure the performance;
3. Place the driver in the room condition again, and then, measure the performance;

Figure A.2 displays failure criteria of the suitability test. If no failure is detected, this type of driver can be tested in the accelerated conditions.

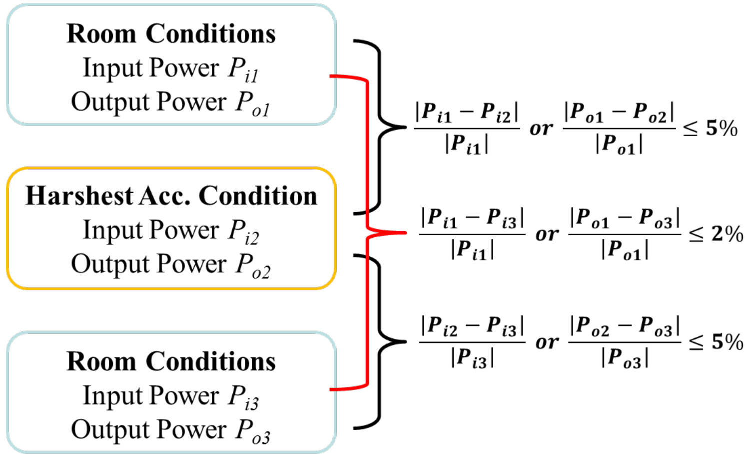

Figure A.2: Suitability Test Criteria.

A.1.3. ACCELERATED TEST METHODS

Figure A.3 shows the test procedures of the accelerated test. The performance of each sample at time zero and after aging is measured in the procedure of initial test and measuring performance. Two accelerated conditions were selected for this accelerated test method: the high temperature & humidity and the power thermal cycling.

For temperature & humidity operation test, the high temperature ($358K \pm 3K$) and high humidity ($85\% \pm 3\% RH$) is applied to test samples. The accelerated factor AF can be calculated by the Peck Model:

$$AF = \left(\frac{RH_{field}}{RH_{test}}\right)^{-q} \cdot e^{\frac{E_a}{k} \cdot \left(\frac{1}{T_{field}} - \frac{1}{T_{test}}\right)} \tag{A.2}$$

where, the typical value of related humidity of field condition RH_{field} is 65%, related humidity of the test condition is 85%, the typical value of the humidity coefficient q is

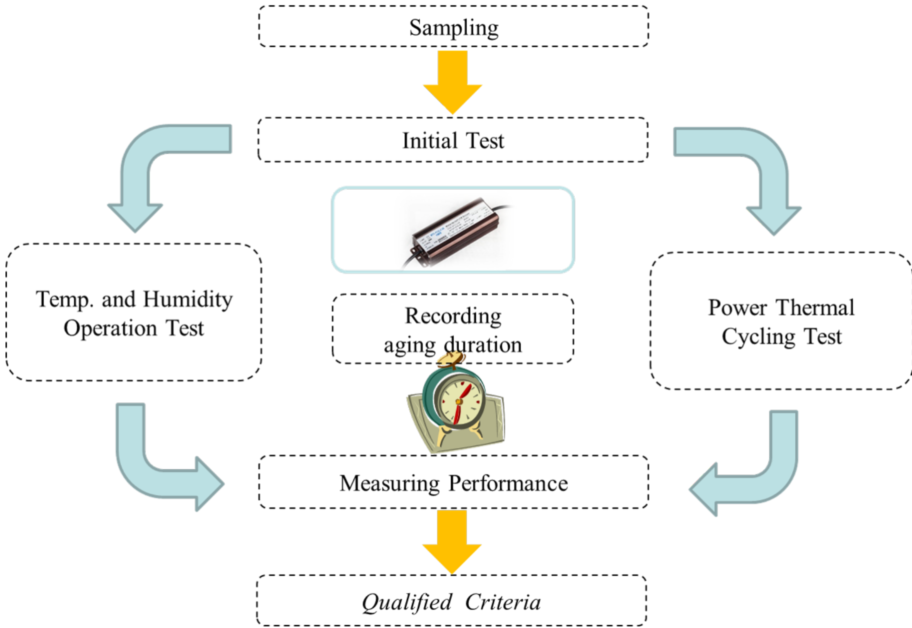

Figure A.3: Accelerated Test Procedures.

2.5, T_{field} is driver's temperature in field condition and T_{test} is driver's temperature in the test condition.

In power temperature cycling test, periodic temperature cycling and input power cycling are applied to test samples. A temperature cycling period contains four steps: heating, high-temperature dwelling ($353K \pm 3K$), cooling and low-temperature dwelling ($253K \pm 3K$). Duration of each dwelling period is 40 minutes. The heating and cooling rate is $\pm 5K/\text{min}$, heating and cooling duration is 20 minutes. As a result, total period for each temperature cycle is 120 minutes.

A power cycling period contains two steps: ON state and OFF state. The duration for each state is 10 minutes, thus, total period for each power cycle is 20 minutes.

Figure A.4 displays the temperature cycling curve in this test. The accelerated factor AF follows the Norris-Landzberg Model:

$$AF = \left(\frac{\Delta T_{field}}{\Delta T_{test}}\right)^{-n} \cdot \left(\frac{f_{field}}{f_{test}}\right)^{-m} \cdot e^{\frac{E_a}{k} \cdot \left(\frac{1}{T_{max,field}} - \frac{1}{T_{max,test}}\right)} \tag{A.3}$$

where, ΔT_{field} is the temperature difference in field condition, ΔT_{test} is the temperature difference in the test condition, the typical value of the temperature difference co-

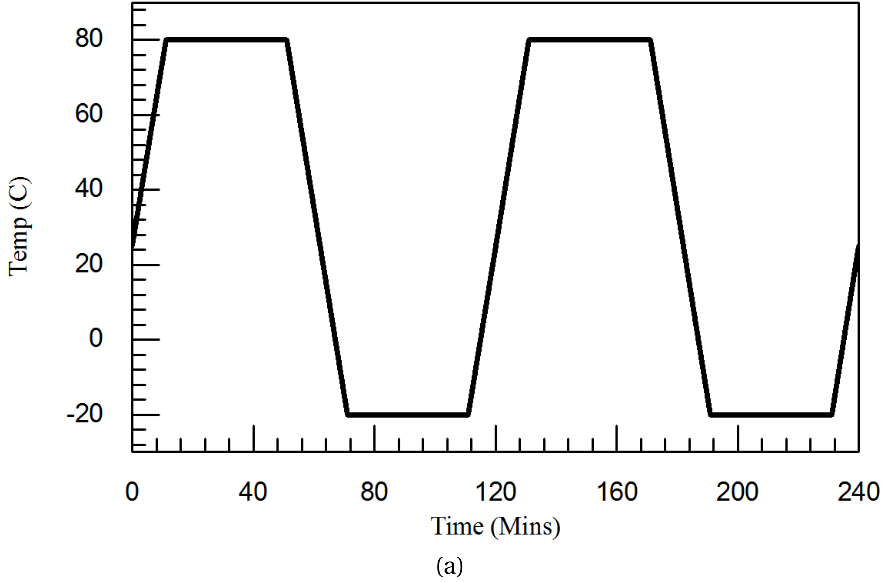

(a)

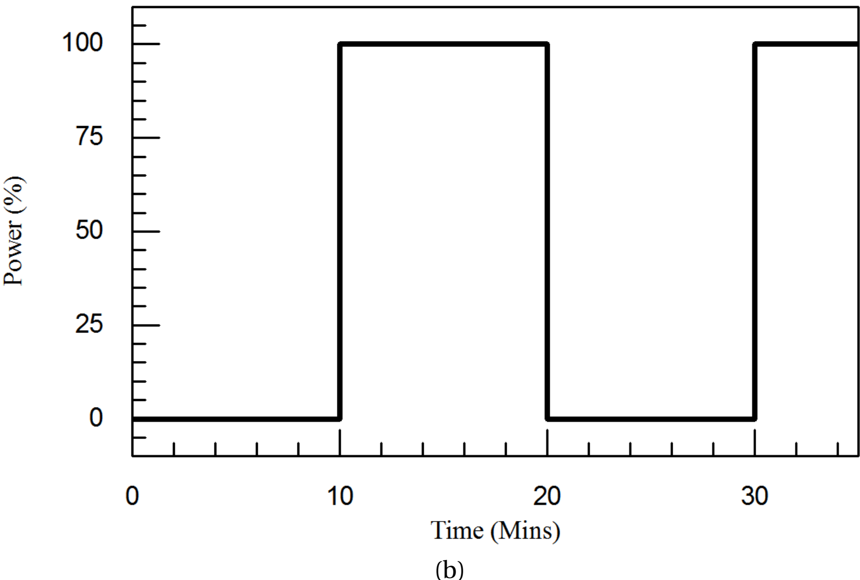

(b)

Figure A.4: (a) Temperature Cycling and (b) Power Cycling Curve.

efficient n is 2.0, f_{field} is frequency of the temperature cycling in field condition and f_{test} is frequency in the test condition, the typical value of the frequency coefficient m is 0.33, $T_{max,field}$ is driver's maximum temperature in field condition and $T_{max,test}$ is

Table A.2: Activation Energy

Component	Activation energy (eV)
Digital Microcircuit	0.10 - 0.15
Low Frequency Diode	0.17
High Frequency Diode	0.18
Bipolar Transistor	0.18
Si MOSFET	0.17
Power Transistor	0.25 - 0.50
GaAs MOSFET	0.37
Thyristor	0.27
Isolator and Emitter	0.24
Resistor	0.08 - 0.20
Capacitor	0.15 - 0.35
Transformer and Inductor	0.11
Relay	0.17 - 0.19
Connector	0.14
Lead Free Solder	0.53

maximum temperature in the test condition.

Table A.2 lists the activation energy of several critical components in LED drivers [8].

A.1.4. FAILURE CRITERIA

Current IEC standards specify many indicators of a driver, but not every indicator can be considered as failure criteria. Table A.3 lists the selected failure criteria: output voltage, output current, output power and power factor. Output properties have direct impacts on LEDs' performance. Deviations of these parameters will bring deviations of LEDs' lumen flux and color temperature. As a high power device, power factor is crucial to safety and efficiency of the entire power grid. For LED modules, keeping a low level of voltage/ current ripple has great help to avoid flicker and color shift of LEDs.

Table A.3: Failure Criteria

Indicators	Reliability Level
Output Current	$\pm 10\%$
Output Voltage	$\pm 10\%$
Output Power	$\pm 10\%$
Power Factor	-5%

If any failure is detected, the whole batch of samples is considered as fail to pass this

test.

REFERENCES

[1] B. Sun, C. A. Yuan, X. J. Fan, S. W. Koh, and G. Q. Zhang, *An accelerated lifetime test method for DC or AC supplied electronic control gear for led modules of outdoor led lighting products*, in *2013 10th China International Forum on Solid State Lighting (ChinaSSL)* (2013) pp. 65–68.

[2] *CSA-029-2015 Accelerated Test Method for DC or AC Supplied Electronic Control Gear for LED Modules of Outdoor Lighting Products* (China Solid State Lighting Alliance, 2015).

[3] W. D. van Driel and X. J. Fan, *Solid state lighting reliability: components to systems* (Springer Science & Business Media, 2012).

[4] *LED luminaire lifetime: recommendations for testing and reporting, Third Edition* (Department of Energy (DoE), United States, 2014).

[5] C. Qian, X. J. Fan, J. Fan, C. Yuan, and G. Q. Zhang, *An accelerated test method of luminous flux depreciation for LED luminaires and lamps*, Reliability Engineering & System Safety **147**, 84 (2016).

[6] *Hammer Testing Findings for Solid-State Lighting Luminaires* (Department of Energy (DoE), United States, 2013).

[7] L. Han and N. Narendran, *An accelerated test method for predicting the useful life of an LED driver*, Power Electronics, IEEE Transactions on **26**, 2249 (2011).

[8] *MIL-HDBK-217F: Reliability Prediction of Electronic Equipment* (Department of Defense (DoD), United States, 1995).

B

Appendix B

B.1. Supporting Information for Chapter 2

Table B.1: Parameter Extraction Tests of the Electrolytic Capacitor Degradation Model

	Test 1	Test 2	Test 3
Simple Size	40	20	60
Target Parameters	A_0, C_0, E_{a1}, E_{a2}	CAP_0, ESR_0 B, D	σ_{CAP}, σ_{ESR} P_{CAP}, P_{ESR}
Aging Temperature	339K to 399K	-	-
Testing Temperature	298K	308K to 378K	298K
Aging Duration	300 Hrs	0 Hrs	0 Hrs
Load Level	Rated	OFF	OFF

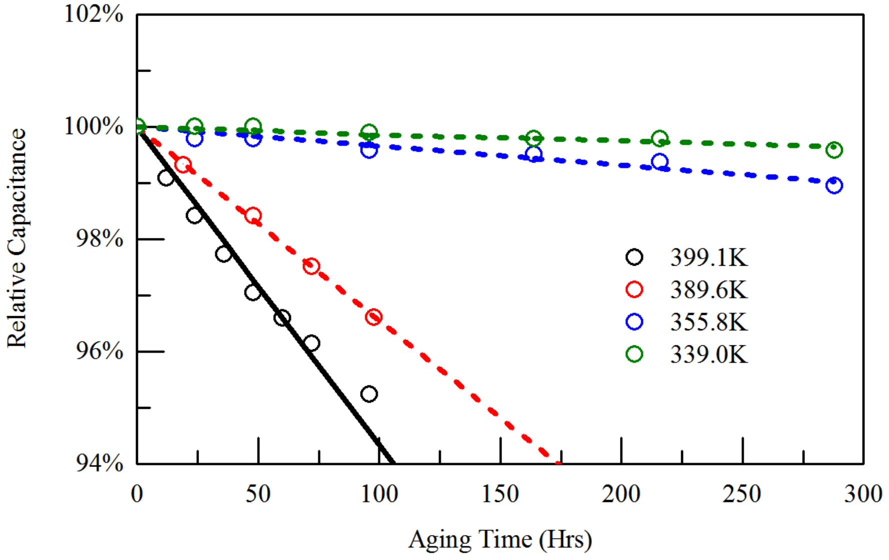

(a)

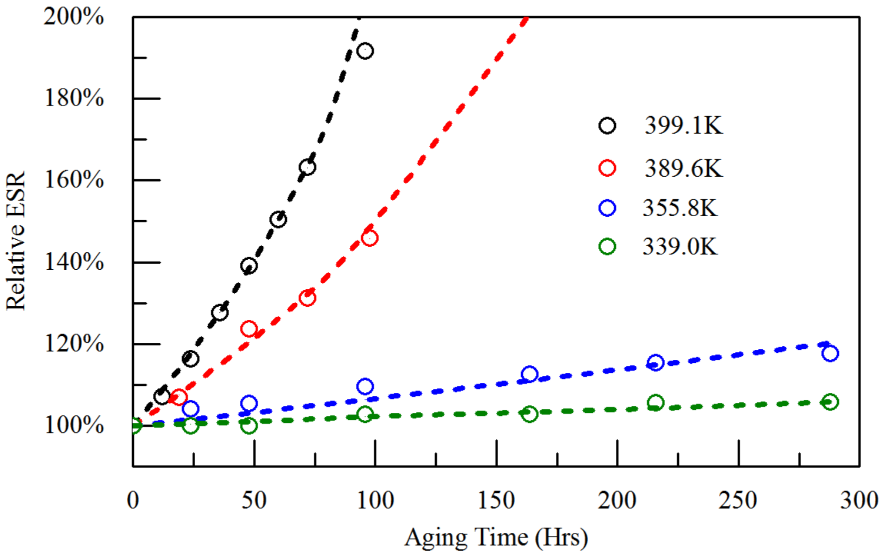

(b)

Figure B.1: Relative (a) Capacitance and (b) ESR of the Electrolytic Capacitor VS. Aging Time.

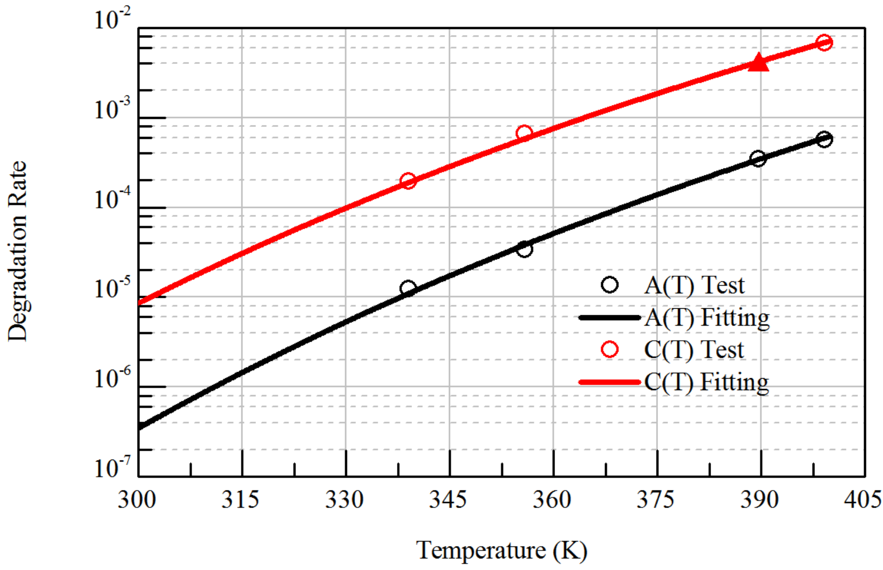

Figure B.2: Degradation Rates of Capacitance and ESR of the Electrolytic Capacitor VS. Aging Temperature.

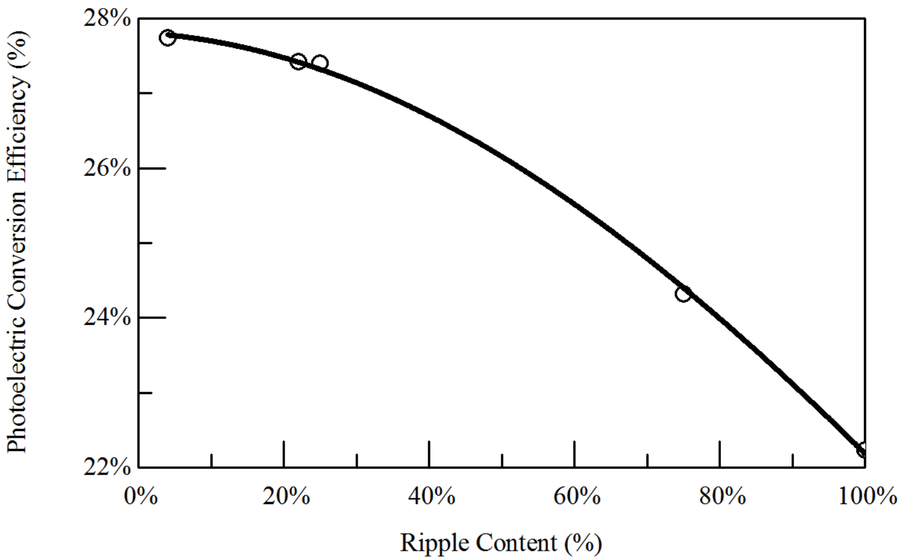

Figure B.3: Photoelectric Conversion Efficacy of the LED Load vs Current Ripple.

B

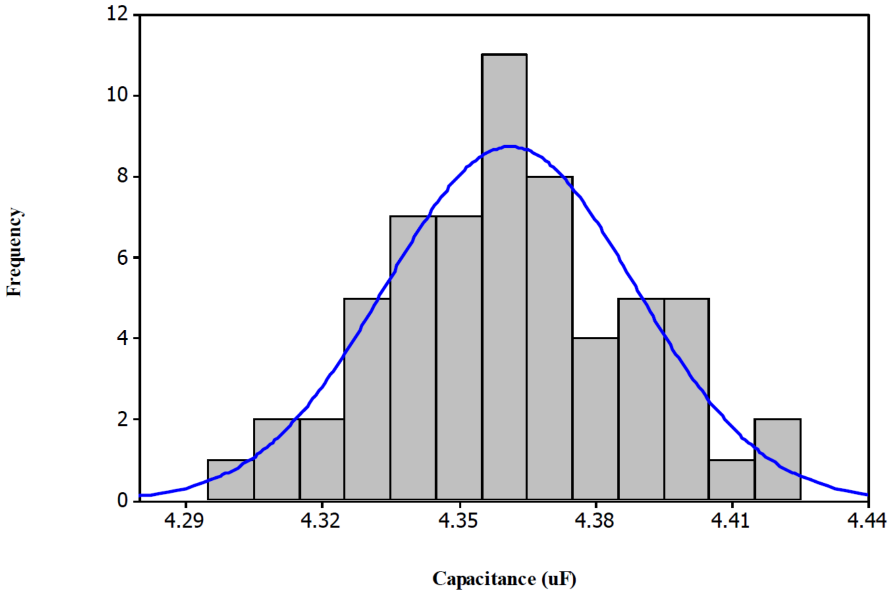

(a)

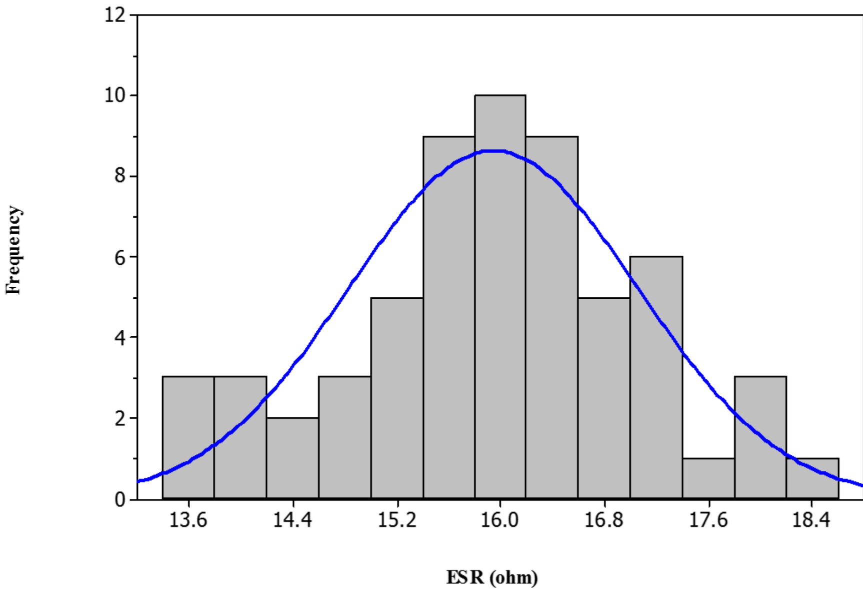

(b)

Figure B.4: Distribution of (a) Capacitance and (b) ESR of the Electrolytic Capacitor.

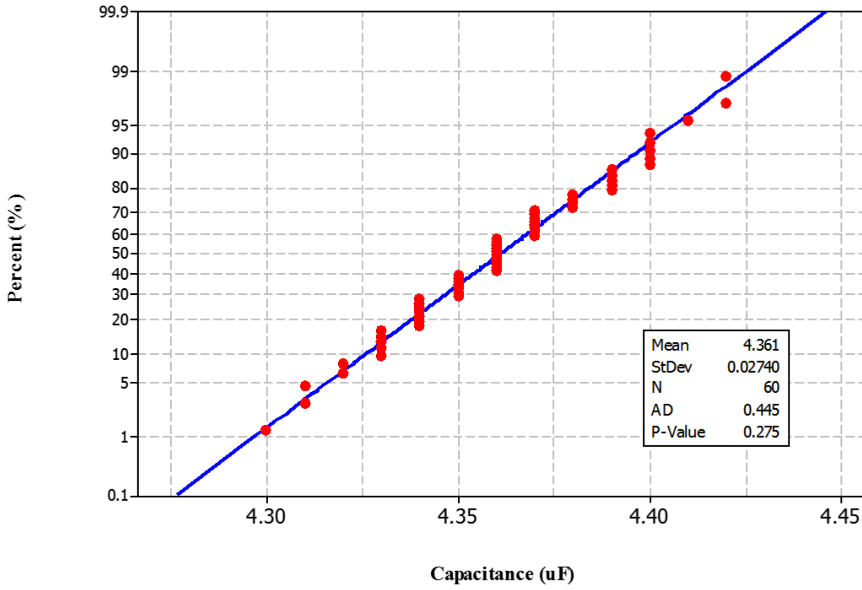

(a)

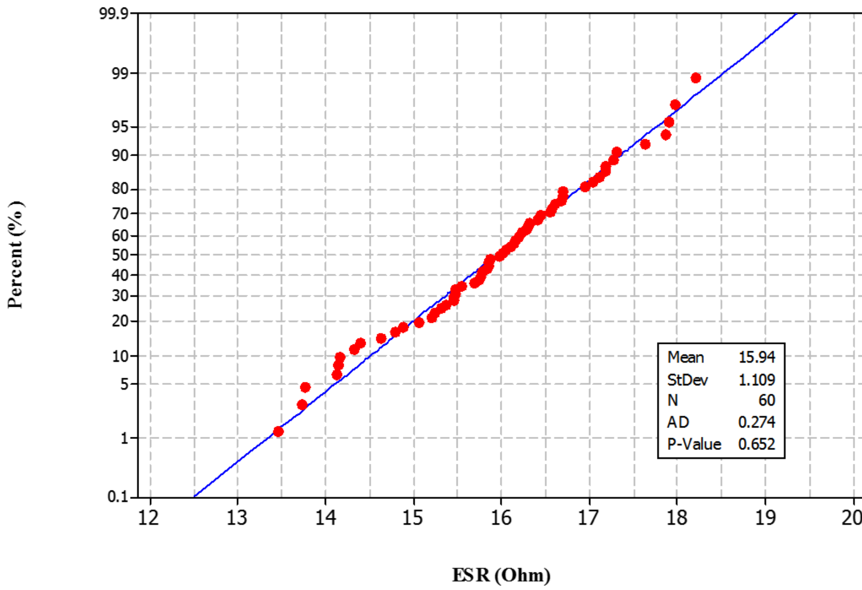

(b)

Figure B.5: Normality Test Results for (a) Capacitance and (b) ESR of the Electrolytic Capacitor.

C

APPENDIX C

C.1. SUPPORTING INFORMATION FOR CHAPTER 3

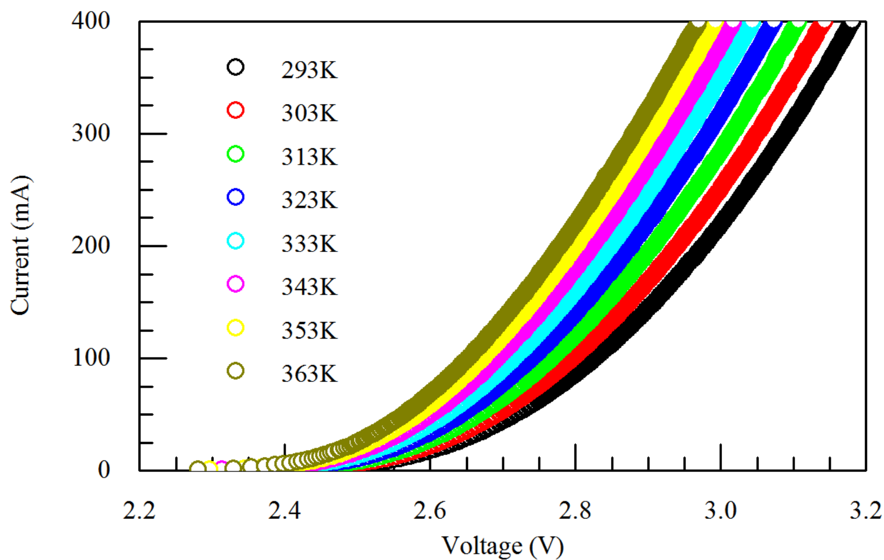

Figure C.1: I-V Curves of LEDs for Different Junction Temperature.

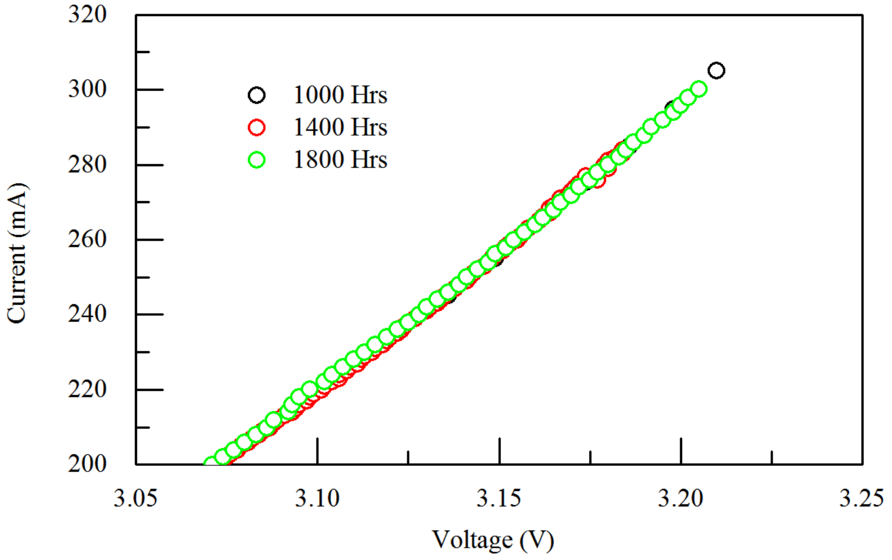

Figure C.2: I-V Curves of LEDs for Different Aging Duration.

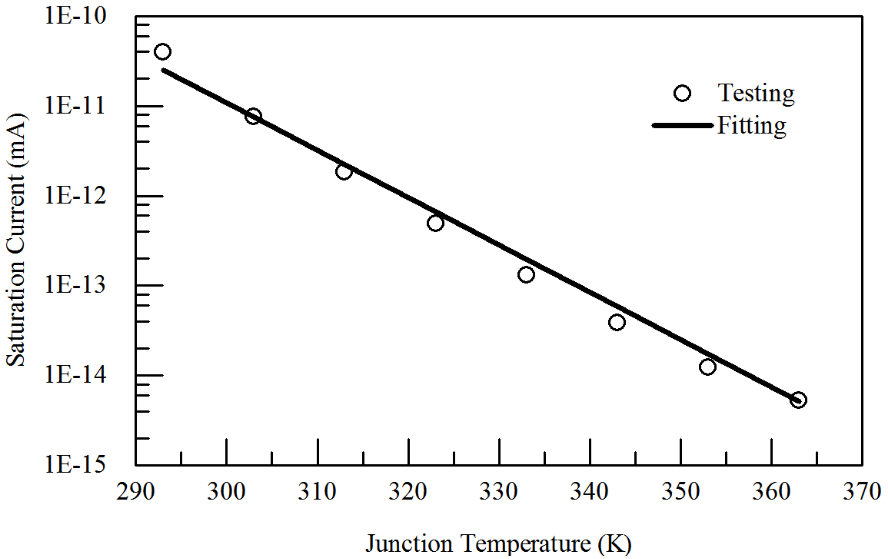

Figure C.3: Saturation Current of LEDs vs Junction Temperature.

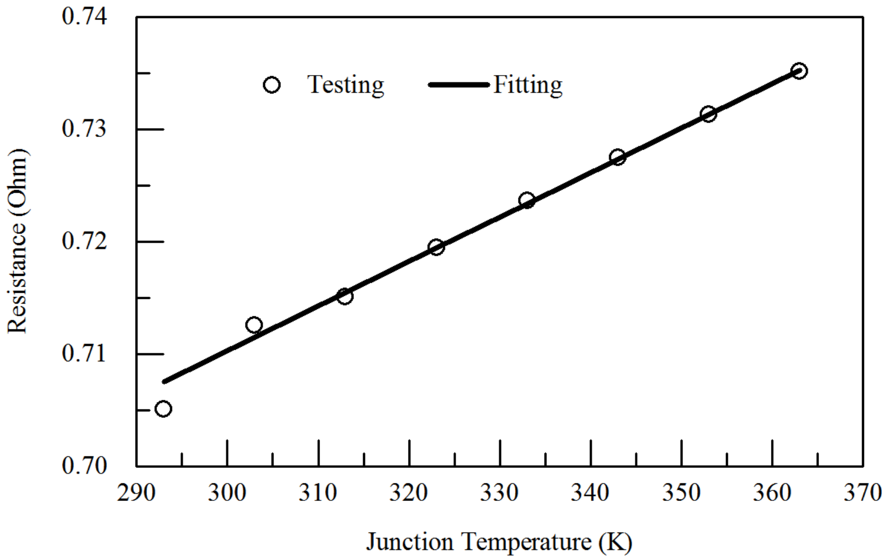

Figure C.4: Series Resistance of LEDs vs Junction Temperature.

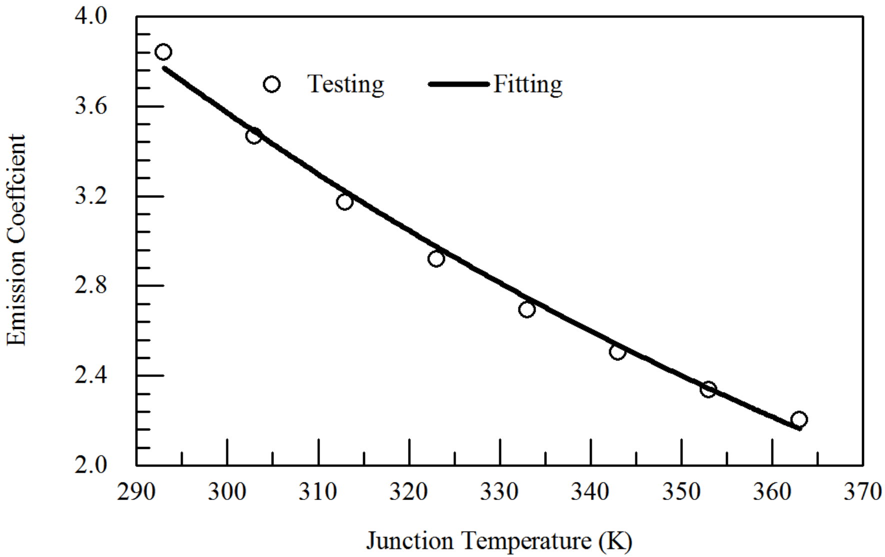

Figure C.5: Emission Coefficient of LEDs vs Junction Temperature.

C

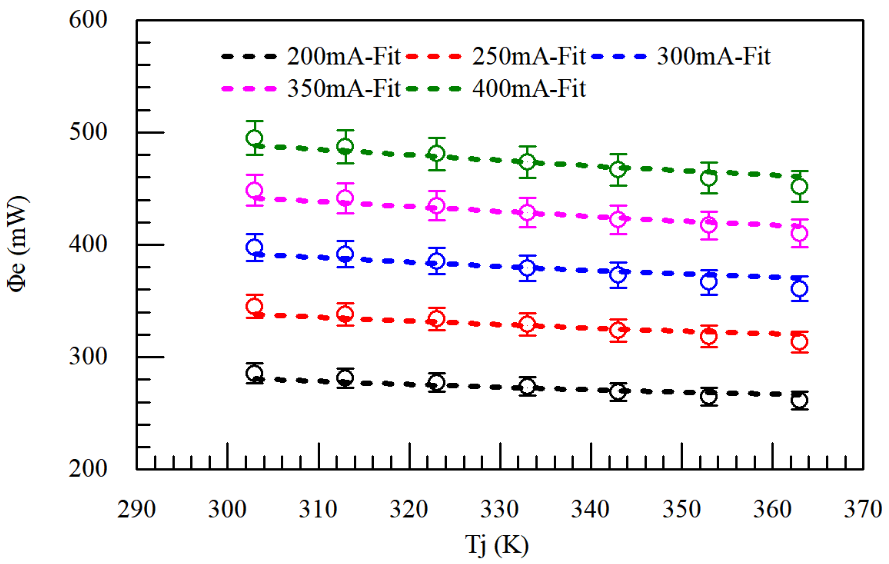

Figure C.6: Optical Power of LEDs vs Junction Temperature.

Abbreviations, Acronyms and Notation

Abbreviations and Acronyms

AC	Alternating Current;
AF	Accelerated Factor;
ALT	Accelerated Life Time Test;
CCM	Constant Current Mode;
CFL	Compact Fluorescent Lamp;
CFD	Computational Fluid Dynamics;
CL	Confidence Level;
CLO	Constant Light Output;
CSP	Chip Scale Package;
DC	Direct Current;
ESL	Equivalent Series Inductance;
ESR	Equivalent Series Resistance;
FEA	Finite Element Analysis;
GTR	Giant Transistor;
HEMT	High Electron Mobility Transistor;
HALT	High Accelerated Life Time Test;
IGBT	Insulated Gate Bipolar Transistor;
J-droop	Current-droop;
L70%	Time to 70% of Lumen Maintenance;
LC Filter	Inductor Capacitor Filter;
LED	Light Emitting Diode;
MESFET	Metal-Epitaxial-Semiconductor Field-Effect Transistor;
MOSFET	Metal-Oxide-Semiconductor Field-Effect Transistor;
MBTF	Mean Time between Failure;
MTTF	Mean Time to Failure;

PC	Power Control;
PET	Polyethylene Terephthalate;
PoF	Physics of Failure;
PWM	Pulse Width Modulation;
RC	Resistor Capacitor;
RH	Relative Humidity;
RMS	Root Mean Square;
SEPIC	Single-Ended Primary Inductor Converter;
SMPS	Switch Mode Power Supply;
SPICE	Simulation Program with Integrated Circuit Emphasis;
SSL	Solid State Lighting;
StDev	Standard Deviation;
T-droop	Temperature-droop;
VoT	Variable on-time;
ZCS	Zero Current Switching;
ZVS	Zero Voltage Switching;

NOTATION

CHAPTER 2

t	Aging duration;
Δt	Time increment;
t_F	Lifetime of component;
$P_{th,Cap}$	The thermal power of electrolytic capacitors;
I_{RMS}	The root mean square value of current;
ESR	Equivalent series resistance of electrolytic capacitor;
R_{th1}	Thermal conduction resistance of electrolytic capacitor
R_{th2}	Convective thermal resistance of electrolytic capacitor
ΔT_{cap}	Temperature rise of electrolytic capacitor;
CAP	Capacitance of electrolytic capacitor;
CAP_T	Initial capacitance of electrolytic capacitor;
ESR_T	Initial equivalent series resistance of electrolytic capacitor;
CAP_0	Basic capacitance of electrolytic capacitor;
ESR_0	Basic equivalent series resistance of electrolytic capacitor;
CAP_{mean}	Mean value of capacitance of electrolytic capacitor;

ESR_{mean}	Mean value of equivalent series resistance of electrolytic capacitor;
A	Degradation rate of the capacitance of electrolytic capacitor;
C	Degradation rate of the ESR of electrolytic capacitor;
A_0	Basic degradation rate of the capacitance of electrolytic capacitor;
C_0	Basic degradation rate of the ESR of electrolytic capacitor;
E_{a1}	Activation energy of the capacitance of electrolytic capacitor;
E_{a2}	Activation energy of the ESR of electrolytic capacitor;
κ	Boltzmann constant;
A_{cap}	Surface area of electrolytic capacitor;
σ	Conductivity of electrolytic capacitor;
σ_A	Base conductivity of electrolytic capacitor;
ε	Relative permittivity of electrolytic capacitor;
ε_0	Absolute permittivity of electrolytic capacitor;
$\varepsilon^{(0)}$	Base permittivity of electrolytic capacitor;
B	Temperature coefficient of relative permittivity;
d	Average foil distance of electrolytic capacitor;
D	Temperature coefficient of conductivity;
T_{Cap}	Average core temperature of electrolytic capacitor;
T_A	Ambient temperature;
f_{CAP}	Probability density of capacitance;
f_{ESR}	Probability density of equivalent series resistance;
σ_1	Standard deviation of capacitance;
σ_2	Standard deviation of equivalent series resistance;
$g(t)$	Cumulative failure rate of electrolytic capacitor;
t_{MTTF}	Mean time to failure of electrolytic capacitor;
N	Sample size;
t_{MAX}	Total operation time of the whole group of samples;

CHAPTER 3

T_j	Junction temperature of the LED light source;
ΔT_j	Junction temperature increment of the LED light source;
$I(t)$	Current of the LED light source at time t;
t	Aging duration;
$\Phi_{lm}(t)$	Absolute luminous flux at time t;
$\Phi(I)$	Luminous flux as a function of I;

β	Depreciation rate of the LED light source;
A_β	Pre-exponential factor of the LED depreciation;
$E_{a,\beta}$	Activation energy of the LED light source;
κ	Boltzmann constant;
Δt	Time increment;
$\eta(t)$	Efficacy of the LED light source at time t;
η_0	Basic efficacy of the LED light source;
Φ_0	Absolute luminous flux before aging;
V_f	Forward voltage of the LED light source;
a	Linear non-radiative recombination rates of LED;
b	Radiative recombination rate of LED;
c	3rd-order non-radiative recombination rates of LED;
A_e	Linear non-radiative current coefficient of LED;
B_e	Radiative current coefficient of LED;
C_e	3rd-order non-radiative current coefficient of LED;
V_{ref}	Reference voltage of the LED driver;
R_{ref}	Overall current control resistance of the LED driver;
A_0	Basic degradation rate of the LED driver;
A	Degradation rate of the LED driver;
T_D	Average temperature of the LED driver;
$E_{a,D}$	Overall activation energy of the LED driver;
R_0	Initial current control resistance of the LED driver;
R_s	Equivalent series resistance of the LED light source;
R_{s0}	Basic equivalent series resistance of the LED light source;
I_S	Saturation current of LED;
I_{s0}	Basic saturation current of LED;
A_I	Temperature coefficient of saturation current of LED;
A_N	Temperature coefficient of ideality factor of LED;
A_s	Temperature coefficient of series resistance of LED;
B_N	Non-thermal coefficient of ideality factor of LED;
C	Ratio of radiative power and luminous flux;
N	Ideality factor of LED;
n	Average carrier density of the LED light source;
P_L	Thermal power of the LED light source;
P_D	Thermal power of the driver;
P_{in}	Input power of the driver;

T_A	Ambient temperature;

CHAPTER 4

T_j	Junction temperature of the LED light source;
A_e	Linear non-radiative current coefficient of LED;
B_e	Radiative current coefficient of LED;
C_e	3rd-order non-radiative current coefficient of LED;
t	Aging duration;
$I_{LED}(t)$	Current of the LED light source at time t;
β	Depreciation rate of the LED light source;
A_β	Pre-exponential factor of the LED depreciation;
V_f	Forward voltage of the LED light source;
T_{MAX}	Maximum junction temperature of the LED light source;
$E_{a,\beta}$	Activation energy of the LED light source;
κ	Boltzmann constant;
η_0	Basic efficacy of the LED light source;
R_0	Initial current control resistance of the LED driver;
R_s	Equivalent series resistance of the LED light source;
R_{s0}	Basic equivalent series resistance of the LED light source;
I_S	Saturation current of LED;
I_{s0}	Basic saturation current of LED;
A_I	Temperature coefficient of saturation current of LED;
A_N	Temperature coefficient of ideality factor of LED;
A_s	Temperature coefficient of series resistance of LED;
B_N	Non-thermal coefficient of ideality factor of LED;
N	Ideality factor of LED;
$T_{j,i}$	Junction temperature of the component i;
$R_{th,i}$	Thermal resistance from junction to surface;
$P_{th,i}$	Thermal power of the component i;
f_{Driver}	Failure probability density of the LED driver;
f_M	Failure probability density of the MOSFET;
f_D	Failure probability density of the diode;
$I_M(t)$	Average current of the MOSFET at time t;
$T_M(t)$	junction temperature of the MOSFET at time t;
f_{M0}	Basic failure probability density of the MOSFET;

I_{Rated}	Rated current of the MOSFET;
T_A	Ambient temperature;
p	Current accelerated coefficient;
$E_{a,M}$	Activation energy of the MOSFET;
$T_{Di}(t)$	junction temperature of the diode at time t;
f_{D0}	Basic failure probability density of the diode;
$E_{a,D}$	Activation energy of the diode;
$MTTF$	Mean time to failure;
t_{MAX}	Total operation time;

CHAPTER 5

t	Aging duration;
$\Phi(t)$	Lumen maintenance at time t;
β	Depreciation rate of the LED light source;
$W(t)$	Stochastic distribution of the lumen depreciation at time t;
α	Increasing rate of the standard deviation;
$p[\Phi(t)]$	Probability density for $\Phi(t)$;
P_{LED}	Total power of the LED light source;
P_{Opt}	Optical power of the LED light source;
$R_D(t)$	Driver's survival probability at time t;
$f_D(t)$	Probability density of the driver's failures at time t;
f_{Di}	Failure probability density of the power diode;
f_{IC}	Failure probability density of the control IC;
$T_{j,Di}$	Junction temperature of the power diode;
$T_{j,IC}$	Junction temperature of the control IC;
λ_{Di}	basic failure probability density of the power diode;
λ_{IC}	basic failure probability density of the control IC;
$E_{a,Di}$	Activation energy of the power diode;
$E_{a,IC}$	Activation energy of the control IC;
κ	Boltzmann constant;
$MTTF$	Mean time to failure;
T_A	Ambient temperature;
$T_{A,in}$	Air temperature inside the lamp;
$T_{C,Di}$	Case temperatures of the power diode;
$T_{C,IC}$	Case temperatures of the control IC;

R_{th1}	Thermal resistance between the air surrounding the driver and the lamp's case;
R_{th2}	Thermal resistance between the lamp's case and the ambient;
$R_{th1,Di}$	Convective thermal resistance of the power diode;
$R_{th1,IC}$	Convective thermal resistance of the control IC;
$R_{th2,Di}$	Conductive thermal resistance of the power diode;
$R_{th2,IC}$	Conductive thermal resistance of the control IC;
$P_{th,LED}$	Thermal power of the LED light source;
$P_{th,Di}$	Thermal power of the power diode;
$P_{th,IC}$	Thermal power of the control IC;

APPENDIX A

N	Minimum sample size;
CL	Confidence level;
R	Reliability level;
P_{i1}	Input power in room conditions before acceleration;
P_{o1}	Output power in room conditions before acceleration;
P_{i2}	Input power in harshest accelerated conditions;
P_{o2}	Output power in harshest accelerated conditions;
P_{i3}	Input power in room conditions after acceleration;
P_{o3}	Output power in room conditions after acceleration;
AF	Accelerated factor;
RH_{field}	Related humidity in field conditions;
RH_{test}	Related humidity in test conditions;
q	Humidity coefficient of Peck Model;
T_{field}	Driver's temperature in field conditions;
T_{test}	Driver's temperature in test conditions;
ΔT_{field}	Temperature difference in field conditions;
ΔT_{test}	Temperature difference in test conditions;
n	Temperature difference coefficient of Norris-Landzberg Model;
f_{field}	Frequency in field condition;
f_{test}	Frequency in test conditions;
m	Frequency coefficient of Norris-Landzberg Model;
E_a	Activation energy;
κ	Boltzmann constant;

$T_{max,field}$	Driver's maximum temperature in field condition;
$T_{max,test}$	Driver's maximum temperature in test conditions;

SUMMARY

LIGHT-Emitting Diodes (LEDs) have become a very promising alternative lighting source with the main advantages of a longer lifetime and a higher efficiency than traditional ones. However, the LED lamp's lifetime is compromised by its driver's reliability. Although extensive studies have been made on the reliability of LEDs, the research on the lifetime prediction for LED drivers, and the interaction of the reliability between LEDs and driver in an LED system is still lacking. This dissertation investigates the lifetime predictions for LED drivers and LED lamps using physics of failure (PoF) based reliability simulations. Various reliability and statistical methods, such as the Monte Carlo method, the fault-tree method, the Markov Chain method, and the Wiener process, are applied and integrated with the electronic-thermal simulation in order to investigate various problems. They are summarized as followed:

Chapter 2 focuses on the reliability of electrolytic capacitor in LED drivers. In this study, a validated reliability model is used to describe degradation behavior of electrolytic capacitor. A single inductor buck-boost driver is simulated to investigate the impact of capacitor degradation on the entire system. It has been found that the temperature of an output stage capacitor increases significantly during operation time. Therefore, electrolytic capacitors degrade faster than that with constant temperature assumption. The capacitor's performance without taking temperature change into account results in an overestimated lifetime of a driver.

Chapter 3 studies the coupling effect of LED and driver's degradations on LED lamp's lifetime. An integrated LED lamp with an electrolytic capacitor-free driver is considered to investigate the coupling effects of both LED and driver's degradations on lamp's lifetime. The electrolytic capacitor-less buck-boost driver is designed to have a comparable life as the LED light source. It has been found that the erroneous results will be obtained if LED's degradation is not taken into considerations. Under the combined effects of the reduced current in LEDs and the lumen dependence over time, the LED lamp's lifetime is reduced significantly. The proposed method will provide a reliability design tool for selecting different drivers and LED light sources.

Chapter 4 investigates the interaction of LED driver's catastrophic failure and LED luminous flux decay. Two distinct operation modes of an electrolytic capacitor-free LED

driver are performed to study such interactions respectively: constant optical output (CLO) mode and constant current mode (CCM). Under CLO mode, the LED's current increases exponentially to maintain the constant light output. As a result, the junction temperatures of LEDs, MOSFETs and power diodes in driver rise significantly, leading to a much shorter MTTF, and faster luminous flux depreciation. However, under the CCM mode, the junction temperatures of LEDs, MOSFETs and diodes change modestly. Therefore, the driver's MTTF and LED's luminous flux decay are not affected much by the variation of temperatures during LED's degradation process under CCM mode.

Chapter 5 considers the effect of LED's stochastic lumen degradation on LED driver's reliability. Stochastic properties of LEDs degradation are described by the Wiener process. A compact thermal model of a commercial LED light bulb is used to obtain the temperature distribution. A temperature dependent reliability model is utilized to driver's survival probability. It has been found that the statistical properties of LEDs life data will lead to a broad range of the driver's survival probability. The stochastic analysis of LEDs life data from accelerated degradation testing can improve the accuracy of the prediction of the LED driver and LED lamp.

In conclusion, the validated electronic-thermal simulation method is a valuable tool to assess the reliability of (integrated) LED drivers and/or LED Lamps.

SAMENVATTING

LIGHT-Emitting Diodes (LED's) zijn een veelbelovende lichtbron geworden ten opzichte van traditionele met als belangrijkste voordelen een langere levensduur en een hogere efficiëntie. Echter, de levensduur van een LED-lamp wordt mede bepaald door de betrouwbaarheid van zijn elektronica. Hoewel veel studies zijn gedaan over de betrouwbaarheid van LED's, is er minder onderzoek naar de levensduurvoorspelling voor de interactie tussen LED en elektronica. Dit proefschrift onderzoekt de levensduur voor LED-eletronika in LED-lampen met behulp van de physics of failure (PoF) benadering. Verschillende methoden, zoals Monte Carlo, fault-trees, Markov Chains en het Wiener proces zijn toegepast en geïntegreerd met elektronische thermische simulaties om verschillende problemen te onderzoeken. Zij worden samengevat als volgt:

Hoofdstuk 2 is gericht op de betrouwbaarheid van elektrolytische condensatoren in LED drivers. In deze studie wordt een gevalideerd betrouwbaarheidsmodel gebruikt om de degradatie van elektrolytische condensatoren te beschrijven. Buck-boost elektronica wordt gesimuleerd om de impact van de condensator degradatie op het hele systeem te onderzoeken. Gebleken is dat de temperatuur gedurende de tijd aanzienlijk verhoogt. Om die reden degraderen elektrolytische condensatoren sneller dan wanneer een constante temperatuur wordt veronderstelt.

Hoofdstuk 3 bestudeert de interaktie tuseen LED's en elektronica op de levensduur van een LED-lamp. Een elektrolytische vrije less buck-boost elektronica is ontworpen met een vergelijkbare levensduur als de lichtbron. Gebleken is dat verkeerde resultaten worden verkregen indien de degradatie van de LEDs niet naar behoren is overwogen. Door de gecombineerde effecten van de gereduceerde stroom in LEDs en de licht afhankelijkheid in de tijd, wordt de levensduur van de LED lamp aanzienlijk verminderd. De voorgestelde simulatie methode is een betrouwbaar design tool voor het selecteren van verschillende drivers en LED-lichtbronnen.

Hoofdstuk 4 onderzoekt de interactie van catastrofaal falen van de LED-driver en het LED licht verval. Twee verschillende werkingsmodi van een elektrolytische condensator-vrije LED-driver zijn gesimuleerd om dergelijke interacties te bestuderen, te weten constante optische output (CLO) en de constante stroom modus (CCM). Onder de CLO-modus neemt de LED's stroom exponentieel toe om de constante lichtopbrengst te be-

houden. Hierdoor nemen de temperaturen van de LEDs, MOSFETs en diodes aanzienlijk toe, wat leidt tot een veel kortere gemiddelde tijd tot falen (MTTF) en een snellere afname van de lichtstroom. Echter, onder de CCM-modus verandert de temperatuur van de LED's, MOSFET's en diodes maar bescheiden. Daarom zal de MTTF onder de CCM wijze minder varieren over de tijd.

Hoofdstuk 5 beschouwt het effect van de stochastische licht degradatie van LEDs als functie van de betrouwbaarheid van de LED elektronica. De stochastische eigenschappen van de LED degradatie worden beschreven door het Wiener proces. Een compact thermisch model van een commerciële LED lamp wordt gebruikt om de temperatuur te berekenen. Gebleken is dat de statistische eigenschappen van LEDs leidt tot een breed scala van de faalkansen van de elektronica. Het meenemen van deze stochastische analyse kan de nauwkeurigheid van de voorspelling van de LED elektronica en LED lamp significant verbeteren.

Tot slot, de gevalideerde elektronische thermische simulatie methode is een waardevol instrument om de betrouwbaarheid van (geïntegreerde) LED-elektronica en / of LED lampen te beoordelen.

List of Publications

Journal Papers

1. **B. Sun**, X.J. Fan, C. Qian and G.Q. Zhang, *PoF-Simulation-Assisted Reliability Prediction for Electrolytic Capacitor in LED Drivers*, IEEE Transactions on Industrial Electronics **63(11)**, 6726-6735, (2016).

2. **B. Sun**, X.J. Fan, W.D. van Driel, H.Y Ye, J.J. Fan, C. Qian and G.Q. Zhang, *A Novel Lifetime Prediction for Integrated LED Lamps by Electronic-Thermal Simulation*, Reliability Engineering & System Safety, **163**, 14-21, (2017).

3. **B. Sun**, X.J. Fan, H.Y Ye and G.Q. Zhang, *A Reliability Prediction for Integrated LED Lamp with Electrolytic Capacitor-Free Driver*, IEEE Transactions on Components, Packaging and Manufacturing Technology, **7(7)**, 1081-1088, (2017).

4. **B. Sun**, X.J. Fan, C.Q. Chui and G.Q. Zhang, *A Stochastic Process Based Reliability Prediction Method for LED Lamps*, Reliability Engineering & System Safety, **Submitted**, (2017).

5. H.Y Ye, A.M. Gheitaghy, H. Tang, **B. Sun**, C. Qian, X. Chen, X.J. Fan, C.Q. Chui and G.Q. Zhang, *Thermal Management on IGBT Power Electronic Devices and Modules*, IEEE Access, **Submitted**, (2017).

6. C. Qian, **B. Sun**, J.S. Cao, *Accelerated Luminous Depreciation Testing for LED Lighting Products*, China Standardization **68**, Setp./Oct. 2014.

Conference Papers and Presentations

1. **B. Sun**, X.J. Fan, J.J. Fan, C. Qian, G.Q. Zhang. A PoF and Statistics Combined Reliability Prediction for LED Arrays in Lamps. In *IEEE International Conference on Thermal, Mechanical and Multi-Physics Simulation and Experiments in Microelectronics and Microsystems (EuroSIME)*, Dresden, Germany, April 2017.

2. **B. Sun**, X.J. Fan, Willem van Driel, G.Q. Zhang. A systematic approach for reliability assessment of electrolytic capacitor-free LED drivers. In *IEEE International Conference on Thermal, Mechanical and Multi-Physics Simulation and Experiments in Microelectronics and Microsystems (EuroSIME)*, Montpellier, France, April 2016.

3. **B. Sun**, X.J. Fan, Willem van Driel, Thomas Michel, Jiang Zhou, G.Q. Zhang. Lumen decay prediction in LED lamps. In *IEEE International Conference on Thermal, Mechanical and Multi-Physics Simulation and Experiments in Microelectronics and Microsystems (EuroSIME)*, Montpellier, France, April 2016.

4. **B. Sun**, X.J. Fan, Cadmus Yuan, Cheng Qian, G.Q. Zhang. A Degradation Model of Aluminum Electrolytic Capacitors for LED Drivers. In *IEEE International Conference on Thermal, Mechanical and Multi-Physics Simulation and Experiments in Microelectronics and Microsystems (EuroSIME)*, Budapest, Hungary, April 2015.

5. **B. Sun**, X.J. Fan, Cadmus Yuan, Sau Wee Koh, G.Q. Zhang. A Lifetime Prediction Method for Solid State Lighting Power Supply Based on SPICE and FEA Simulations. In *IEEE International Conference on Thermal, Mechanical and Multi-Physics Simulation and Experiments in Microelectronics and Microsystems (EuroSIME)*, Ghent, Belgium, April 2014.

6. **B. Sun**, X.J. Fan, Cadmus Yuan, Sau Wee Koh, G.Q. Zhang. Accelerated Lifetime Test for Isolated Components in Linear Drivers of High-Voltage LED System. In *IEEE International Conference on Thermal, Mechanical and Multi-Physics Simulation and Experiments in Microelectronics and Microsystems (EuroSIME)*, Wroclaw, Poland, April 2013.

7. Sau Wee Koh, Cadmus Yuan, **B. Sun**, Bo Li, X.J. Fan, G.Q. Zhang. Product Level Accelerated Lifetime Test for Indoor LED Luminaires. In *IEEE International Conference on Thermal, Mechanical and Multi-Physics Simulation and Experiments in Microelectronics and Microsystems (EuroSIME)*, Wroclaw, Poland, April 2013.

8. **B. Sun**, Sau Wee Koh, X.J. Fan, Cadmus Yuan, G.Q. Zhang. An Accelerated Lifetime Test Method for DC or AC Supplied Electronic Control Gear for LED Modules of Outdoor LED Lighting Products. In *China International Forum on Solid State Lighting (ChinaSSL)*, Beijing, China, November 2013.

9. Guangjun Lv, Cadmus Yuan, **B. Sun**, Bo Li, X.J. Fan, G.Q. Zhang. Validation of the methodology of lumen depreciation Acceleration of LED lighting. In *China International Forum on Solid State Lighting (ChinaSSL)*, Beijing, China, November 2013.

10. **B. Sun**, Sau Wee Koh, X.J. Fan, Cadmus Yuan, G.Q. Zhang. Single-Component Accelerated Life Test Method for LED Drivers in AC LED Systems. In *China International Forum on Solid State Lighting (ChinaSSL)*, Guangzhou, China, November 2012.

STANDARD CONTRIBUTIONS

1. Standardization Administration of China. *GB/T-33720: Accelerating Depreciation Test Method for LED Lighting Products*. 2017.

2. Standard Committee of China Solid Stare Lighting Alliance. *CSA-029: Accelerated Lifetime Test Method for DC or AC Supplied Electronic Control Gear for LED Modules of Outdoor LED Lighting Products.* 2014.

3. Standard Committee of China Solid Stare Lighting Alliance. *CSA-020: Accelerating Depreciation Test Method for LED Lighting Products.* 2013.

BOOK CHAPTER

1. **B. Sun**, X.J. Fan, Willem van Driel, H.Y Ye, C. Qian, J.J. Fan, G.Q. Zhang. *Driver Reliability: A Physics of Failure Approach for Driver Reliability Prediction*, SSL Reliability: from components to systems - Part II (2017).

PATENT

1. **B. Sun**, J. Wei, Y. Li, Y.Y. Leung, T. Fang, X.J. Fan, G.Q. Zhang. *Desktop card tablet recreation system.* State Key Lab of Solid State Lighting of China, CN205832553U, China Patent, 2016.

2. S.W. Koh, X.J. Fan, Z.Y. Wang, **B. Sun**, C.A. Yuan, G.Q. Zhang. *Method and device for accelerated detection of lumen maintenance of lighting device.* State Key Lab of Solid State Lighting of China, CN102980747A, China Patent, 2013.

3. S.W. Koh, **B. Sun**, X.J. Fan, C.A. Yuan, G.Q. Zhang. *Method and device for detecting service life of illumination driver.* State Key Lab of Solid State Lighting of China, CN102967786B, China Patent, 2012.

4. S.W. Koh, X.J. Fan, Zhiying Wang, **B. Sun**, C.A. Yuan, G.Q. Zhang. *Detection method and device for failure probability of illuminating system.* State Key Lab of Solid State Lighting of China, CN102982241B, China Patent, 2012.

5. C.Y. Wong, G. Fan, L. Niu, **B. Sun**, L. Liu, J. Guo, Y.Y. Leung, J. Wei, M. Dong, L. Zhao, S.W. Koh, C.A. Yuan, G.Q. Zhang. *Polarized fluorescent powder, fluorescent powder polarization method and method for manufacturing light-emitting diode (LED) luminescent devices.* State Key Lab of Solid State Lighting of China, CN102983251B, China Patent, 2012.

6. C.Y. Wong, G. Fan, L. Niu, **B. Sun**, L. Liu, J. Guo, Y.Y. Leung, J. Wei, M. Dong, L. Zhao, S.W. Koh, C.A. Yuan, G.Q. Zhang. *Color temperature adjustable light-emitting diode (LED) light-emitting device and manufacturing method thereof.* State Key Lab of Solid State Lighting of China, CN102983252B, China Patent, 2012.

WORKSHOPS

1. **B. Sun**, Sau Wee Koh, Bob Li, *Off-Grid Lighting System Reliability*,The 2nd Workshop of Sino-German Cooperation Program: Off-Grid Lighting, Beijing, China, 2013.

2. **B. Sun**, Sau Wee Koh, Bob Li, *Multi-physical Reliability Simulation of LED Drivers for Solid State Lighting*,The 3rd Workshop of Sino-German Cooperation Program: Off-Grid Lighting, Jena, German, 2014.

ACKNOWLEDGEMENTS

THIS dissertation was completed in February 2017. Writing this final part of my dissertation, I realize many people have contributed to my Ph.D. research.

First of all, I would like to express my deepest appreciation to my promoter Prof. dr. Guoqi Zhang for the continuous support of my Ph.D. study and related research, for his patience, motivation, and immense knowledge. You gave me a precious opportunity to enroll in the Ph.D. program in Beijing Research Center (BRC). I could not have imagined having a more insightful promoter for Ph.D. study.

I would like to dedicate my sincere gratitude to Prof. Xuejun Fan, my daily supervisor, who has the attitude and the substance of a true academic researcher: he continually and convincingly conveyed a rigorous and pragmatic spirit in regard to research. You are always available for discussion regardless of time, location and distance. Without your guidance and persistent help, this dissertation would not have been possible.

I am grateful to my co-promoter, Dr. Willem van Driel, for his guidance from the angle of both academic research and industrial experience. My sincere thanks also go to Dr. Changann Yuan, Dr. Cheng Qian, Dr. Jiajie Fan and Dr. Bob Li, who provided me opportunities to join their team as a reliability engineer. Without their support, it would be hard to conduct this research. I owe sincere thankfulness to Dr. Huaiyu Ye and Dr. Jia Wei for their advice on my research and selfless help in my life in the Netherlands. In addition, a thank you to Prof. Jelena Popovic who gave me valuable comments to my paper as an expert of Power Electronics.

I would like to acknowledge the financial support of the National High-Tech Research and Development Program of China (863 Program, 2015AA03A101), International Science and Technology Cooperation Program of China (2015DFG52110) and EMRP JRP ENG62 MESaIL which was carried out with funding by the European Union.

It was pleasure work with brilliant colleagues from ECTM ,EKL and BRC: Prof. Lina Sarro, Dr. Sau Wee Koh, Dr. Stanely Leung, Dr. Cell Wong, Dr. Jianfei Dong, Dr. Fabio Santagata, Dr. Elina Iervolino, Dr. Sima Tarashioon, Dr. Jing Zhang, Dr. Maryam Yazdan Mehr, Dr. Rene Poelma, Dr. Jianlin Huang, Dr. Mingzhi Dong, Dr. Pan Liu, Dr. Pengfei Sun, Haining Wu, Hongyu Tang, Cinzia Silvestri, Zahra Kolahdouz Esfahani, Yelena Grachova, Xueming Li, Guangjun Lu, Hao Zhang, Manjunath Ramachandrappa Venkatesh,

Robert Sokolovskij, Hengqian (Daniel) Yi, Boyao Zhang, Brahim Mansouri, Aleksandar Jovic, Yuan Gao, Jianwen Sun, Dongbin Cai, Yingjie Shen, Jian Li. I am obliged to all my colleagues in China State Key Laboratory of Solid State Lighting, for their professional support in the laboratory, for their unforgettable training about social skills and for the sleepless nights we were working together. I would like to thank all other the professors, PhDs, post-docs, master students and technicians inside or outside our department for their presentations, feedback, cooperation, help and friendship.

I would like to thank my wife, Sang Wu, who appeared in my life just when I need her most. Her support, tolerance, encouragement, quiet patience and unwavering love are unshakable bedrocks of my life. I thank my parents for supporting me spiritually throughout my life. I grew up with their constant care and love. Whenever I get into trouble, they come over first to support me and encourage me. I am thankful for my best friend Andy Han. We have common interests, despite the fact that we come from different backgrounds. He always help me to think about scientific problems in different ways.

Finally, and the most importantly, I am truly grateful to all the people who have promoted the international cooperation program of Beijing Research Center of TU Delft. They have built a bridge between Europe and China for young researchers all over the world. Until today, I still miss the days and nights in Delft, Beijing and Changzhou where I worked with talents from both universities and industries. Perhaps in the future, teammates in my PhD period will be my research partners.

CURRICULUM VITÆ

BO SUN

May 1986	Born in Taiyuan, China, P.R.

EDUCATION

2004–2008 Bachelor of Science in Microelectronics
School of Physical Science and Technology
South China University of Technology, Guangzhou, China

2009–2011 Master of Engineering Science in Electrical Engineering
Phillip M. Drayer Dept. of Electrical Engineering, College of Engineering
Lamar University, Beaumont, Texas, USA

Thesis:	Transmission Gate Technique for Soft Error Mitigation in Nanometer CMOS Circuit
Supervisor:	Prof. S. Sayil

2012–2017 PhD. Reliability Engineering in Opto-electronics System
Delft University of Technology, Delft, the Netherlands

Dissertation:	The Lifetime Prediction of LED Drivers and Lamps
Promotor:	Prof. dr. G.Q. Zhang
Co-Promotor:	Prof. dr. W.D. van Driel
Daily Supervisor:	Prof. X.J. Fan

WORK EXPERIENCE

2008–2009 Process Quality Control Assistant Engineer
Founder High Tech. PCB Ltd, Co., Zhuhai, China

2010–2011 Research and Teaching Assistant
Lamar University, Beaumont, Texas, USA

2012–2017 Reliability Engineer
State Key Laboratory of Solid State Lighting, Changzhou, China

PROJECTS

2012–2013 China Solid State Lighting Alliance Project: CSA-020 Accelerating Depreciation Test Method for LED Lighting Products.

2013–2015 International Science and Technology Cooperation Program: Off-Grid Lighting System.

2013–2014 China Solid State Lighting Alliance Project: CSA-029 Accelerated Test Method for DC or AC Supplied Electronic Control Gear for LED Modules of Outdoor LED Lighting Products.

2013–2015 International Science and Technology Cooperation Program: 2015DFG62430 Cyclic Utilization and Life-Cycle Management of LED Luminaries.

2014–2016 EU European Metrology Research Programme: EMRP JRP ENG62 MESaIL Metrology for Efficient and Safe Innovative Lighting.

2015–2017 National High-Tech Research and Development Program of China: 2015AA03A101 Research on reliability and controllable life of LED lighting system based on failure mechanism.

2015–2017 International Science and Technology Cooperation Program: 2015DFG52110 Construction of the Innovation Cooperation Platform for Solid State Lighting Technology in BRICS Countries.

AWARD

2013	Global SSL Events of the Year 2013 International Solid State Lighting Association (ISA)